NASA CR-66344

THE DEVELOPMENT OF TECHNOLOGY REQUIRED FOR THE SUCCESSFUL DEPOSITION OF ALUMINUM ALLOYS AND BERYLLIUM

By Ronald Guidotti and Kenneth Lui

Prepared under Contract No. NAS1-7418 by

ELECTRO-OPTICAL SYSTEMS, INC.
A Xerox Company

for

NATIONAL AERONAUTICS AND SPACE ADMINISTRATION

NASA CR-66344

THE DEVELOPMENT OF TECHNOLOGY REQUIRED FOR THE SUCCESSFUL DEPOSITION OF ALUMINUM ALLOYS AND BERYLLIUM

By Ronald Guidotti and Kenneth Lui

Prepared under Contract No. NAS1-7418 by

ELECTRO-OPTICAL SYSTEMS, INC.
A Xerox Company

for

NATIONAL AERONAUTICS AND SPACE ADMINISTRATION

ABSTRACT

Trial syntheses of beryllium Grignards yielded insufficient quantities of material required for the successful electrodeposition of beryllium. Aluminum-alloy and hardened-aluminum plating baths were developed through the use of inorganic and organic compound additives to an aluminum plating bath ($AlCl_3$ and $LiAlH_4$ in diethyl ether). The ultimate yield strength of the aluminum deposits from the improved baths was in the range of 145 - 228 MN/m^2 (21K to 33K psi). A voltammetric technique using a triangular waveform was used to scan a large number of electrolytes in uncovering the improved plating baths. The triangular-wave voltammetric scan also was found to be a useful method in monitoring for signs of deterioration of the plating bath.

ACKNOWLEDGMENT

The authors wish to acknowledge the support given by Jimmie Brower in the preparation of the large number of test solutions.

CONTENTS

CONTENTS (contd)

ILLUSTRATIONS

SECTION 1

INTRODUCTION

Hollow-core (modified honeycomb) solar panel substrates of high-strength, lightweight, and nonmagnetic metals are very desirable for space applications. The only metal suitable for electroforming a nonmagnetic structure at present is pure aluminum. However, the electroformed aluminum possesses a relatively low yield strength and modulus of elasticity. The present contract work is concerned with the development of the technology required for the successful electrodeposition of high-strength aluminum alloys and other strong, nonmagnetic light metals such as beryllium.

The present contract work, therefore, is divided into three main areas. The first area is concerned with the development of a beryllium plating bath utilizing an ethereal solution of a beryllium Grignard. During previous NASA work (NASA Report CR-66427), a plating bath was developed for the electrodeposition of pure magnesium utilizing an ethereal solution of a magnesium Grignard. The work effort was to be concentrated on a study of various beryllium Grignard preparation methods for obtaining suitable quantities for use in a plating solution.

The second area is concerned with development of a hardened aluminum or aluminum-alloy plating bath. The basic aluminum plating solution (APS) of aluminum chloride and lithium aluminum hydride in ethyl ether produces a very soft and weak electrodeposit. The work in the second area, then, involves the use of inorganic and organic compound additives to the APS to increase the physical strength of the aluminum electrodeposit through hardening and/or alloy formation.

The third area of work is concerned with the molecular-level electrochemical scanning studies of mixed-solvent systems, mixed-salt systems, and combinations of systems that could potentially produce aluminum-alloy electrodeposits with greater physical properties than pure aluminum. A single-sweep, repetitive, voltage-time triangular waveform was to be used.

Flat plate and hollow-core demonstration samples (10 cm x 15 cm) were to be electroformed from the best beryllium, best hardened aluminum, and best aluminum-alloy plating baths.

SECTION 2

SUMMARY

Attempts were made under the present contract to develop a plating bath (of the Grignard type) for the electrodeposition of high-purity beryllium metal. Studies were also made of the basic aluminum bath to improve and strengthen the aluminum electrodeposit through the use of various bath additives. Screening of the various additives were performed using an electrolyte-voltammetric-scanning method.

Several methods of preparing beryllium Grignard were investigated during the study. The direct preparation method of heating beryllium metal, an alkyl halide, and a catalyst together in ethyl ether produced very low yields of beryllium Grignard. The indirect method of preparing beryllium alkyls *in situ* was somewhat more successful. Mixing $BeCl_2$ etherate with an ethereal solution of ethyl magnesium bromide (EMB) produced a solution of dialkyl beryllium along with magnesium halides. Only powdery Mg-Be alloy electrodeposits were obtained from this solution. The use of a solution of ethyl lithium (in benzene), instead of EMB, with the $BeCl_2$ etherate also produced a poor electrodeposit of beryllium.

Alloys of aluminum and beryllium were obtained by electrolysis of mixtures of $BeCl_2$ etherate with ethereal $LiAlH_4$ or the standard aluminum plating solution (APS= 3.73M $AlCl_3$, 0.33 M $LiAlH_4$). The $BeCl_2$-$LiAlH_4$ system produced brittle, inferior alloy deposits compared to the $BeCl_2$-APS system. The best alloy deposit was obtained at a $BeCl_2$ concentration of 1.25M in the APS. The deposit contained 0.04% Be; it had an average ultimate strength of 110 MN/m^2 (16,000 psi).

The ZnX_2-APS systems yielded Zn-Al alloys on electrolysis, but the deposits were extremely brittle with no structural strength.

Plating baths formulated from ethereal EMB and $LiAlH_4$ produced Mg-Al alloys which were thin, peeled, and highly stressed. Many of the solutions were poor conductors.

An aluminum alloy containing titanium was obtained from the APS containing 0.03-0.04M titanyl acetylacetonate. The deposit contained 0.07% Ti; it had an average yield strength (0.2% offset) of 99 MN/m^2 (14,400 psi) and an average ultimate strength of 120 MN/m^2 (17,400 psi).

Several hundred solution combinations of the APS containing inorganic and organic compound additives were examined in attempts to develop a hardened aluminum plating bath. Of all the compounds tested, the following gave the most improved, hardened electrodeposit: $BeCl_2$ (1.25M), titanyl acetylacetonate (0.03-0.04M), carbanilide (0.114M), bis (2-butoxyethyl) ether (17% by volume), benzonitrile (0.175M), ferrocene (0.188M), oxydianiline (0.0895M), and pyridine (0.124M). Of these, pyridine produced the hardest and strongest electrodeposit. It had a yield strength (0.2% offset) of 198 MN/m^2 (28,700 psi) and an ultimate strength of 222 MN/m^2 (32,300 psi).

Many of the solutions tested in the electrodeposition studies were examined through the use of single-sweep voltammetry using a triangular waveform. Voltage derivative curves (dV/dt-V) were obtained of the various solutions to observe the values of the reduction potentials. The voltage derivative curves were found useful for correlating the

nature of the electrodeposit (i.e., metallic or nonmetallic) to the type of plating solution. Signs of deterioration of the plating bath were found to be detectable by the single-sweep technique.

Large flat-plate and hollow-core (10 x 15 cm) samples were electroformed from the APS-titanyl acetylacetonate, APS-beryllium chloride, and APS-pyridine plating solutions.

SECTION 3
TECHNICAL DISCUSSION

3.1 ELECTRODEPOSITION OF BERYLLIUM

3.1.1 SYNTHESIS OF BERYLLIUM GRIGNARDS

3.1.1.1 Direct Synthesis

Since Grignard reagents have been used with success in this laboratory (in the THF-ether solution) for the electrodeposition of magnesium, it was decided to attempt preparation of the beryllium counterpart for subsequent beryllium electrodeposition tests. Successful preparation or organoberyllium halides was reported by Gilman and Schulze (1) by heating beryllium (and a catalyst) with alkyl halides in ether solution for more than 15 hours at 353 to 363°K (80°C to 90°C).

Since ethyl ether has a very high vapor pressure at temperatures over 373°K (100°C), a stainless steel pressure cylinder rated at 13.4 MN/m^2 (1800 psi) was chosen as the reaction vessel. It was equipped with a thermocouple and pressure gauge so that the reaction conditions could be monitored. After loading, it was placed in an oven at the desired temperature. All transfers and loading took place in the glove box under a dry nitrogen atmosphere.

Before use, the alkyl halides were twice distilled over $CaSO_4$ to remove any water. The anhydrous ethyl ether was distilled over $LiAlH_4$ in the glove box to remove the last traces of moisture. Just before loading into the reaction vessel, the beryllium chips (or powder) were

ground in a mortar to expose fresh metal surfaces for reaction. Attempts were made to prepare large quantities of ethyl beryllium iodide and ethyl beryllium bromide by heating an ethyl ether solution of the respective alkyl halide with beryllium metal powder for several days at 388°K to 423°K. Beryllium chloride, mercury(II) chloride, and ethyl magnesium chloride were each used as catalysts. While it appears that organoberyllium halides can be synthesized in the above manner, the method suffers from very poor yields. As a result, it is not a practical method of preparing suitable quantities of beryllium Grignard for electrodeposition tests.

3.1.1.2 Indirect Synthesis

As the direct-synthesis approach proved to be neither practical nor fruitful, it was discarded in favor of an indirect-synthesis approach. The Grignard reagent is reported to be a mixture of compounds according to the following equilibrium (2,3):

$$2RMgX \rightleftarrows R_2Mg + MgX_2$$

Addition of $BeCl_2.2Et_2O$ to the above solution causes the following reaction to take place (4,5):

$$2RMgX + BeCl_2.2Et_2O \rightarrow R_2Be + MgX_2 + MgCl_2 + 2Et_2O$$

Addition of more $BeCl_2.2E_2O$ to an ether solution of R_2Be (in a 1:1 mole ratio) should then yield the equivalent of an ether solution of RBeX.

The Grignard solutions (3M) were obtained commercially and the $BeCl_2 \cdot 2Et_2O$ solution was prepared in the laboratory. When $BeCl_2$ is added to ethyl ether, $BeCl_2 \cdot 2Et_2O$ is formed. The etherate dissolves only enough ether to form a solution which is approximately 2.6M in the etherate. The denser etherate solution is not miscible with ethyl ether and is, therefore, easily separated from it. Thus, a 2.6M solution of $BeCl_2 \cdot 2Et_2O$ is readily obtained.

The $BeCl_2$ etherate solution was mixed with various ethereal Grignard reagents in various proportions ($BeCl_2$:Grignard mole ratio = 0.10 to 4.1:1.0), and the precipitate which formed was removed by filtration. The resulting filtered solution was then electrolyzed (aluminum anodes and copper cathodes) at room temperature with 6.4 mm (¼") electrode spacings. Qualitative analyses were performed on any significant electrodeposits for the major metallic constituents.

The better electrodeposits were obtained using the EtMgBr Grignard, but even these were not satisfactory in terms of obtaining a deposit with any structural strength. Most of the deposits were dull, powdery, and brittle. The majority of the solutions examined were not very conductive. Alloy Mg-Be electrodeposits were obtained in the majority of cases. Deposits of pure beryllium could possibly be obtained if the Et_2Be or Me_2Be were isolated in the pure state for electrolysis studies. Addition of the dialkyl beryllium compounds to $BeCl_2$-ether solutions in a 1:1 mole ratio should then produce the beryllium Grignard.

The $BeCl_2$ etherate solution was also reacted with EtLi to produce Et_2Be:

$$2EtLi + BeCl_2 \cdot Et_2O \rightarrow \underline{2LiCl} + Et_2Be + Et_2O$$

The LiCl was removed by filtration and more $BeCl_2$ etherate solution was added to the Et_2Be solution (in a 1:1 mole ratio) to form EtBeCl, theoretically.

However, since the EtLi was obtainable commercially in only benzene or other hydrocarbons, the resulting solution was a very poor conductor. Only a thin, black film was obtained after an hour of electrolysis at 1 mA/cm^2.

3.1.2 BERYLLIUM CHLORIDE ETHERATE SOLUTION

For comparative purposes, the $BeCl_2.2Et_2O$ ether solution was electrolyzed to observe the nature of the deposit. At a current density of 6 mA/cm^2 (copper cathode, beryllium anode, 6.4 mm spacing), a cell voltage of 40V was required. After three hours the voltage required had risen to 74V. Gassing was observed at both the cathode and anode. The Be deposit obtained was in the form of a thin, black, powdery film which could easily be wiped off.

3.2 ELECTRODEPOSITION OF ALUMINUM ALLOYS

3.2.1 BERYLLIUM-ALUMINUM ALLOYS

3.2.1.1 Beryllium Chloride Etherate-Lithium Aluminum Hydride Solution

In an attempt to improve the electrodeposit from the BeCl etherate solution, $LiAlH_4$-ether solution (1.7M) was added in increasing amounts. Any precipitate which formed was removed by filtration and the resulting solution electrolyzed at 6 to 10 mA/cm^2. ($BeCl_2$:$LiAlH_4$ mole ratio $\simeq$ 0.76 to 30:1.0).

At low $BeCl_2$:$LiAlH_4$ mole ratios (<2:1) much precipitation occurred, the resulting solutions were poor conductors, and very poor electrodeposits were obtained from these solutions. However, as the ratio increased, good aluminum electrodeposits were obtained. When the $BeCl_2$:$LiAlH_4$ mole ratio exceeded about 5:1, beryllium was codeposited with aluminum to form a Be-Al alloy. At higher ratios, the amount of beryllium in the electrodeposit became greater. Precipitation of LiCl did not occur when the mole ratio of $BeCl_2$ to $LiAlH_4$ exceeded 30:1. All of the Be-Al alloys were brittle or powdery and possessed essentially no structural strength.

3.2.1.2 Beryllium Chloride Etherate-Aluminum Plating Solution

As unsatisfactory electrodeposits were obtained from the $BeCl_2$-$LiAlH_4$ ether solutions, the $LiAlH_4$ was added in the form of the standard aluminum plating solution (APS). The composition of the solution was 3.46M $AlCl_3$ and 0.35M $LiAlH_4$ in ether. When the APS was added to the $BeCl_2$ etherate solution in increasing amounts ($BeCl_2$:$LiAlH_4$ mole ratio= 1.5 to 30:1.0), no precipitation occurred as in the case of the $LiAlH_4$-ether solution. The resultant solutions were electrolyzed at 6 to 13 mA/cm^2 (copper cathodes and aluminum anodes).

In the case of the $BeCl_2$-$LiAlH_4$ electrodeposition tests, codeposition of beryllium with aluminum did not occur until the mole ratio of $BeCl_2$ to $LiAlH_4$ approached 5. In the case of the $BeCl_2$-APS electrodeposition tests, codeposition of beryllium did not occur until the mole ratio of $BeCl_2$ to $LiAlH_4$ reached almost 20. The results obtained with the $LiAlH_4$ in the form of the APS with $BeCl_2$ were much better than those obtained with the $LiAlH_4$-ether solution added alone to the

$BeCl_2$-ether solution. In the present case, however, a smooth, coherent Be-Al alloy deposit was obtained when the $LiAlH_4$ was added in the form of the APS with a $BeCl_2$ to $LiAlH_4$ mole ratio of about 20 to 25:1.0 ($[BeCl_2] \simeq 1.9M$). The electrodeposit in this case contained 2.7% Be and 97% Al. At lower ratios, mainly aluminum was deposited. At higher ratios, the deposit became powdery.

3.2.2 ZINC-ALUMINUM ALLOYS

As a result of hydrogen overvoltage, zinc can be readily electrodeposited from aqueous solutions of its salts. Sinc zinc halides are relatively soluble in ethyl ether, attempts were made to electrodeposit Zn-Al alloys from various plating baths prepared by mixing ethereal solutions with ether solutions of several aluminum salts.

3.2.2.1 Zinc Chloride

When a $ZnCl_2$-ether solution was added to an $AlCl_3$-ether solution and the resulting solution electrolyzed, a bright silvery deposit was obtained that contained only zinc. Even at low concentrations of $ZnCl_2$, only zinc was electrodeposited.

The next series of experiments was performed using the aluminum plating solution (3.4M $AlCl_3$, 0.38M $LiAlH_4$) instead of the $AlCl_3$-ether solution. A $ZnCl_2$-ether solution was added to the APS in increasing amounts ($ZnCl_2$: $LiAlH_4$ mole ratio = 1.00 to 2.00:1.00), and the resulting solutions were filtered and then electrolyzed at 6.8 mA/cm^2 (copper cathodes, aluminum anodes).

When the ethereal $ZnCl_2$ solution was added to the APS, a flocculent white precipitate was formed which darkened upon standing. When the precipitate was added to water, hydrogen was evolved leaving mossy zinc behind. This would indicate that the precipitate is ZnH_2 - formed probably by the following reaction : (6)

$$LiAlH_4 + 2ZnCl_2 \xrightarrow{Et_2O} LiCl + AlCl_3 + \underline{2ZnH}_2$$

Codeposition of any significant amounts of zinc with aluminum occurred over a very limited initial mole-ratio range of $ZnCl_2$ to $AlCl_3$. Traces of zinc in the electrodeposit were first noted at an initial mole ratio of $ZnCl_2$: $LiAlH_4$ of 1.22 to 1.25: 1.00 at a current density of 6 mA/cm^2. The presence of zinc in the deposit caused it to become somewhat brittle.

At an initial $ZnCl_2$ to $LiAlH_4$ mole ratio of about 1.33 to 1.43:1.00, fair amounts of zinc were present in the alloy deposit. The best deposit was obtained at an initial mole ratio of $ZnCl_2$:$LiAlH_4$ of 1.45 to 1.47:1.00. The deposit was silvery in appearance, hard, but very brittle, Unfortunately. The deposits obtained at higher current densities (10 to 15 mA/cm^2) appeared to become somewhat powdery relative to those obtained at lower current densities (4 to 6 mA/cm^2).

3.2.2.2 Zinc Iodide

When ZnI_2-ether solution was used instead of the $ZnCl_2$-ether solution with the APS, precipitation of ZnH_2 was considerably delayed, and the initial ZnI_2 to $LiAlH_4$ mole ratio had to be reduced to a value of 0.107:1.00 before aluminum was detected in the electrodeposit.

This would indicate a very low reduction potential for zinc under these conditions. The nature of the Zn-Al alloy electrodeposit using ZnI_2-ether solution with the APS was less satisfactory than that for the case of the $ZnCl_2$-ether solution with APS.

3.2.3 MAGNESIUM-ALUMINUM ALLOYS

Electrodeposition tests were carried out with ethyl magnesium bromide (EMB)-ether solution containing various amounts of $LiAlH_4$ in hopes that codeposition of aluminum with magnesium would occur. The $LiAlH_4$ was added in the form of $LiAlH_4$-ethyl ether solution to the EMB solution (3.1M, in ethyl ether). No satisfactory combination of $LiAlH_4$ with EMB was obtained. For mixtures where aluminum was found in the electrodeposit, the conductivity of the resulting solutions was found to be very poor ($LiAlH_4$: EMB mole ratio$\simeq$0.38 to 0.57:1.0). Mixtures which were fairly conductive ($LiAlH_4$: EMB mole ratio$\simeq$0.11 to 0.33:1.0) produced poor deposits which were powdery, brittle (or both), or stressed. The addition of $LiAlH_4$ to the EMB in the form of the aluminum plating solution resulted in precipitate formation.

3.3 ELECTRODEPOSITION STUDIES

To complement data obtained from the electrolyte scanning studies, a series of electrodeposition tests were conducted with the APS containing various additives. The aim of these studies was to observe whether hardening of the aluminum electrodeposit would take place with the addition of various amounts of different solvents and salts to the plating bath. To facilitate the testing, small test cells were

constructed from small, commercially available bottles. Figure 1 is a diagram of the test cell. The volume of solution used for each test was 50 to 60 cm^3. To define the plating area (6.05 cm^2), the upper portions of the electrodes were covered with heat-shrinkable TFE tubing. The glove box was employed for preparing the various solutions and for filling the test cells.

After the filled cells were removed from the glove box, they were placed in a holder so that 10 test cells could be run simultaneously (providing the power supply capability was not exceeded). The cells were then connected in series to a constant current supply and the total current density was adjusted to approximately 22 mA/cm^2. The usual electrolysis time was about 22 hours so that an average electrodeposit thickness of 0.28 mm to 0.38 mm (11 mils to 15 mils) was obtained. A cell containing only APS was included in each series of tests as a control. The cathodes were usually weighed before and after each run to determine the approximate current efficiency. After each run, the electrodeposits were also examined under the microscope for grain structure differences.

3.3.1 INERT ORGANIC SOLVENT ADDITIVES

High concentrations of xylene (20% by volume) caused no hardening of the electrodeposit when added to the APS but did cause an increase in smoothness. At high concentrations of isopropyl ether and n-butyl ether (about 30% by volume), fair hardening of the deposit was noted.

Reduction in current efficiency also was noted. Similar results were noted with bis (2-butoxyethyl) ether, but at only 15% by volume. Bis (2-methoxyethyl) ether was incompatible with the APS, forming a white precipitate.

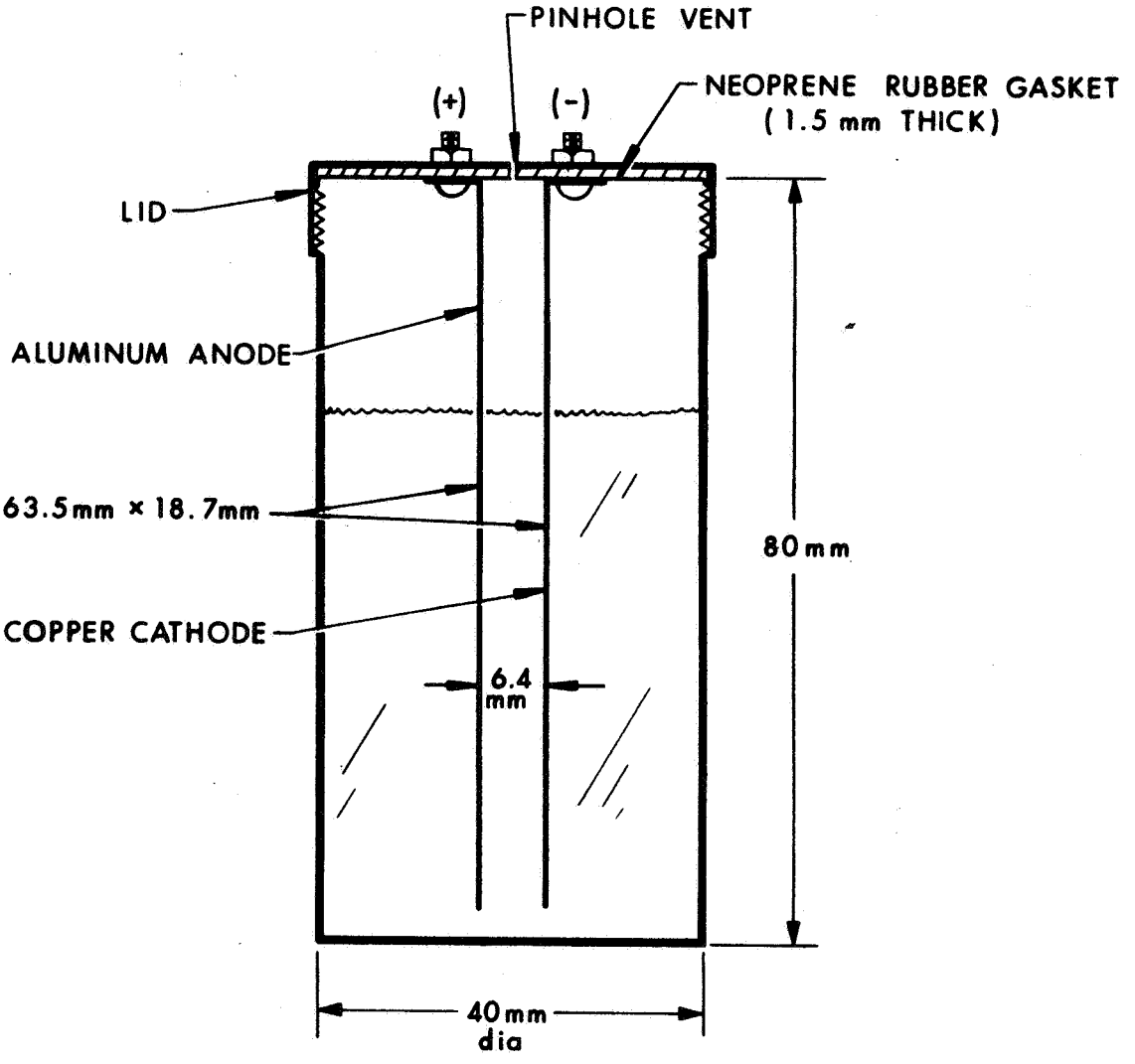

Figure 1. Plating Test Cell

3.3.2 INERT SALT ADDITIVES

A number of anhydrous inert salt additives were examined as possible additives to the APS. The salt additives which showed little or no effect upon the aluminum electrodeposit when added to the APS at a concentration of 0.1M were: potassium chloride, ammonium chloride, lithium chloride, lithium iodide, magnesium chloride, boron fluoride, aluminum isopropoxide, sodium acetate, potassium acetate, beryllium acetate, beryllium chloride, copper(II) chloride, copper(I) bromide, and copper(I) cyanide.

At a concentration of $BeCl_2$ of 1.3 to 1.9M in the APS, a slightly brittle but hardened Be-Al electrodeposit was obtained. The copper salts studied were apparently reduced by the hydride of the APS to copper metal sponge.

Salts which caused a marked deterioration (e.g., embrittlement) of the aluminum electrodeposit to occur when added to the APS at a concentration of 0.1M were: lithium perchlorate, magnesium perchlorate, potassium thiocyanate, ammonium thiocyanate, chromium(III) chloride, iron(III) chloride, and titanium(IV) chloride. Titanium was detected in the deposit from the APS containing 0.05M to 0.10M $TiCl_4$. The deposit exhibited increased resistance to attack by concentrated HCl over that of pure aluminum.

Salts which were insoluble in the APS after fifteen minutes of stirring were: disodium maleate, sodium formate, disodium hydrogen phosphate, potassium cyanide, lithium aluminate, manganese(II) chloride, manganese(II) bromide, cobalt(III) fluoride, and tin(IV) chloride (precipitate formation).

3.3.2.1 Acetylacetonate Salt Additives

A number of acetylacetonate salt compounds were investigated as possible hardening additives to the APS. The acetylacetonate compounds of the following elements were studied: cobalt, iron, magnesium, beryllium, aluminum, uranium, zirconium, nickel, chromium, manganese, copper, vanadium, molybdenum, and titanium. At concentration of 0.05M in the APS, all of the acetylacetonates, except for the case of titanyl acetylacetonate, caused a marked deterioration of the electrodeposit. In most cases, the deposit became brittle and crumbly, and peeled from the cathode. When the concentration was reduced to 0.025M, the deposits improved but were still unsatisfactory in the majority of the cases.

Only three of the acetylacetonates studied showed any promise as APS additives - uranyl acetylacetonate, chromium(III) acetylacetonate, and titanyl acetylacetonate. Extremely small concentrations of these additives were necessary to harden the electrodeposit (0.0074M, 0.0011M, and 0.04M, respectively - the lowest optimum additive concentrations encountered in the electrodeposition studies.) The optimum additive concentration ranges, in these cases, were also extremely narrow.

Of these three acetylacetonates, titanyl acetylacetonate gave the most satisfactory electrodeposit. Its optimum concentration range in the APS was the largest, also (0.025M to 0.040M). The electrodeposit in this case contained traces of titanium, which made it more resistant to attack by concentrated HCl than pure aluminum.

3.3.3 NITROGEN COORDINATIVE ADDITIVES

By changing the nature of the platable solution species, it is possible to change the nature of the electrodeposit. In the present case, it was desirable to modify the aluminum complex in solution in such a manner as to cause a hardening of the resulting aluminum electrodeposit. One possible way to modify the complex is by changing the solution characteristics. By changing the nature of the solvent (as in the case of the ether additives,) the characteristics of the solvent coordination with the complex are also changed.

To study the effects of nitrogen coordination upon the solution species in the APS and upon the resulting electrodeposit, various types of nitrogen-containing organic compounds were investigated as additives. The solutions were subjected to scanning tests as well as plating tests in the hopes of obtaining some type of correlation between the nature of the solution and its electrodeposit.

3.3.3.1 Amines

The following amine additives were studied as APS additives at concentrations of 0.05M to 0.30M: 2,4-dimethylaniline, phenylhydrazine hydrochloride, diphenylamine, tetraethyl ammonium chloride, 4-aminophenyl ether, hydrazine, and ethylenediamine.

Hydrazine and ethylenediamine could not be used as additives to the APS due to immediate precipitate formation upon addition, while hydrazine hydrobromide was insoluble in the APS. Tetraethylammonium chloride caused a considerable softening of the electrodeposit at a concentration

of 0.06M. Of all the amines studied as APS additives, only 4-aminophenyl ether gave satisfactory results (0.05M to 0.10M). The majority of the other amine additives caused embrittlement as well as hardening of the electrodeposit to occur.

3.3.3.2 Amides

Similar results were obtained with the amide compounds studied as APS additives as with the amine compounds. The amide additives which caused the electrodeposit to be brittle and peeled in the concentration range of 0.05M to 0.10M in the APS were acetamide, phenylacetamide, acetoacetanilide, and oxanilide. Reduction of the additive concentration did not improve the electrodeposit.

Some of the amide additives had little or no effect upon the electrodeposit at a concentration of 0.05M to 0.10M (e.g., dimethyl formamide, benzanilide, acetanilide, urea, and phenylurea), while others caused the electrodeposit to become somewhat hardened but fairly brittle (e.g., benzamide, p-toluamide, and p-aminoacetanilide). Only carbanilide, of all the amides studied, produced a satisfactory hardened, but not brittle, aluminum electrodeposit (at a concentration of 0.10M in the APS).

3.3.3.3 Nitriles

Since the use of aliphatic nitriles as APS additives resulted in non-metallic, black electrodeposits (even for the case of 0.13M heptanenitrile), the studies were mainly concerned with the aromatic nitriles. The aromatic nitriles studied which caused hardening without embrittlement, of the aluminum electrodeposit to occur at a concentration of 0.10M to

0.15M in the APS were: benzonitrile, p-tolunitrile, m-tolunitrile, and phthalonitrile. Of these, benzonitrile, m-tolunitrile, and p-tolunitrile appeared to give the best results as nitrile hardening additives. The optimum concentration range for the above three nitrile additives was 0.15M to 0.18M in the APS.

Nitriles which caused the electrodeposit to become hardened but somewhat brittle in the concentration range of 0.10M to 0.15M in the APS were: 1-naphthaleneacetonitrile, 2-naphthoylacetonitrile, terephthalonitrile, phenylacetonitrile, pentafluorobenzonitrile, and 4-biphenylcarbonitrile. However, reduction of the concentration of 4-biphenylcarbonitrile to 0.05M in the APS eliminated the brittleness of the electrodeposit.

3.3.3.4 Heterocyclic Compounds

Heterocyclic compounds are organic ring compounds in which a nitrogen atom has been substituted for a carbon atom. They may be thought of as cyclic amines. Small amounts of pyridine added to the APS at a concentration of 0.12M to 0.15M resulted in one of the hardest and strongest electrodeposits of aluminum. At higher concentrations ($>$0.23M), however, the deposit became quite brittle and weak.

The use of 2-bromopyridine and 2,2'-bipyridine as additives resulted in a severe deterioration of the electrodeposit at concentrations of 0.24M and 0.10M, respectively, in the APS. 3-Acetylpyridine reacted violently with APS, while morpholine formed a white precipitate with the APS. Quinoline and 8-quinolinol were found to be insoluble in the APS.

3.3.3.5 Nitro Compounds

The results of the use of aliphatic and aromatic nitro compounds as APS additives were not favorable. No metallic deposits were obtained in any of the cases. Addition of nitromethane to the APS resulted in gassing, heat generation, and a high-resistance solution (7). The addition of nitrobenzene to the APS caused a delayed reaction to occur, generating large amounts of gas suddenly through formation of a diazonium salt, probably (8).

Addition of a nitro-substituted benzonitrile to the APS produced results similar to those for nitrobenzene, even at a concentration as low as 0.031M. As a result of their reactivity with the APS, therefore, nitro compounds could not be used as additives.

3.3.4 OTHER COORDINATIVE ADDITIVES

3.3.4.1 Esters

Several organic and inorganic esters were examined as possible hardening additives to the APS. Only an insignificant amount of hardening was noted for the organic esters ethyl acetate and phenyl benzoate at concentrations of 0.10M to 0.20M in the APS. For the case of the inorganic ester, tri-n-butyl phosphate, the considerable hardening of the aluminum electrodeposit was accompanied by severe embrittlement at concentrations of 0.05M to 0.10M in the APS.

3.3.4.2 Organometallic Compounds

Concentrations of ferrocene of 0.1M to 0.2M in the APS caused considerable hardening of the electrodeposit without embrittlement. However, at somewhat higher concentrations (> 0.23M), the deposit became brittle. No iron was detected in the electrodeposit on a qualitative basis. The titanium counterpart of ferrocene, titanocene dichloride, caused a severe deterioration of the electrodeposit - even at a concentration of 0.02M.

3.4 SCALE-UP OF HARDENED-ALUMINUM FLAT-PLATE ELECTROFORMING - 5.1 x 15 CM SIZE

Of the several hundred aluminum test baths formulated in the electrodepositions studies, about fifteen solutions produced satisfactory, nonbrittle, hardened aluminum electrodeposits. Of these, eight test solutions were selected for scale-up to about 1.5 ℓ (from 0.05 ℓ), so that 5.1 x 15 cm flat-plate samples could be electroformed for physical property testing.

The experimental setup for the 5.1 x 15 cm flat-plate electroforming consisted of a large Pyrex tube (7.5 cm in diameter) as the solution container, and a large rubber stopper for the lid. The stopper contained electrical feed throughs, as support for the electrodes, and a small valve to relieve excess gas pressure. The aluminum anode was wrapped in TFE woven cloth (to contain the anode slime),

and was separated from the cathode by TFE spacers. This arrangement ensured rigidity and maintained a constant electrode separation. A magnetic stirrer was used to circulate the solution. A current density of 15-20 mA/cm^2 was used with copper cathodes and aluminum anodes.

The results of physical testing are presented in Table I. The physical properties of the regular aluminum electrodeposit from the APS (9) and the physical properties of the mixed-ether (anisole-ethyl ether) electrodeposit (10) are included for comparison.

3.4.1 BERYLLIUM CHLORIDE ADDITIVE

A low-melting bismuth alloy was used as the mandrel material for the Be-Al flat-plate electroforming, since the alloy would not adhere to stainless very readily and adhered too strongly to copper. After electrodeposition of the alloy, the mandrel was removed by melting, leaving the alloy electroform behind.

An electrode spacing of 13 mm was used, with a bath temperature of about $308^{o}K$. The heat generated during electrolysis was absorbed by the solution itself - no external source of cooling was employed.

The Be-Al plating solution which was formulated during the electrodeposition studies consisted of three volumes of $BeCl_2$ etherate and one volume of APS ($[BeCl_2] = 1.9M$).

TABLE I

PHYSICAL PROPERTIES OF SOME HARDENED ALUMINUM ELECTRODEPOSITS FROM APS* CONTAINING VARIOUS ADDITIVES

No.	Additive	Yield Strength** (MN/m^2)	Ultimate Strength (MN/m^2)	Percent Elongation (5.08 cm)	Knoop Hardness
1.	Beryllium chloride, 1.25M	---- ----	109 (15,800 psi) 112 (16,200)	0 0	54
2.	Titanyl acetylacetonate, 0.0398M	91.0 (13,200 psi) ***	93.2 (13,500 psi) 110 (16,000 psi)	2.5 1.0	56
3.	Carbanilide, 0.114M	103 (15,000 psi) 104 (15,100 psi)	118 (17,000 psi) 111 (16,100 psi)	5.0 1.5	45
4.	Bis (2-butoxyethyl) ether, 17% by vol.	114 (16,400 psi) 102 (14,600 psi)	130 (18,800 psi) 126 (18,100 psi)	3.0 8.0	64

TABLE I (Cont'd)

PHYSICAL PROPERTIES OF SOME HARDENED ALUMINUM ELECTRODEPOSITS FROM APS* CONTAINING VARIOUS ADDITIVES

No.	Additive	Yield Strength** (MN/m^2)	Ultimate Strength (MN/m^2)	Percent Elongation (5.08 cm)	Knoop Hardness
5.	Benzonitrile, 0.175M	113 (16,200 psi)	126 (18,200 psi)	2.0	56
		113 (16,300 psi)	134 (19,300 psi)	3.5	
6.	Ferrocene, 0.188M	126 (18,200 psi)	153 (21,600 psi)	10	70
		110 (15,900 psi)	144 (20,900 psi)	11	
7.	Oxydianiline, 0.0895	143 (20,500 psi)	152 (21,800 psi)	3.5	61
		149 (21,400 psi)	159 (22,900 psi)	2.0	
8.	Pyridine, 0.124M	200 (29,000 psi)	219 (31,700 psi)	2.5	88
		197 (28,600 psi)	226 (32,800 psi)	5.0	
9.	Mixed-ether bath (anisole:ethyl ether = 2:1, by vol.)	148 (21,400 psi)	177 (25,700 psi)	8-10	50-70
10.	None	62.8 (9,100 psi)	76.2 (13,800 psi)	17	---

* APS = Aluminum Plating Solution (3.73M $AlCl_3$, 0.33M $LiAlH_4$)

** 0.2% offset

***Malfunction of test instrument

When a 5.1 x 15 cm sample was electroformed from this solution, it appeared to be quite brittle, however. The $BeCl_2$ concentration was then reduced to the point where a satisfactory electrodeposit was obtained. At this point, the $BeCl_2$ etherate to APS volume ratio was 1:1. ($[BeCl_2]$ = 1.3M).

The 5.1 x 15 cm flat-plate sample from the APS containing 1.3M $BeCl_2$ possessed an average ultimate strength of 110 MN/m^2 (16,000 psi). No yield strength was obtained, as the sample ruptured before 0.2% offset was obtained. The sample had a microhardness of 54 KHN and a beryllium content of 0.04%.

3.4.2 TITANYL ACETYLACETONATE

The first time the APS containing titanyl acetylacetonate was electrolyzed, a brown scum formed on the walls of the test cell and on the anode TFE bagging. This did not occur during subsequent runs, so that some additional electrochemical reaction other than metal deposition must take place initially for only a short period of time.

Some difficulty was encountered in the preliminary electroforming runs using 0.03M to 0.04M $TiO(AcAc)_2$ in the APS. A large electrode spacing of 25 mm was used at first to minimize tapering tendencies and to allow the solution to circulate more readily between the electrodes during stirring to minimize any concentration grandients. However, at this separation, a large IR drop resulted in the solution causing it to become quite warm ($\sim 323^{\circ}K$), which resulted in a considerable amount of sponge formation after a period of time. At the increased solution temperature, the anodic dissolution of aluminum was reduced as evidenced by considerable gassing at the anode during electrolysis.

After removal of sponge, a thin flat-plate was obtained for physical testing. It possessed a yield strength (0.2% offset) of 91.0 MN/m^2 (13,200 psi), an average ultimate strength of 105 MN/m^2 (14,800 psi), and a hardness of 56 KHN. The results of the spectrographic analysis of an electrodeposit from the APS containing TiO(AcAc)$_2$ are presented in Table II. The analysis for a typical soft aluminum electrodeposit is included for comparison. As can be seen, only a very small amount of titanium was present (0.10%), with copper being the largest minor constituent (0.16%).

The above figures are not to be taken as final, since the electrodeposit which was tested was not representative of the APS-TiO(AcAc)$_2$ system. It was subsequently discovered that control of the solution temperature was important for obtaining a satisfactory hardened deposit without sponge formation.

A small portion of the same solution which produced a spongy deposit in the large test cell (1.5 l volume) was electrolyzed in the small test cell (0.050 l volume) used for the electrodeposition study. In this case, the electrode spacing was only 6.4 mm, and a thick, coherent, and hardened plate was now obtained. When no external cooling was used, the electrode spacing played a major role - along with electrode polarization, solution conductivity, and the current density - in determining the resultant equilibrium solution temperature. The solution temperature in the case of the smallest cell was much less than that for the large test cell, and the electrodeposit was considerable improved as a result.

TABLE II

SPECTROGRAPHIC ANALYSIS OF REGULAR AND HARDENED ALUMINUM ELECTRODEPOSITS

Element	Hardened Al APS+0.04M $TiO(AcAc)_2$	Regular Al (APS)
Copper	0.16%	0.00018%
Iron	0.09%	0.002%
Magnesium	Nil	0.0012%
Silicon	0.06%	0.008%
Zinc	0.07%	Nil
Manganese	0.01%	0.011%
Titanium	0.10%	Nil
Chromium	Nil	Nil
Nickel	Nil	Nil
Aluminum	Rem. = 99.51%	Rem. = 99.96%

Several test plates which were subsequently electoformed in the large test cell, at a reduced electrode spacing of 6.5 mm instead of the previous 25 mm, now produced coherent, thicker deposits without accompanying sponge formation. (See Section 3.5 test results for 10 x 15 cm electroformed flat-plates).

3.4.3 CARBANILIDE ADDITIVE

The carbanilide additive was the only amide additive tested which produced a satisfactory hardened aluminum deposit when added to the APS. The APS containing 0.114M carbanilide (26 mm electrode spacing) produced an electrodeposit (5.1 x 15 cm) with an average yeild strength of 103 MN/m^2 (15,000 psi), an average ultimate strength of 114 MN/m^2 (16,500 psi), and a hardness of 45 KNH. The APS-carbanilide bath produced the softest electrodeposit of all of the hardened aluminum plating baths formulated.

3.4.4 BIS (2-BUTOXYETHYL) ETHER ADDITIVE

The physical properties of the electrodeposit from the APS containing the aliphatic ether additive, bis (2-butoxyethyl) ether, were not as great as those of the deposit from the APS containing the aromatic ether additive anisole. The 5.1 x 15 cm flat-plate electroform from the APS containing 17% by volume of bis (2-butoxyethyl) ether, possessed an average yield strength (0.2% offset) of 108 MN/m^2 (15,700 psi), an average ultimate strength of 128 MN/m^2 (18,600 psi), and a hardness of 64 KHN.

Since a 25 mm electrode spacing was used, the solution became fairly warm (IR heating). At a lower solution temperature (smaller electrode spacing), somewhat better results would have been obtained.

3.4.5 BENZONITRILE ADDITIVE

The electrodeposit from the APS containing the aromatic nitrile, benzonitrile (0.175M), was slightly stronger than that from the APS containing 17% bis (2-butoxyethyl) ether. The benzonitrile-APS system produced an electrodeposit with an average yield strength (0.2% offset) of 113 MN/m^2 (16,400 psi), an average ultimate strength of 130 MN/m^2 (18,900 psi), and a hardness of 56 KHN.

3.4.6 FERROCENE ADDITIVE

The electrodeposit from the APS containing 0.188M ferrocene (25 mm electrode spacing) had an average yield strength (0.2% offset) of 116 MN/m^2 (16,800 psi), an average ultimate strength of 148 MN/m^2 (21,500 psi), and a hardness of 70 KHN. This deposit was the second hardest aluminum deposit encountered in the electroforming scale-up studies.

3.4.7 OXYDIANILINE (4-AMINOPHENYL ETHER) ADDITIVE

The electrodeposit from the APS containing 0.089M oxydianiline (25 mm electrode spacing) was the second strongest deposit encountered in the series. It had an average yield strength (0.2% offset) of 146 MN/m^2 and a hardness of 61 KHN.

3.4.8 PYRIDINE ADDITIVE

The addition of pyridine to the APS at a concentration of 0.125M resulted in a bath which produced the hardest and strongest aluminum of all the various baths examined during the flat-plate (5.1 x 15 cm) electroforming studies (13 mm electrode spacing). It had an average yield strength (0.2% offset) of 198 MN/m^2 (28,700 psi), an average ultimate strength of 222 MN/m^2 (32,200 psi), and a hardness of 88 KHN. This deposit was far superior in every way than the best previous deposit obtained - that from the mixed-ether (anisole-ethyl ether) bath.

3.5 10 x 15 CM FLAT-PLATE AND HOLLOW-CORE ELECTROFORMS

Of the eight hardened aluminum plating solutions studies in the preparation of 5.1 x 15 cm flat-plates (for physical property measurements), three were chosen for further scale-up to prepare 10 x 15 cm flat-plates and hollow-core samples. The three were the APS-$TiO(AcAc)_2$, APS-$BeCl_2$, and APS-pyridine baths. The plating apparatus which was used is shown in Figure 2. This apparatus had several advantages over the plating apparatus used for the 5.1 x 15 cm size samples in that there were provisions for filtering, circulation, and cooling the solution. Thus, one could more easily control the temperature of the bath, and thereby, the grain size of the deposit.

3.5.1 TITANYL ACETYLACETONATE ADDITIVE

Two hollow-core samples (10 cm x 15 cm) and two flat-plate samples (12.5 x 15 cm) were electroformed from the APS containing 0.03-0.04M of the $TiO(AcAc)_2$ additive.

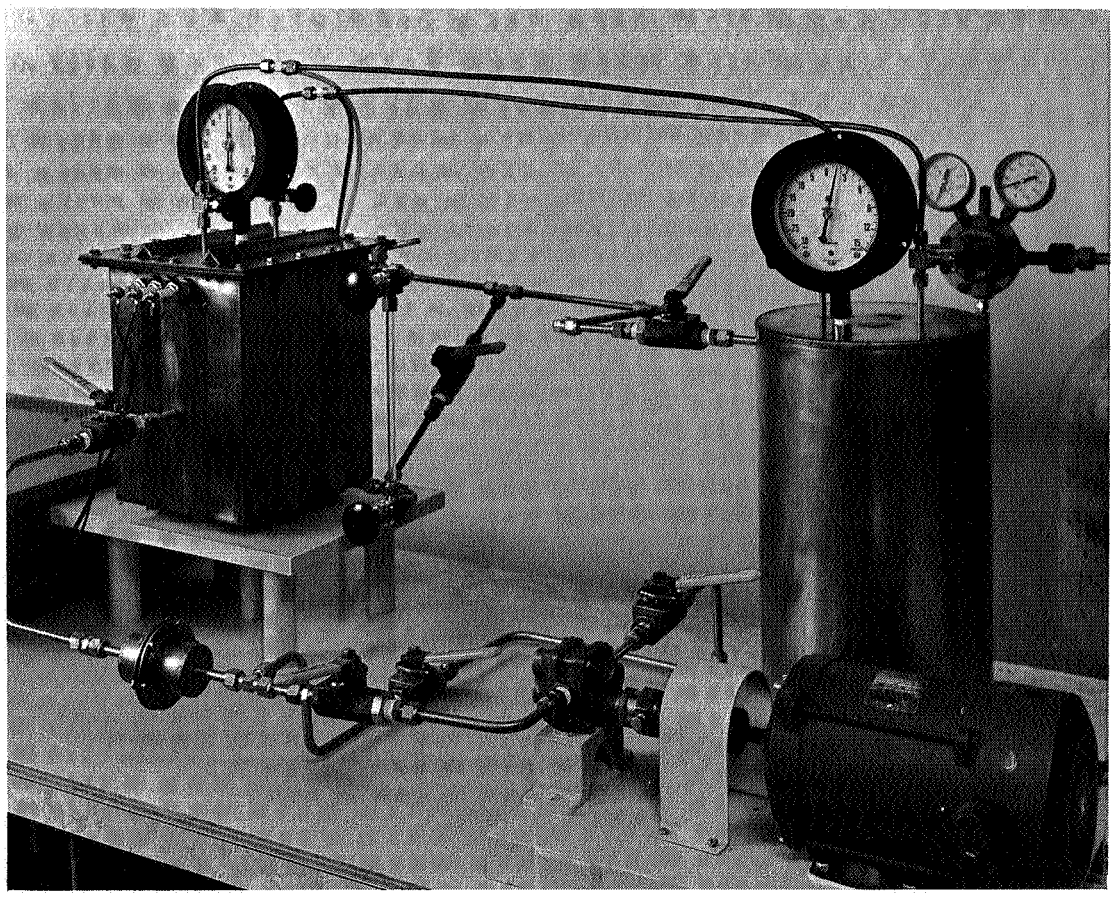

96715

Figure 2. Aluminum Electroplating Apparatus for 10 x 15 cm Electroforms

The first samples were found to be slightly rough where the solution entered the tank and impinged on the mandrel during circulation. However, this was eliminated through the use of a deflection plate mounted on the mandrel. A current density of approximately 16 mA/cm^2 produced an electrodeposit with an unusually fine grain size when the temperature was maintained between 293°K and 298°K during the plating process.

A sample for physical testing was obtained from a wide edge of the hollow-core sample. The sample possessed an average yield strength (0.2% offset) of 99 MN/m^2 (14,400 psi), an average ultimate strength of 120 MN/m^2 (17,400 psi), and a hardness of 74.5 KHN. This sample is more representative of the APS-$TiO(AcAc)_2$ bath than the sample of Section 3.4.2.

The results of a spectrographic analysis of the above samples are given in Table III. The large amount of copper formerly present was absent, and the iron and zinc contents were considerably reduced. While a slight reduction in titanium content occurred (from 0.10% to 0.07%), an increase in chromium and nickel content also occurred. The overall purity of the aluminum deposit increased from 99.51% to 99.81%.

A photomicrograph of the above deposit is presented in Figure 3. A photomicrograph of an aluminum electrodeposit from the mixed ether (anisole-ethyl ether) bath is included for comparison (Figure 4).

3.5.2 BERYLLIUM CHLORIDE ADDITIVE

Two hollow-core samples (10 x 14 cm) and two flat-plate samples (12.5 x 15 cm) were electroformed from the APS containing 1.25M $BeCl_2$ etherate (50% by volume). The mandrels were fabricated out of a low-melting tin-bismuth alloy which was easily removed afterwards by melting.

TABLE III

SPECTROGRAPHIC ANALYSIS OF HOLLOW-CORE ELECTRODEPOSIT FROM APS CONTAINING 0.03M $TiO(AcAc)_2$

Element	Content
Copper	Nil
Iron	0.02%
Magnesium	Nil
Silicon	0.05%
Zinc	0.03%
Manganese	0.01%
Titanium	0.07%
Chromium	0.01%
Nickel	0.001%
Aluminum	Rem. $\simeq$ 99.81%

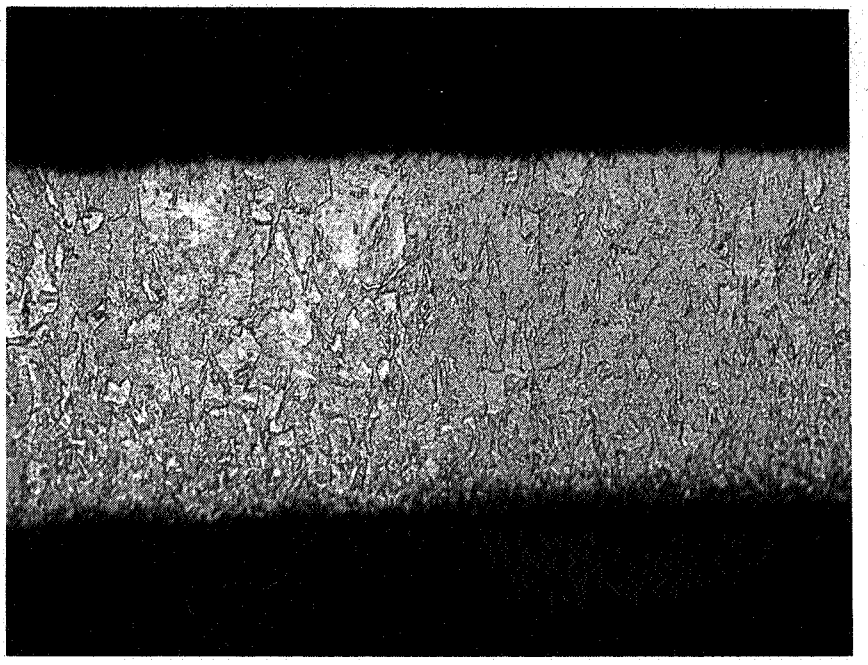

Figure 3. Aluminum Deposit from APS Containing 0.03M $TiO(AcAc)_2$ (Keller Etch, 250X)

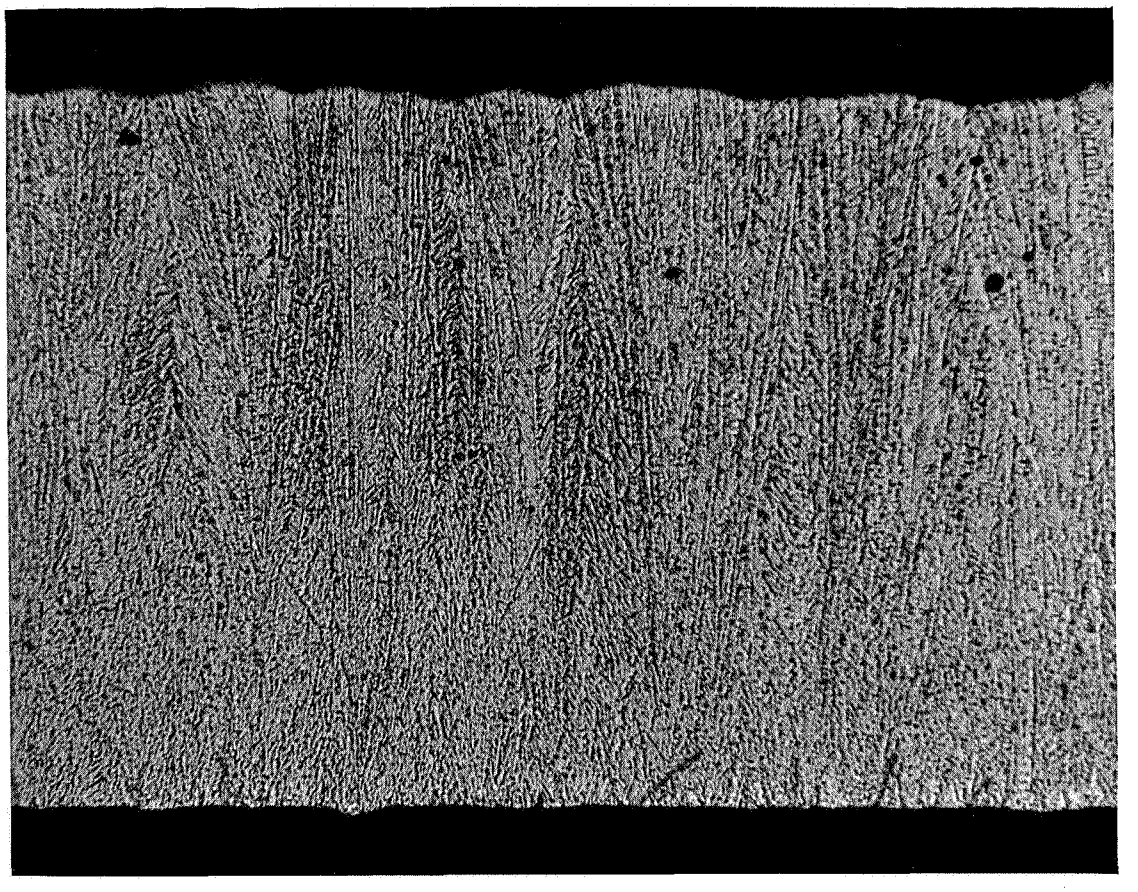

Figure 4. Aluminum Electrodeposit from Mixed Ether Bath (Keller Etch, 250X)

At a current density of 16 mA/cm^2 and a solution temperature of 293° to 298°K, an electrodeposit was obtained which had a rough texture and loosely-packed crystal arrangement. A photomicrograph of the deposit (Figure 5) showed some voids.

The flat-plate sample possessed an average yield strength (0.2% offset) of 84 MN/m^2 (12,200 psi), an average ultimate strength of 102 MN/m^2 (14,800 psi), and a hardness of 62.5 KHN. Relative to the 5.1 x 15 cm size flat-plate (Table I), the elongation and hardness of the sample had increased - from 0 to 4% and 54 KHN to 62.5 KHN, respectively. The ultimate strength did not change substantially.

The results of a spectrographic analysis of the flat-plate sample (12.5 x 15 cm) are presented in Table IV. The beryllium content of the 5.1 x 15 cm flat-plate was 0.04% (Section 3.4.1), but for the case of the large flat-plate, it was nil. This most likely is a result of the lower solution temperature during the plating process for the latter case.

3.5.3 PYRIDINE ADDITIVE

Two hollow-core samples (10 cm x 15 cm) and two flat-plate samples (13 cm x 15 cm) were electroformed from the APS containing 0.098M of the pyridine additive at a solution temperature of 295°K and 14mA/cm^2 current density. The first flat-plate that was electroformed was very hard but stressed enough to cause the deposit to pull away from the mandrel, resulting in a somewhat deformed plate. Addition of a small amount of $LiAlH_4$ (an increase of 0.02M) alleviated this problem.

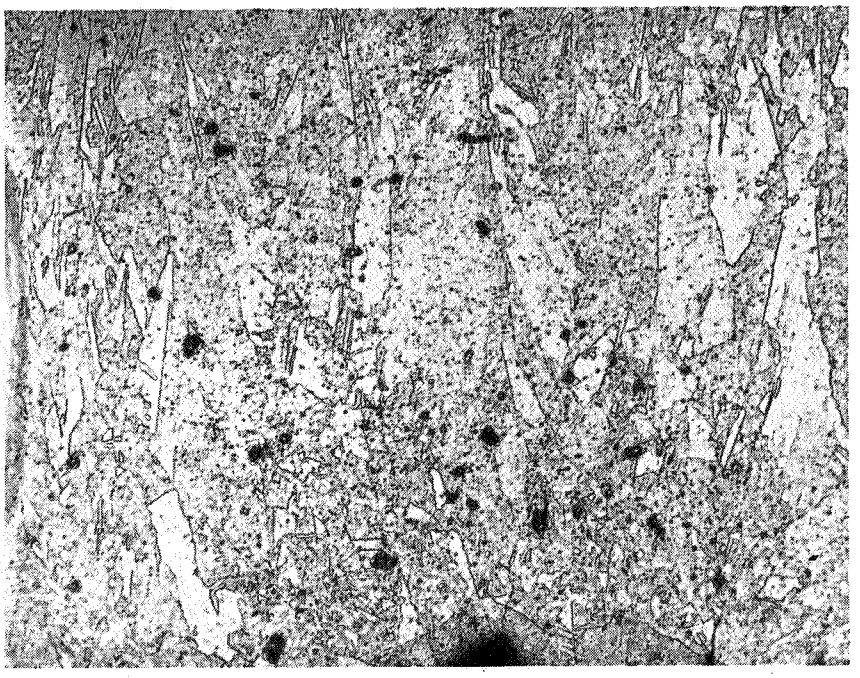

005322

Figure 5. Aluminum Deposit from APS Containing 1.25M $BeCl_2$ (Keller Etch, 250X)

TABLE IV

SPECTROGRAPHIC ANALYSIS OF FLAT-PLATE (12.5 x 15 CM) ELECTRODEPOSIT FROM APS CONTAINING 1.25M $BeCl_2$

Element	Content
Copper	Nil
Iron	0.01%
Magnesium	Nil
Silicon	0.03%
Zinc	0.03%
Manganese	0.01%
Titanium	0.02%
Chromium	Nil
Beryllium	Nil
Aluminum	Rem. = 99.90%

A photomicrograph of the resultant flat-plate aluminum electrodeposit is presented in Figure 6. The grain size was exceedingly small.

The flat-plate sample was found to have an average yield strength (0.2% offset) of 203 MN/m^2 (29,400 psi), an average ultimate strength of 240 MN/m^2 (34,700 psi), and a hardness of 95.0 KHN. The results in the present case were somewhat better than that for the case of the 5.1 x 15 cm flat-plate (Section 3.4.8). A spectrographic analysis of the flat-plate sample (Table V) showed the aluminum to be 99.90% pure.

3.6 ELECTROLYTE SCANNING STUDIES

A large number of test aluminum plating baths were subjected to electrochemical examination at the molecular level using a voltammetric scanning technique employing a triangular waveform. Mixed-solvent systems and mixed-salt systems were studied with this technique. The objective of this study was to screen candidate aluminum-alloy and/or hardened aluminum baths which would produce electrodeposits with considerably improved physical properties over those from the regular APS. The results of this study are presented in the Appendix.

3.7 CONCLUSIONS

3.7.1 ADDITIVES TO ALUMINUM PLATING SOLUTIONS

As a result of tests to date, it appears that there are several types of inorganic and organic compounds that can be used as additives to the APS to harden the aluminum electrodeposit. Each hardening additive

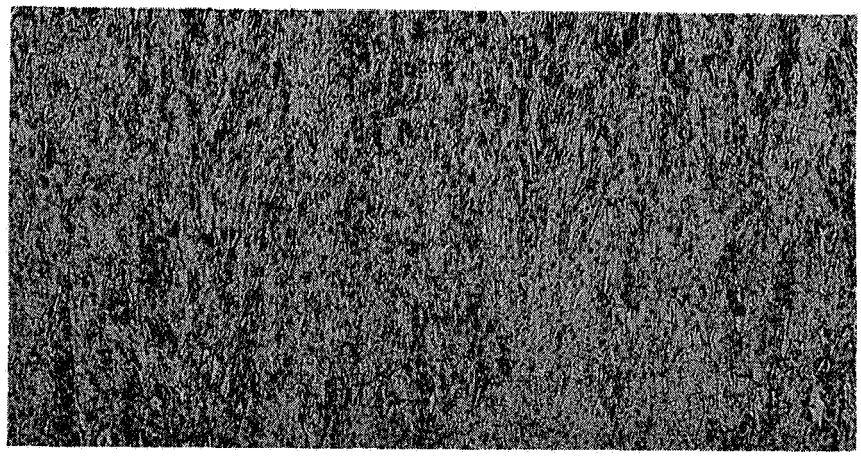

Figure 6. Aluminum Deposit from APS Containing 0.098M Pyridine (Keller Etch, 250X)

TABLE V

SPECTROGRAPHIC ANALYSIS OF ALUMINUM FLAT-PLATE (12.5 x 15 CM) ELECTRODEPOSIT FROM APS CONTAINING 0.098M PYRIDINE

Element	Content
Copper	Nil
Iron	0.02%
Magnesium	Nil
Silicon	0.04%
Zinc	0.03%
Manganese	Nil
Titanium	0.01%
Chromium	Nil
Beryllium	Nil
Aluminum	Rem. = 99.90%

appeared to have somewhat narrow, optimum concentration range in the APS for effective hardening. Below this range, only a slight hardening occurred; above this range, the deposit tended to become brittle and weak.

A much lower concentration of the nitrogen-coordination additives (e.g., nitriles, heterocyclics, amides and amines) were required, relative to the ether (oxygen-coordination) additives for comparable (or better) hardening. The optimum-hardening concentration range was approximately 0.080-0.12M for the nitrogen-coordination additives, while 1-2M for the ether additives.

However, because of the narrow concentration range for optimum hardening, the addition of nitrogen-coordination additives to the APS required more precision than in the case of the ether additives. Of all the inorganic compound additive studies, only several of the acetylacetonates were effective hardening agents. The titanyl acetylacetonate additive required the lowest concentration of all the additives examined (0.03-0.04M) for a satisfactory hardened aluminum deposit.

The nature of the coordination with the aluminum complex of the APS is slightly different for each of the various hardening additives. The degree of coordination in the case of the organic additives is affected by the availability of the free electron pair(s) of the coordinative nitrogen or oxygen of the additive compound. In the case of the inorganic salt additives, the aluminum solution complex is substantially modified, in many instances.

3.7.2 HARDENED-ALUMINUM FLAT-PLATE ELECTROFORMS

The eight hardened-aluminum test baths which were scaled up in volume from 0.05 ℓ to 1.5 ℓ produced 5.1 x 15 cm electroforms which varied in

average ultimate strength from 105 MN/m^2 (14,800 psi) to as high as 240 MN/m^2 (34,700 psi) and which varied in hardness from 45 KHN to 95 KHN. The pyridine additive produced both the strongest and hardest aluminum deposit all the additives tested. The deposit in this case was far superior in every way than the deposit from the mixed-ether bath, which is approximately 3M in anisole. The oyxdianiline additive produced a deposit which was comparable to the latter deposit - but at a much reduced additive concentration (0.09M).

The harder and stronger aluminum electrodeposit were characterized by a very fine grain size, which was generally obtained when the solution temperature was maintained between 288°K and 298°K during electrolysis. At too low a solution temperature (e.g., 273°K), salt precipitation from solution could occur. If the solution temperature became too great (e.g., 333°K), on the other hand, the grain size of the electrodeposit usually increased, with a subsequent reduction in strength. Temperature control was most important for the APS-$TiO(AcAc)_2$ system. At a solution temperature of 295°K, a very satisfactory hardened electrodeposit resulted; at a solution temperature of 323°K, however, excessive sponge formation was observed.

Equally satisfactory results were obtained at current densities ranging from 11-22 mA/cm^2. At 22 mA/cm^2, for example, the aluminum was deposited at approximately 0.025 mm/hr (1 mil/hr).

REFERENCES

1. H. Gilman and F. Schulze, J. Amer. Chem. Soc. 49, 2904 (1927)
2. W. Schlenk and W. Schlenk, Jr. Ber. 62, 920 (1929)
3. H. Gilman and R. E. Fothergill J. Amer. Chem. Soc. 51, 3149 (1929)
4. G. B. Wood and A. Brenner, J. Electrochem. Soc. 104, 29 (1957)
5. H. C. Kawecki, Thesis, Massachusetts Institute of Technology, (1934)
6. G. D. Barbaras, C. Dillard, A. E. Finholt, T. Wartik, K. E. Wilzbach, and H. I. Schlesinger, J. Amer. Chem. Soc. 73, 4585 (1951)
7. R. F. Nystrom, J. Amer. Chem. Soc. 77, 2544 (1955)
8. R. F. Nystrom and W. G. Brown, J. Amer. Chem. Soc. 70, 3737 (1948)
9. K. Lui, Private communication
10. K. Lui, R. Guidotti, and M. Klein, "Research and Development of Magnesium/Aluminum Electroforming Process for Solar Concentrators," Final Report, NASA Contract NAS-1-6218, NASA Report CR-66427, p. 70.

APPENDIX A

ELECTROLYTE SCANNING STUDIES

A.1 EXPERIMENTAL

A commercially available function generator with a frequency range of 0.0015 Hz to 1 MHz was used to supply the triangular waveform. The function generator had a short circuit output capability of $\pm$ 100 mA and an output capability of up to 32V p-p into a 50-ohm load. The generator could also supply square waves, sine waves, and ramp functions with the same frequency range as the triangular waveform, and with similar output capability. Figure 1 A is a schematic of the scanning apparatus used in the earlier studies. In the later studies, the emmitter-follower output stage (Q_1) was replaced by a power supply which was modulated by the input waveform.

The power supply was capable of being modulated over a large frequency range (from dc up to over 1 kHz) with an output capability of up to 60V at 500 mA. However, in the present study, the maximum potential applied to the cell was only 5V, which gave quite satisfactory results. At much higher applied voltages ($\gtrsim$ 10V), noticeable solution decomposition began to occur (i.e., organic reduction processes). An x-y recorder was used to record the data.

All of the electrolyte scanning experiments were conducted in the glove box to minimize contamination of the test solutions. The test cell contained all-platinum electrode system. The counter electrode (anode)

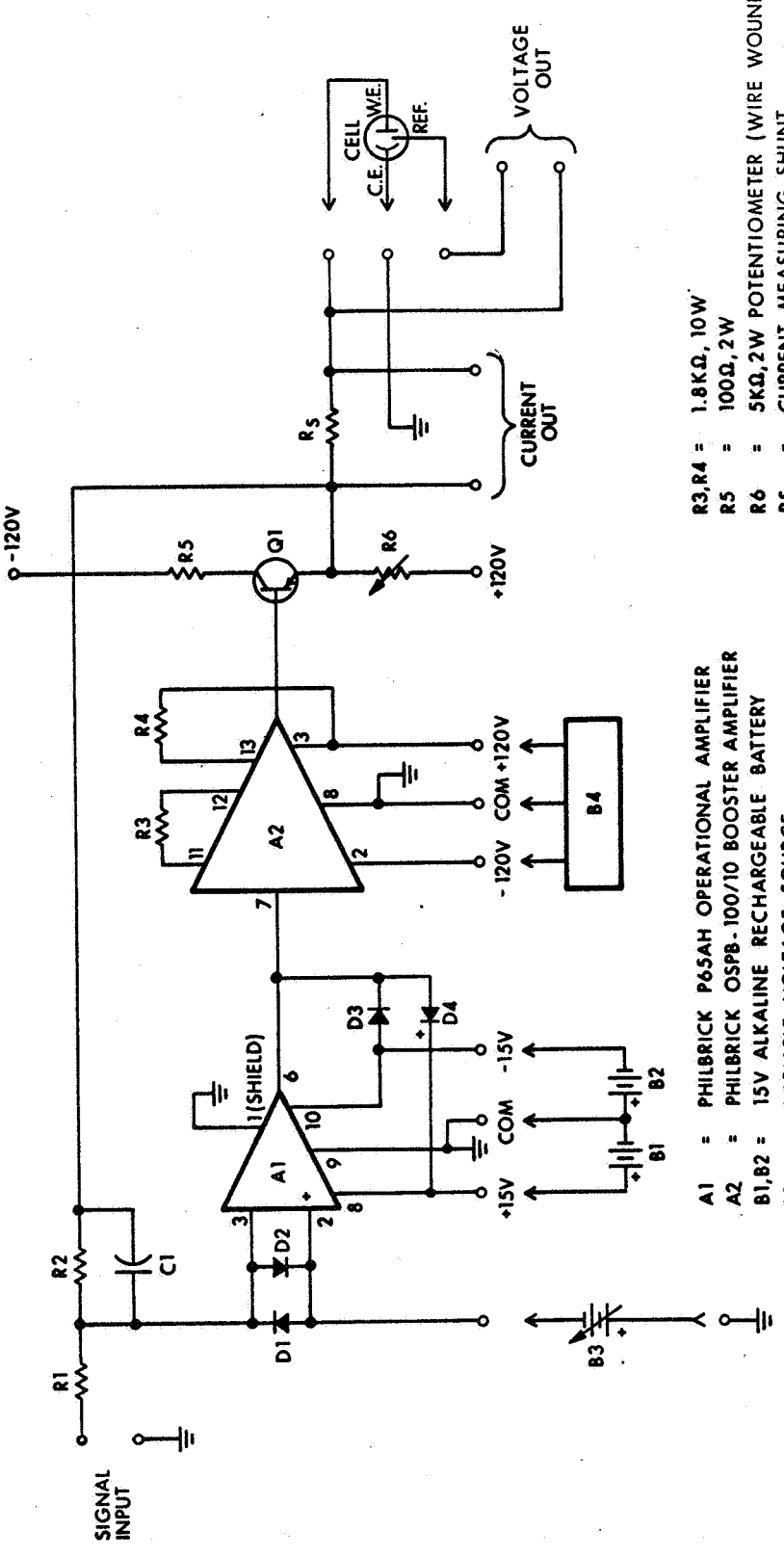

Figure 1A. Schematic of Electrolyte Scanning Apparatus

73629075

was a coiled sheet of platinum gauze. The working electrode (cathode) consisted of a square plate of 0.25 mm platinum (about 2.8 cm^2 in area) which was spot-welded to a platinum lead. In the latter portion of the studies, the platinum-square working electrode was replaced by a platinum wire electrode (0.069 cm^2 area). The much smaller platinum microelectrode appeared to give somewhat sharper incisions at the reduction potential measured by the use of derivative polarography (dV/dt-V) plots. The quasi-reference electrode was a platinum wire positioned so that the tip was less than 1 mm from the working electrode. The electrodes were contained in a cylindrical glass cell with a tight-fitting TFE cover with provisions for the platinum leads to the electrodes. The leads to the reference and working electrodes were enclosed within capillary tubing with TFE caps at the ends immersed in the test solution.

Since the studies were conducted using an x-y recorder to record the various data, a frequency of 0.05 Hz was chosen as to be compatible with the recorder pen response. The same potential range was scanned for each solution under test - 0 to 5V (1 V/sec). All the data were obtained from single sweep measurements, by triggering the function generator for only one cycle, so as to avoid large changes in cell characteristics which could occur during a continuous sweep process (e.g., excessive electrode polarization).

It was found that if the working electrode was not cleaned after each scan in which aluminum was deposited, the subsequent scan was not accurate. When successive scans were run on the same solution, the originally sharp incisions became quite weak and rounded, and sometimes disappeared altogether. However, if a clean working electrode surface was used for each scan, this did not occur, although the measured

reduction potentials were not exactly the same for each run on an individual test solution. The experimental error was relatively higher in the present study (5 to 10% in many cases) - especially in the measurement of the low-valued reduction potentials. Regardless of the experimental error in this case, the results obtained were still quantitative enough for the desired purpose of distinguishing the nature of the electrochemical solution processes.

A.2 DERIVATIVE POLAROGRAPHY

In addition to voltage-current (V-I) and voltage-time (V-t) curves, voltage-derivative functions (dV/dt-t and dV/dt-V) also were recorded of the test solutions using the triangular waveform. Figure 2A shows the curves obtained during a resistive load, the V-I curve is a straight line, while the V-t curve maintains the waveform of the input signal, except that it is slightly reduced in amplitude. The dV/dt-t and the dV/dt-V curves exhibit some rounding but, in theory, should be perfectly square. Figure 3A shows the circuitry used to obtain the derivative curves.

In conventional polarography involving a small concentration of a reducible species in a supporting electrolyte, the derivative voltage-time curve (dV/dt-t) exhibits a sharp incision at the point where reduction occurs (i.e., reduction potential). By correlation with the voltage-time curve, the potential at this point can be determined.

However, by use of a dV/dt-V plot, only a single sweep is required. The position of the incision (or its distance from the potential axis)

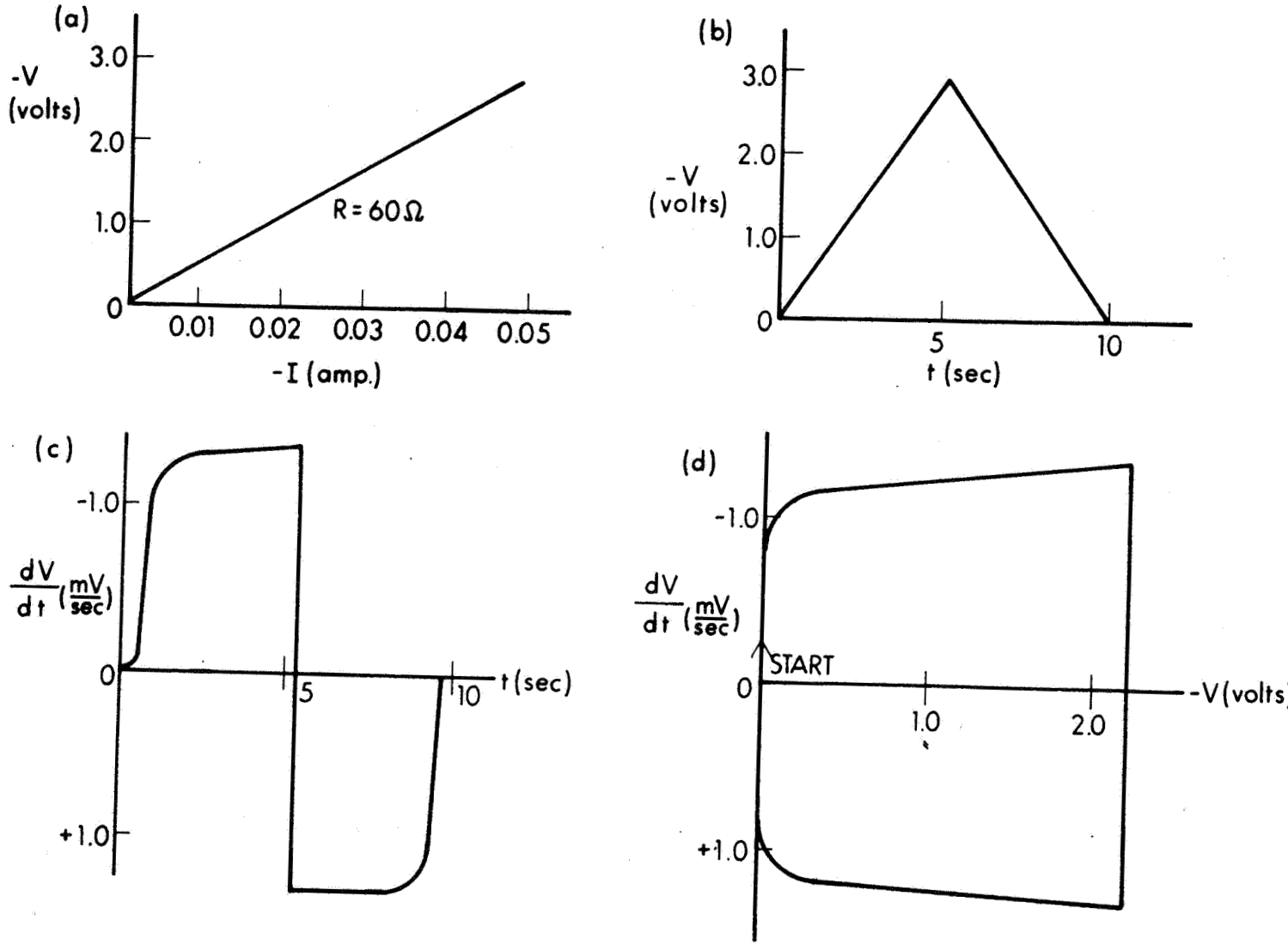

Figure 2A. Single Sweep Data for Resistive Load Using Triangular Waveform

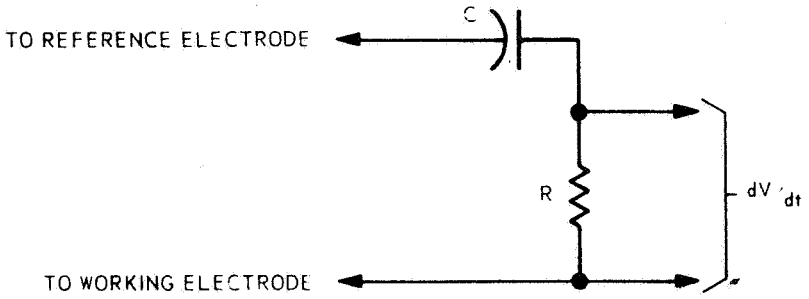

(a) $dV_{dt} - t$

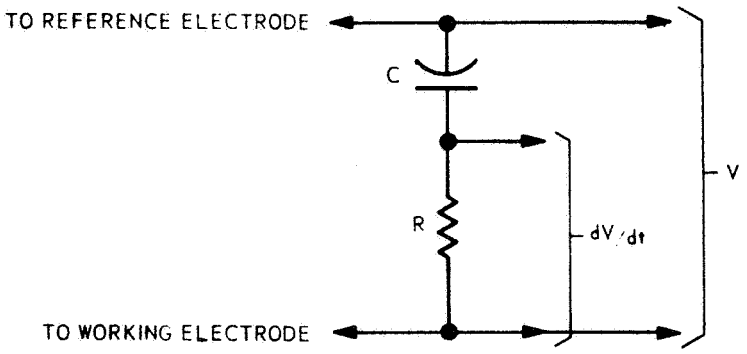

(b) $dV_{dt} - V$

C = 10 μF

R = 1KΩ

Figure 3A. Circuit for Obtaining Derivative Curves

gives a measure of the corresponding concentration. For a reversible reduction, the cathodic and anodic incisions appear at the same potential.

A large number of test solutions that were used in the electrodeposition studies were scanned using the triangular waveform. The voltage derivative (dV/dt-V) curves for many of these solutions are present in the Appendix. The "used" solutions are those that were previously electrolyzed for 20-22 hours at 20 mA/cm^2 (0.05 l solution volume) in the electrodeposition studies. The "new" solutions were not previously electrolyzed. All solutions were scanned at the same sweep rate of 1V/sec to a maximum potential of 5V (0.05Hz). The majority of the data obtained was for the case of the used solutions. Usually, the solutions were scanned immediately after the conclusion of the electrodeposition tests.

A.2.1 Aluminum Plating Solution

Several scanning experiments were conducted with the APS alone to determine what effects extended periods of electrolysis and exposure to the atmosphere would have upon the voltage derivative curves.

Only one strong incision was observed in the case of the new APS - at -0.25V (upper portion of curve). (See Figure 4A(a)). As only one incision was observed, it can be assigned to the electrodeposition of aluminum. Voltage derivative curves of $AlCl_3$-ether solutions obtained as the $LiAlH_4$ content was increased (from 0.02M to 0.30M) exhibited the incision at (or very near) -0.25V. This would indicate a fair degree of reversibility for the aluminum electrodeposition process. Indeed, anodic dissolution of aluminum during electrolysis of the APS has

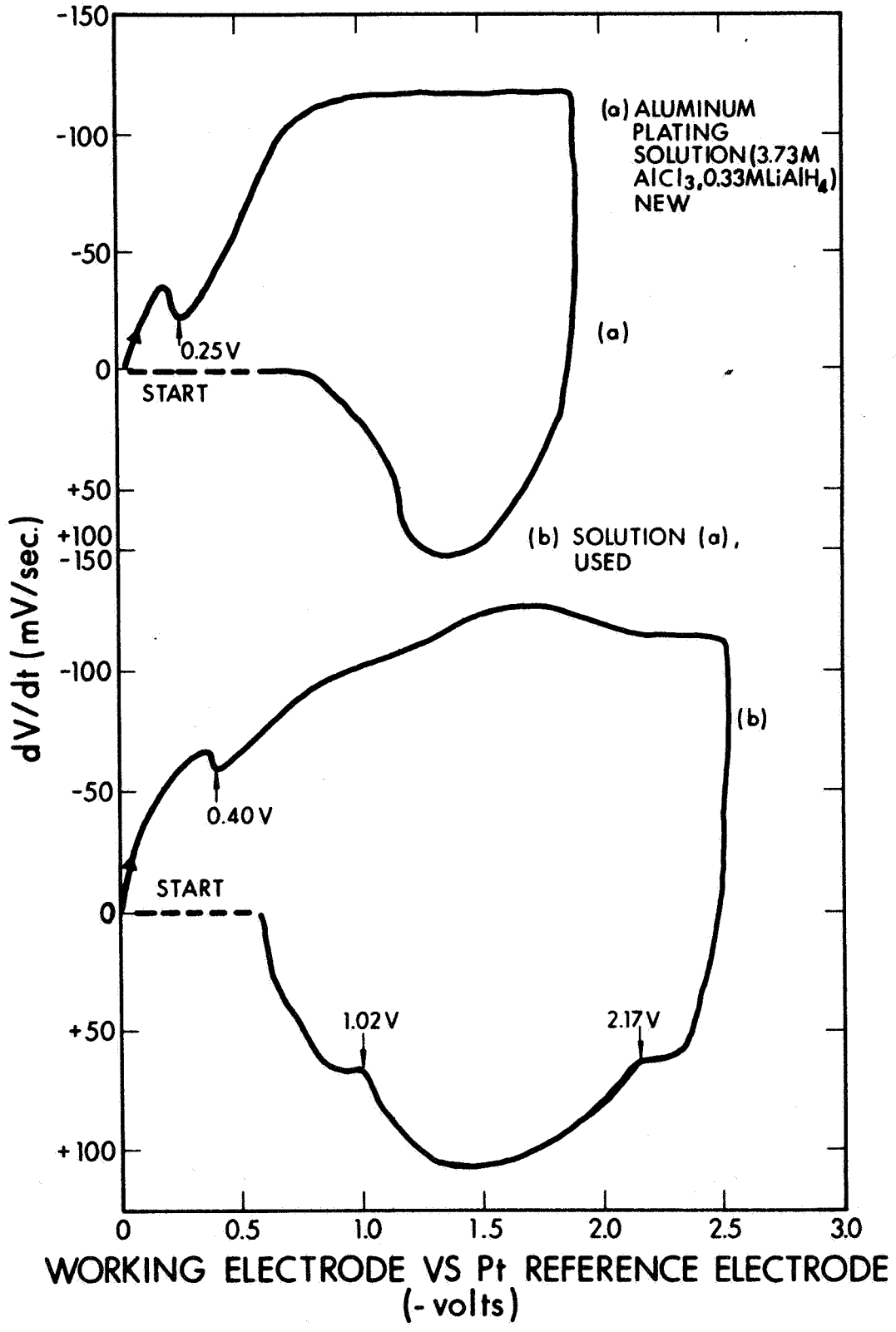

Figure 4A. Voltage Derivative Curves for Regular APS

been found to take place at almost 100% current efficiency.

After the APS had been electrolyzed for 22-24 hours at 22 mA/cm^2, the peak at -0.25V (upper part of curve) was shifted to a much higher potential (-0.40V), and the conductivity of the solution was reduced. In addition, several new peaks were observed in the bottom portion of the curve in the -2.12V to -2.17V range and in the -1.02V to -1.0V range. (Figure 4A(b). The curve still exhibited about 0.5V of residual polarization as in the case of the new APS.

Upon deterioration of the electrolyzed solution by exposure to the atmosphere air for a period of time (40 minutes), the peak near -0.40V was still present (-0.46V) but now had become considerable broader and much weaker in intensity. The peak at -2.1V no longer was present, and the strong peak at -1.0V had been replaced by two weak peaks at -1.1V and -1.2V. (Figure 4 A(c)). Also, the polarization after each scan had dropped to almost zero. Thus, by use of the voltage derivative curves, one can monitor the plating characteristics of the APS, and thereby, determine whether or not the APS has deteriorated.

A.2.2 Inert Organic Solvent Additives

In general, in the case of the inert organic solvent additives, the first sharp, strong peak observed can be attributed to the aluminum electrodeposition process. For a completely reversible process, the value of the peak obtained on the voltage-increasing (upper) portion of the triangular sweep (upper part of curve) should be very nearly the same as that obtained during the voltage-decreasing (lower) portion

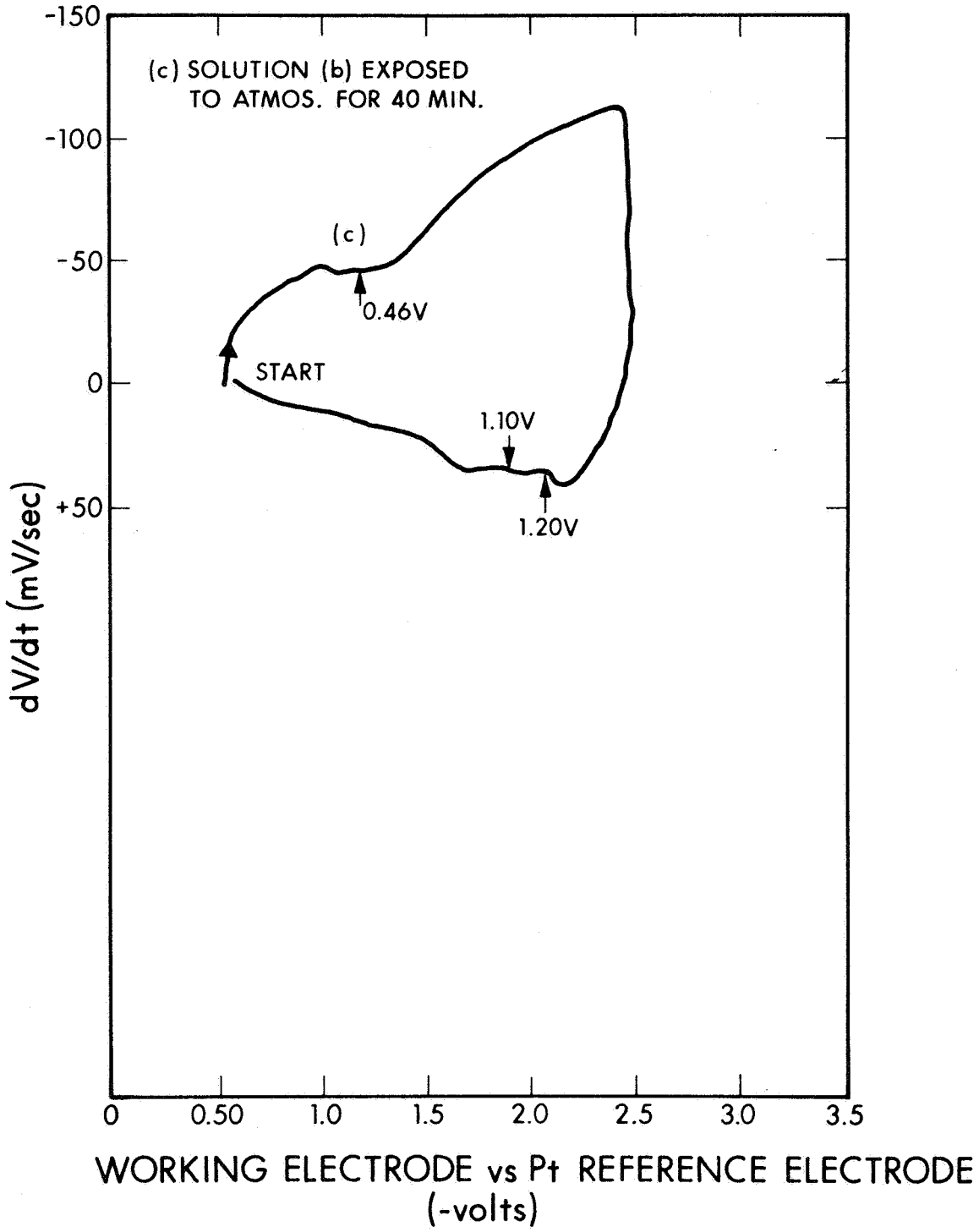

Figure 4A. Voltage Derivative Curves for Regular APS (contd)

of the curve. In the case of xylene (17% by volume), two sets of peaks were obtained (Figure 5A(a)). The set due to aluminum reduction occurred at -0.25V on the upper portion of the curve, and at -0.23V on the lower portion. The remaining peaks were due to some organic reduction process (-1.30V (upper) and -1.85V (lower)). In the case of the APS containing isopropyl ether (29% dilution), an additional peak was observed in the range where aluminum deposition occurs (Figure 5A(b)). During electrolysis, therefore, one would expect a reduction in the cathodic current efficiency as a result. This was found to be true. Some additional electrochemical solution process must be occurring simultaneously with the electrodeposition of aluminum.

Similar results were noted for the APS diluted with 17% bis (2-butoxyethyl) ether (Figure 5A(c)). In this case, the aluminum reduction potential was shifted slightly to more negative values (-0.36V).

The organic reduction process became more pronounced in the case of the APS containing n-butyl ether than for the case of isopropyl ether, bis (2-butoxyethyl) ether, or xylene. A large reduction in the cathodic current efficiency occurred when the dilution with n-butyl ether was increased to 29%.

A.2.3 Nitro Compounds

Very poor non-metallic (or only partially metallic) electrodeposits were obtained when nitro compounds were used as APS additives. In the case of the APS containing nitromethane (0.881M), a thin salt crust covered the cathode after electrolysis. None of the peaks observed could definately be assigned to the aluminum electrodeposition process, in agreement with the experimental results (Figures 6A(a) and 6A(b)).

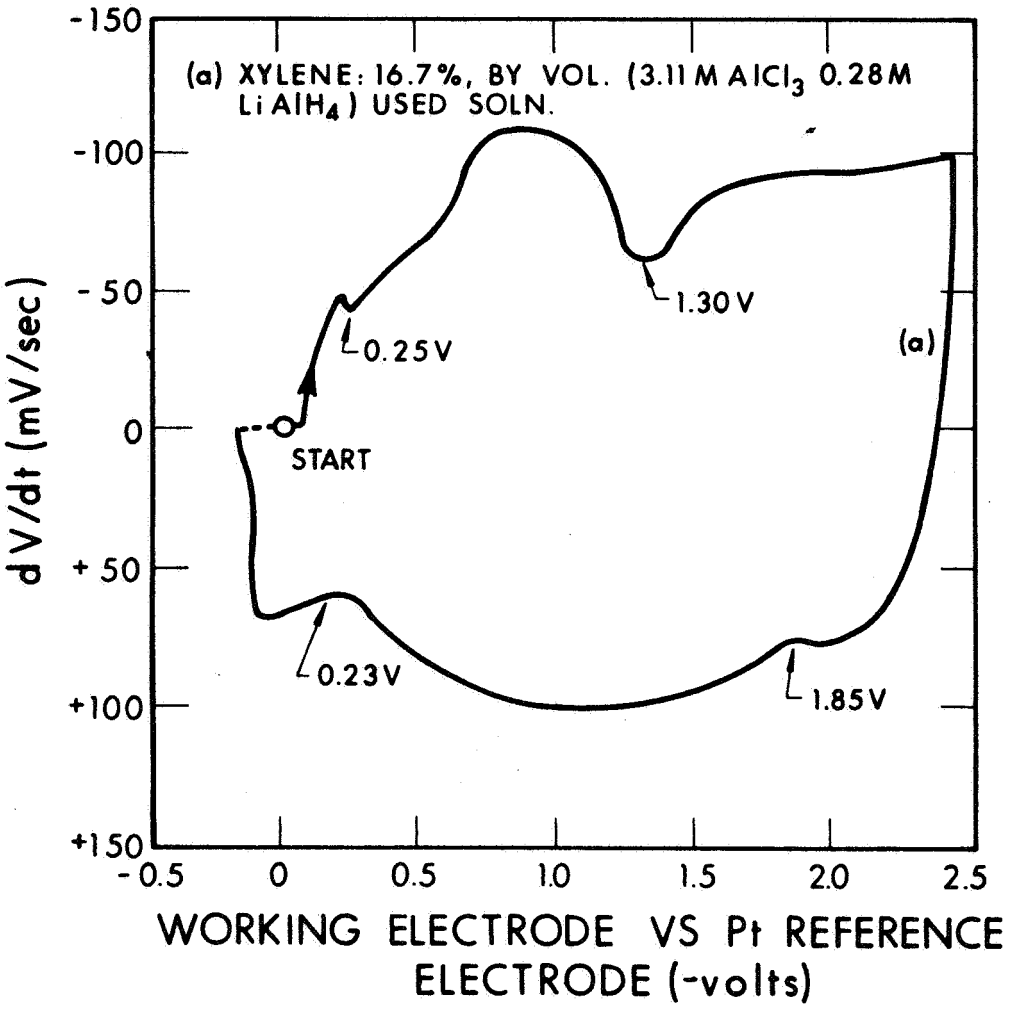

Figure 5A. Voltage Derivative Curves for APS Containing Inert Organic Solvent Additives

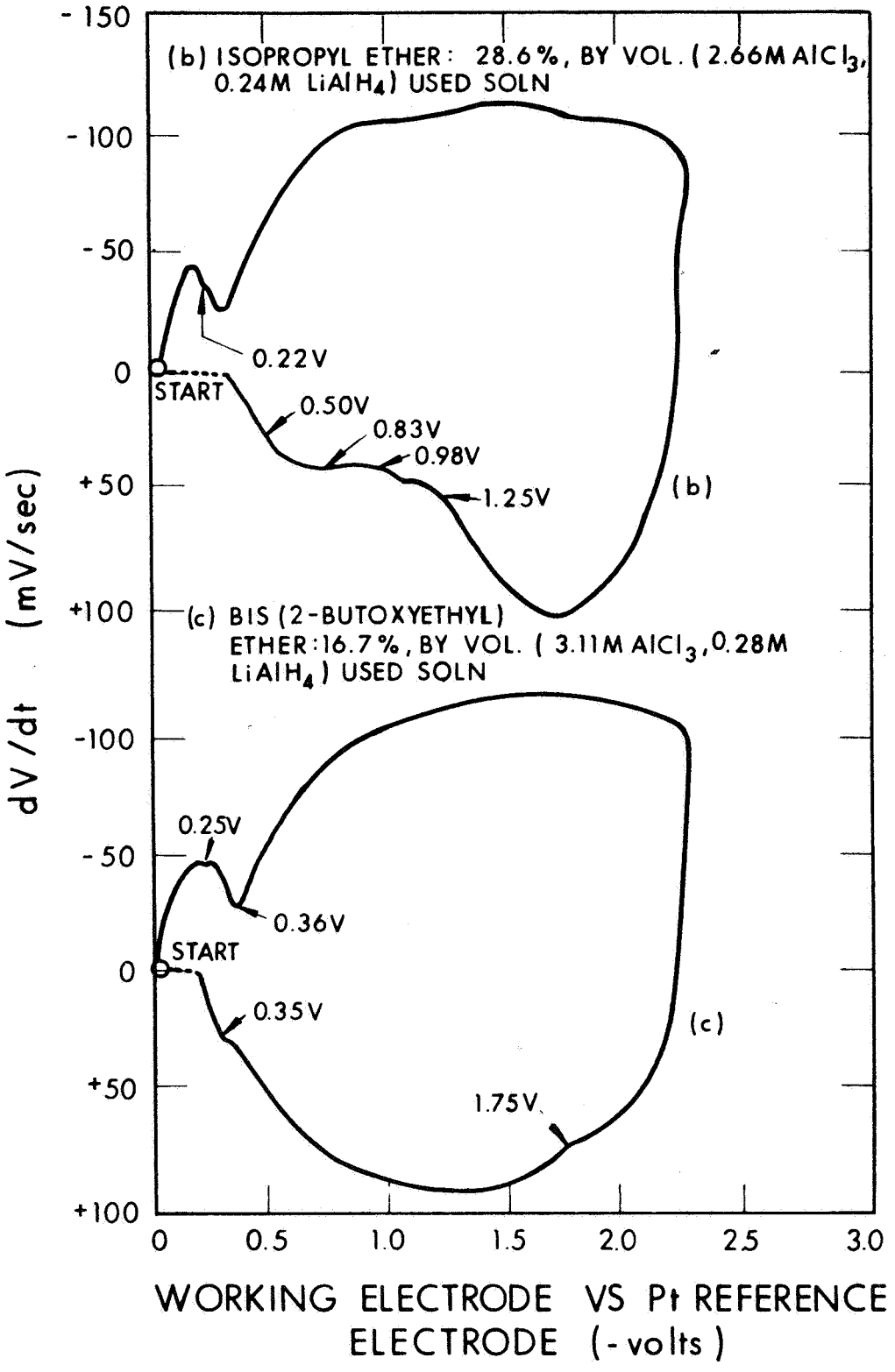

Figure 5A. Voltage Derivative Curves for APS Containing Inert Organic Solvent Additives (contd)

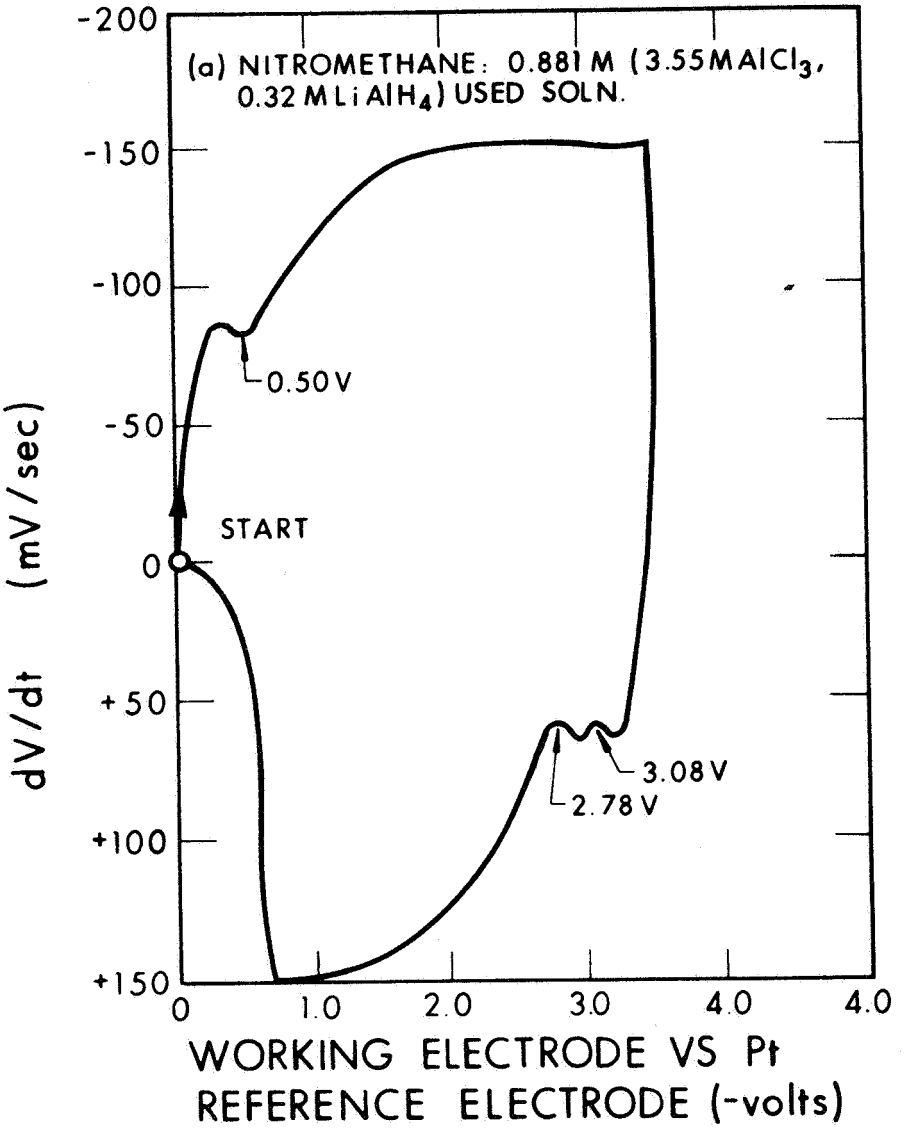

Figure 6A. Voltage Derivative Curves for APS Containing Nitro Compound Additives

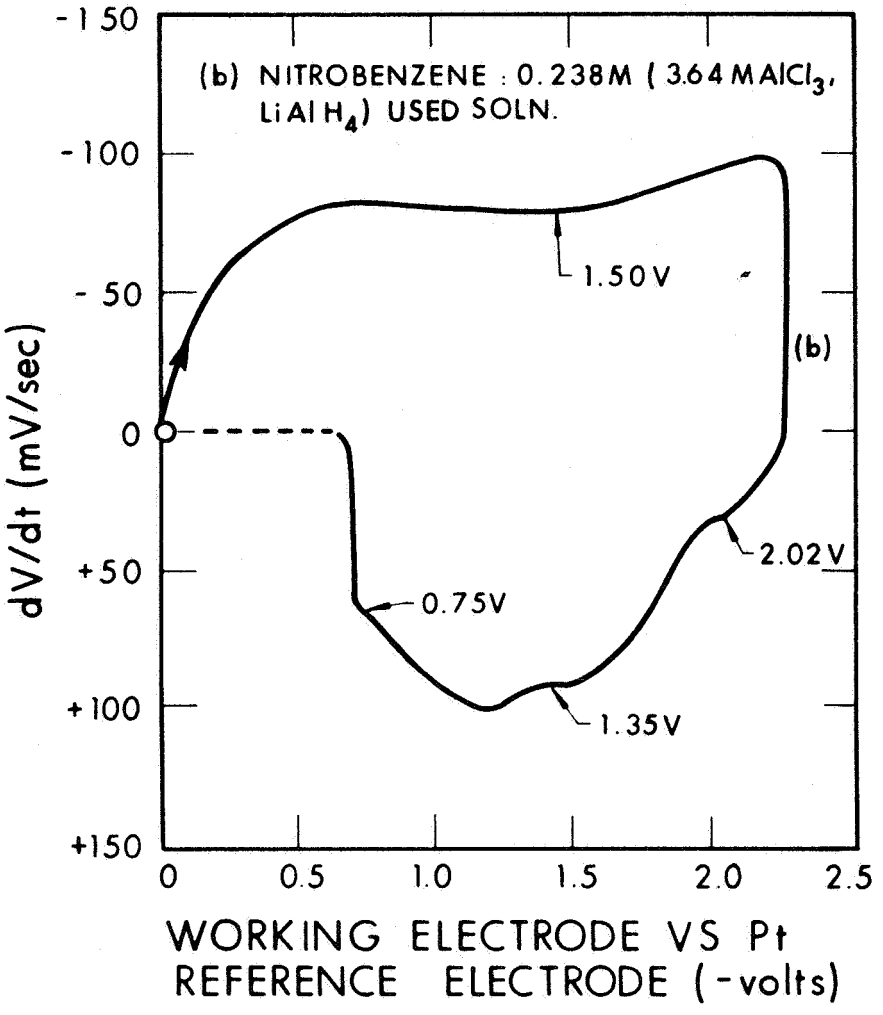

Figure 6A. Voltage Derivative Curves for APS Containing Nitro Compound Additives (contd)

A.2.4 Inert Salt Additives

The aluminum reduction potential was shifted toward a more positive value in the case of many of the halides additives (KCl, NH_4Cl, LiCl, LiBr, and $MgCl_2$ (Figures 7A(a)-7A(e)).

In the case of the acetate additives to the APS (NaAc, KAc, and $BeAc_2$), a strong additional peak was observed after the aluminum peak in the range of -0.9V to -1.5V (upper part of curve). The residual voltage was relatively large for the case of $BeAc_2$ (-0.8V), but negligible for KAc and NaAc (Figures 7A(f)-7A(h)).

An additional peak was observed in the potential range of aluminum electrodeposition in the case of the thiocyanate salt additives (NH_4SCN and KSCN). The residual voltage was large also (-0.5V to -0.7V). The nature of the resultant deposit (partially metallic, crumbly, flaky) corroborates the scanning data (Figures 7A(i)-7A(k)). The thiocyanate anion apparently interacts strongly with the aluminum solution complex to prevent the electrodeposition of pure aluminum.

The derivative curves for the APS containing the perchlorate salt additives ($Mg(ClO_4)_2$ and $LiClO_4$) differed from the curve for the APS alone, mainly in the additional peaks noted on the lower portion of the curve (Figures 7A(l) and 7A(m)). However, the resultant electrodeposits were quite poor, being dark, lamellar, and very crumbly.

In the case of the APS containing $BeCl_2$ (0.12M), and additional strong peak was observed near -2.40V (Figure 7A(n)). However, no beryllium was detected in the deposit at this concentration, so that the peak cannot be assigned to a beryllium reduction process.

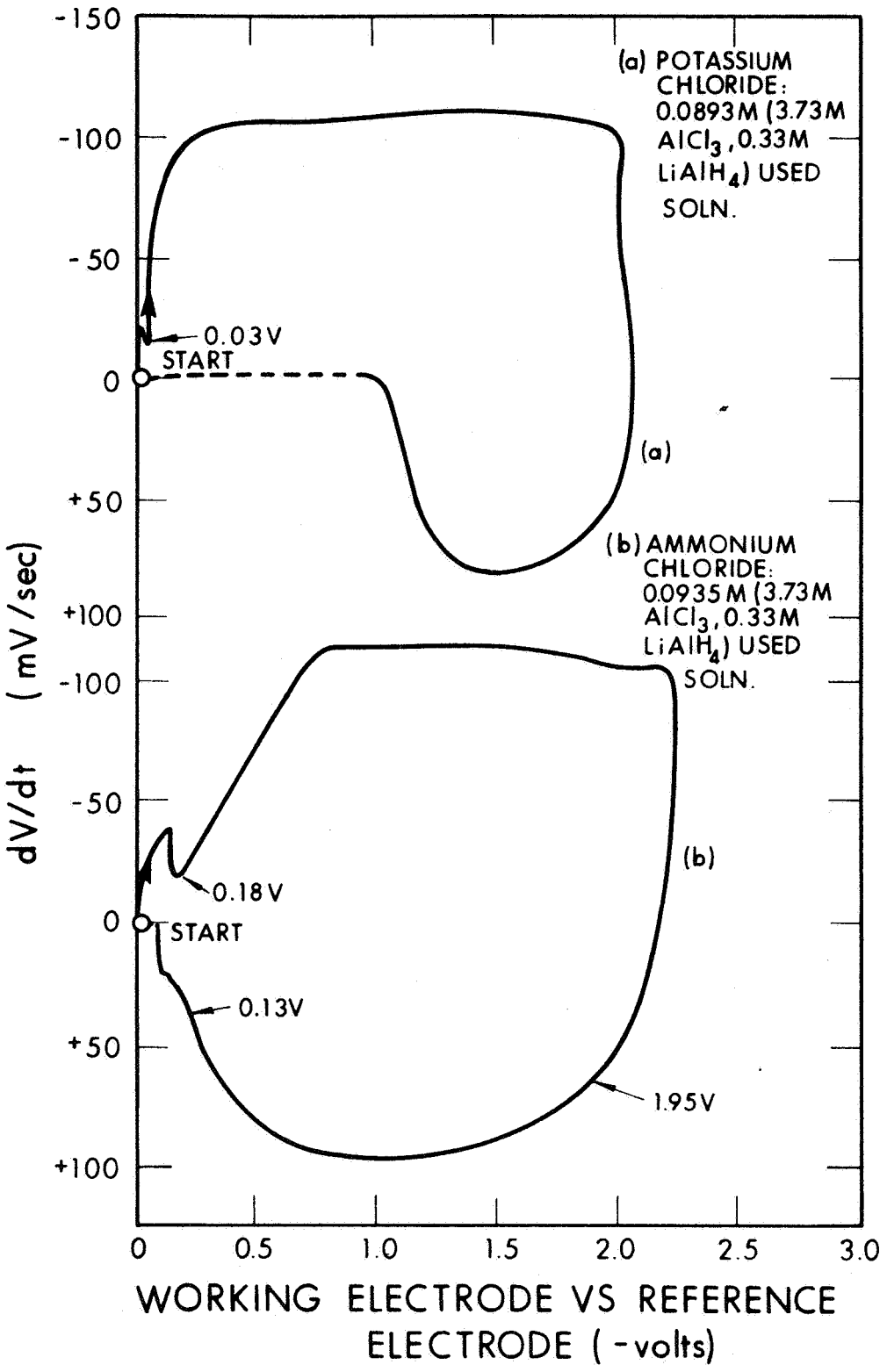

Figure 7A. Voltage Derivative Curves for APS Containing Inert Salt Additives

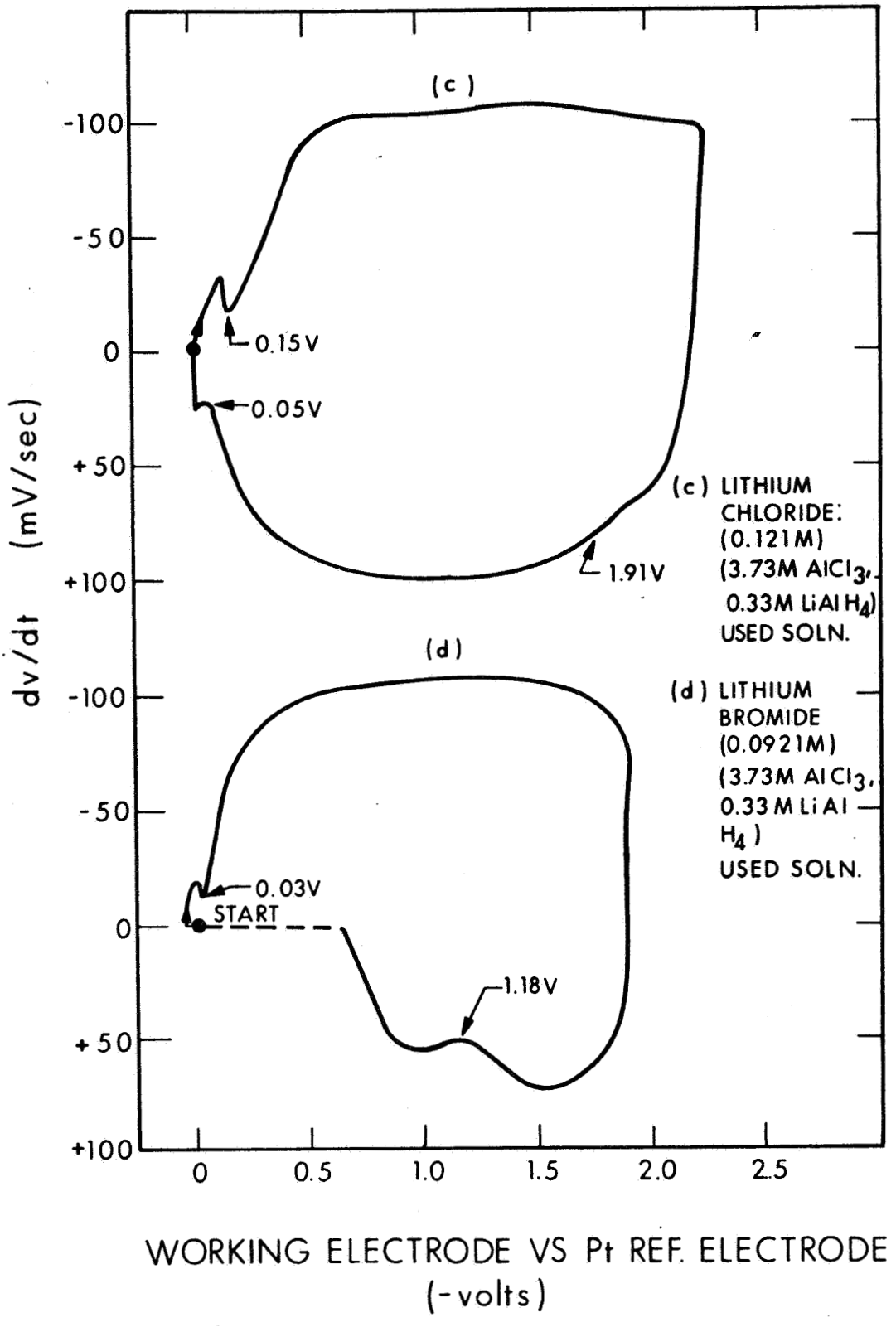

Figure 7A. Voltage Derivative Curves for APS Containing Inert Salt Additives (contd)

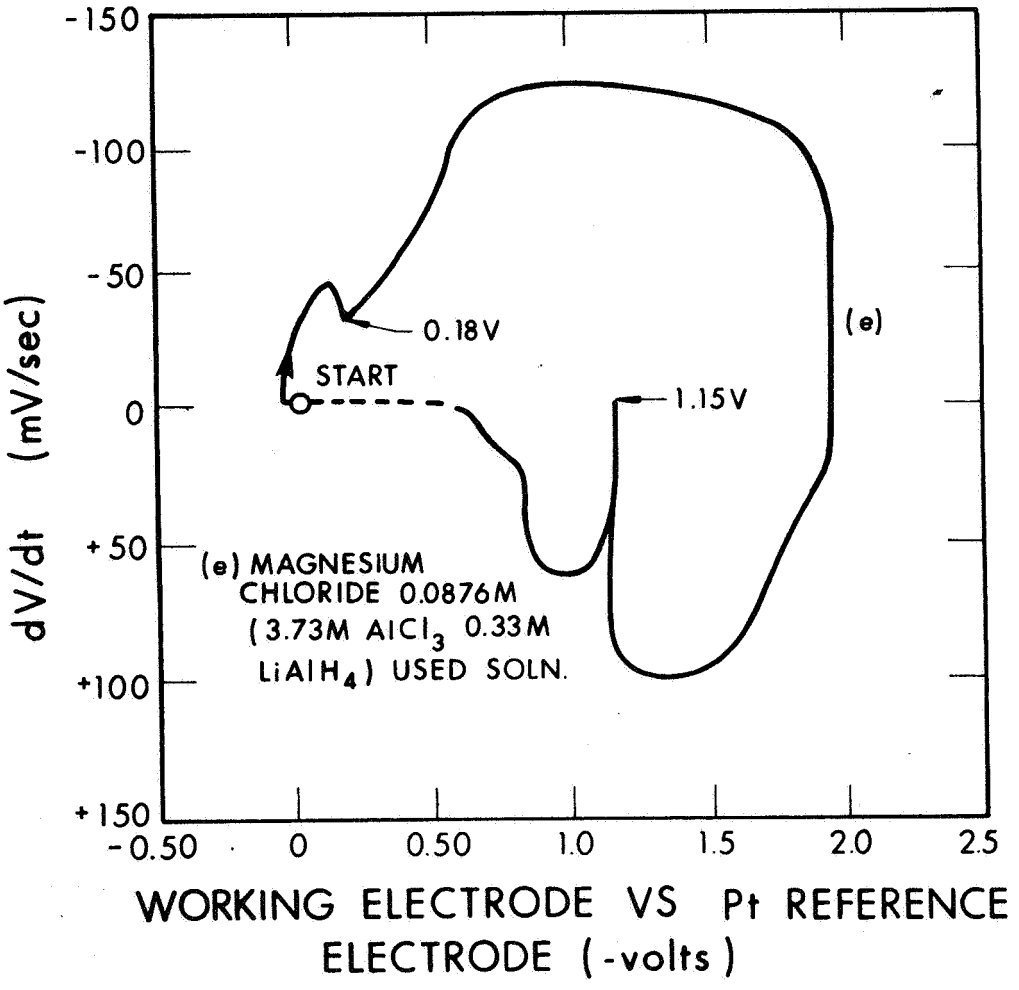

Figure 7A. Voltage Derivative Curves for APS Containing Inert Salt Additives (contd)

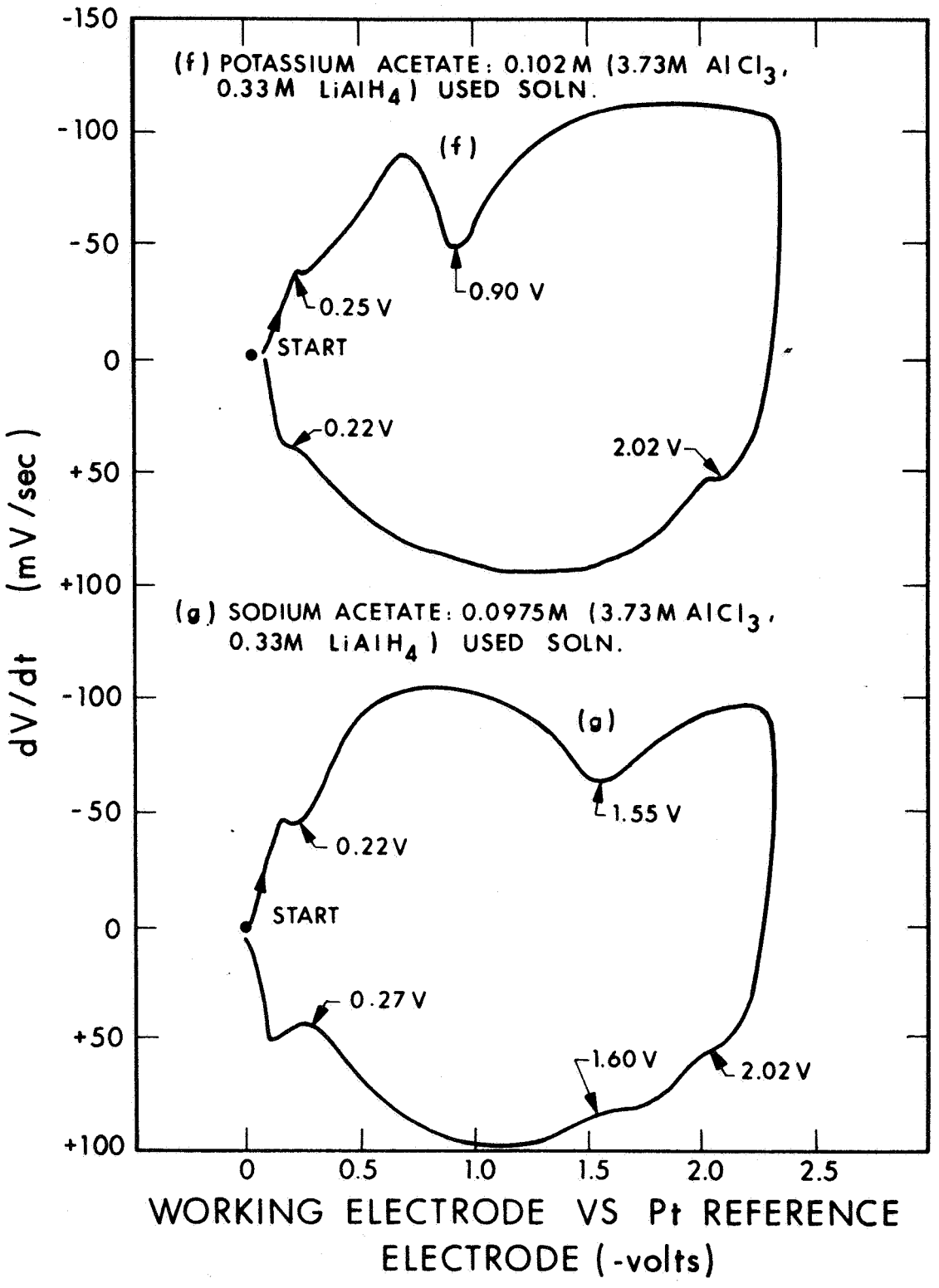

Figure 7A. Voltage Derivative Curves for APS Containing Inert Salt Additives (contd)

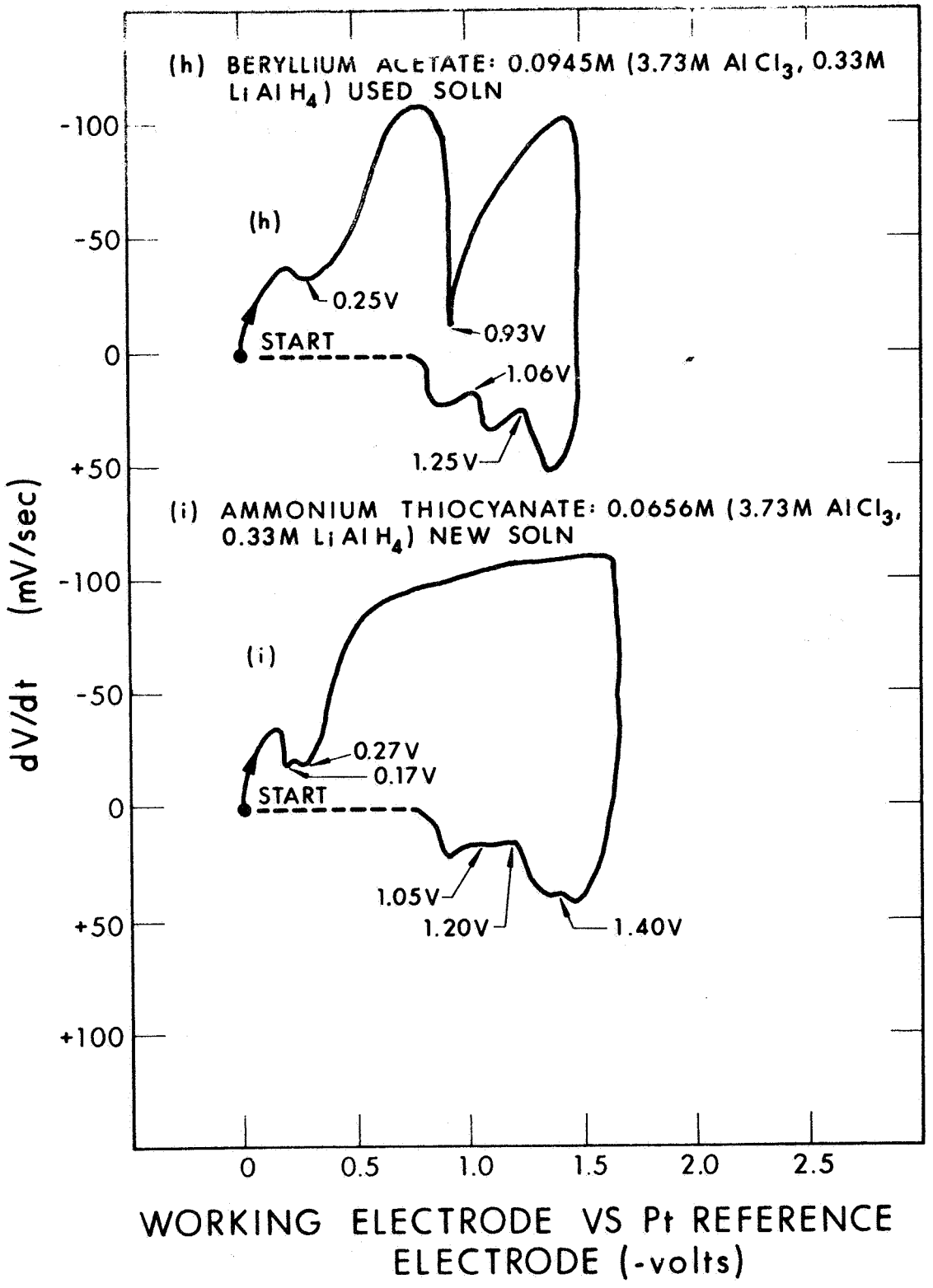

Figure 7A. Voltage Derivative Curves for APS Containing Inert Salt Additives (contd)

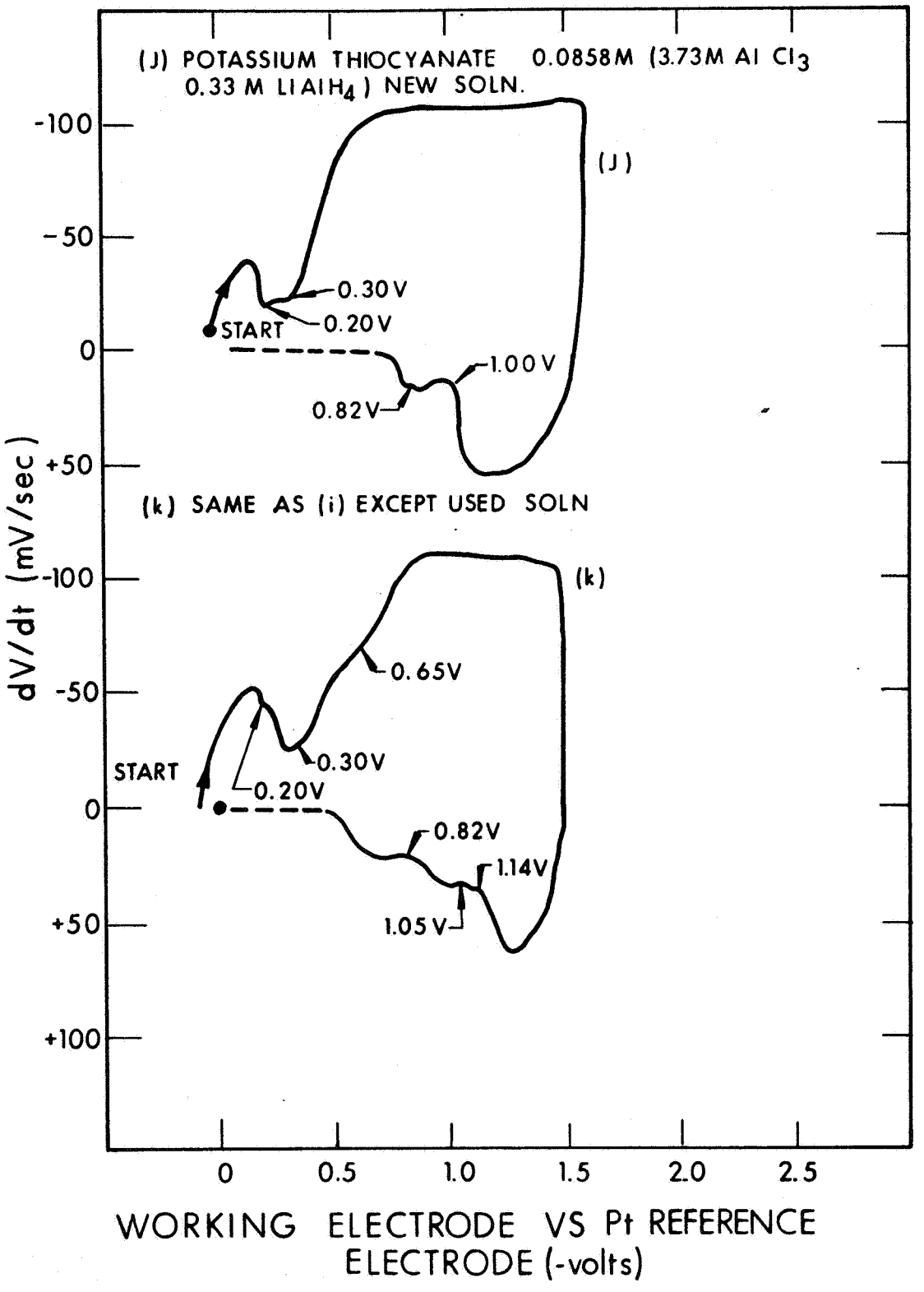

Figure 7A. Voltage Derivative Curves for APS Containing Inert Salt Additives (contd)

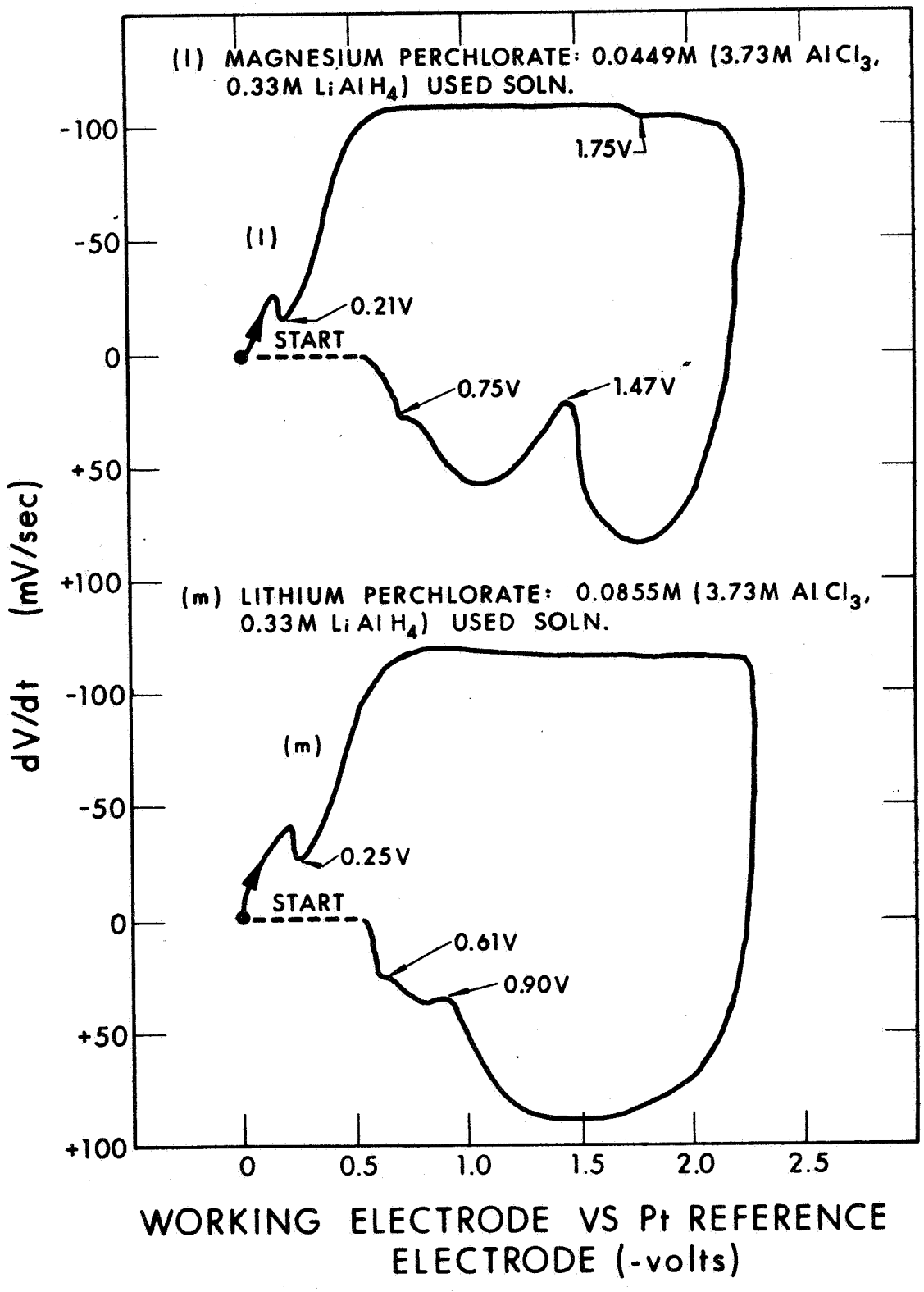

Figure 7A. Voltage Derivative Curves for APS Containing Inert Salt Additives (contd)

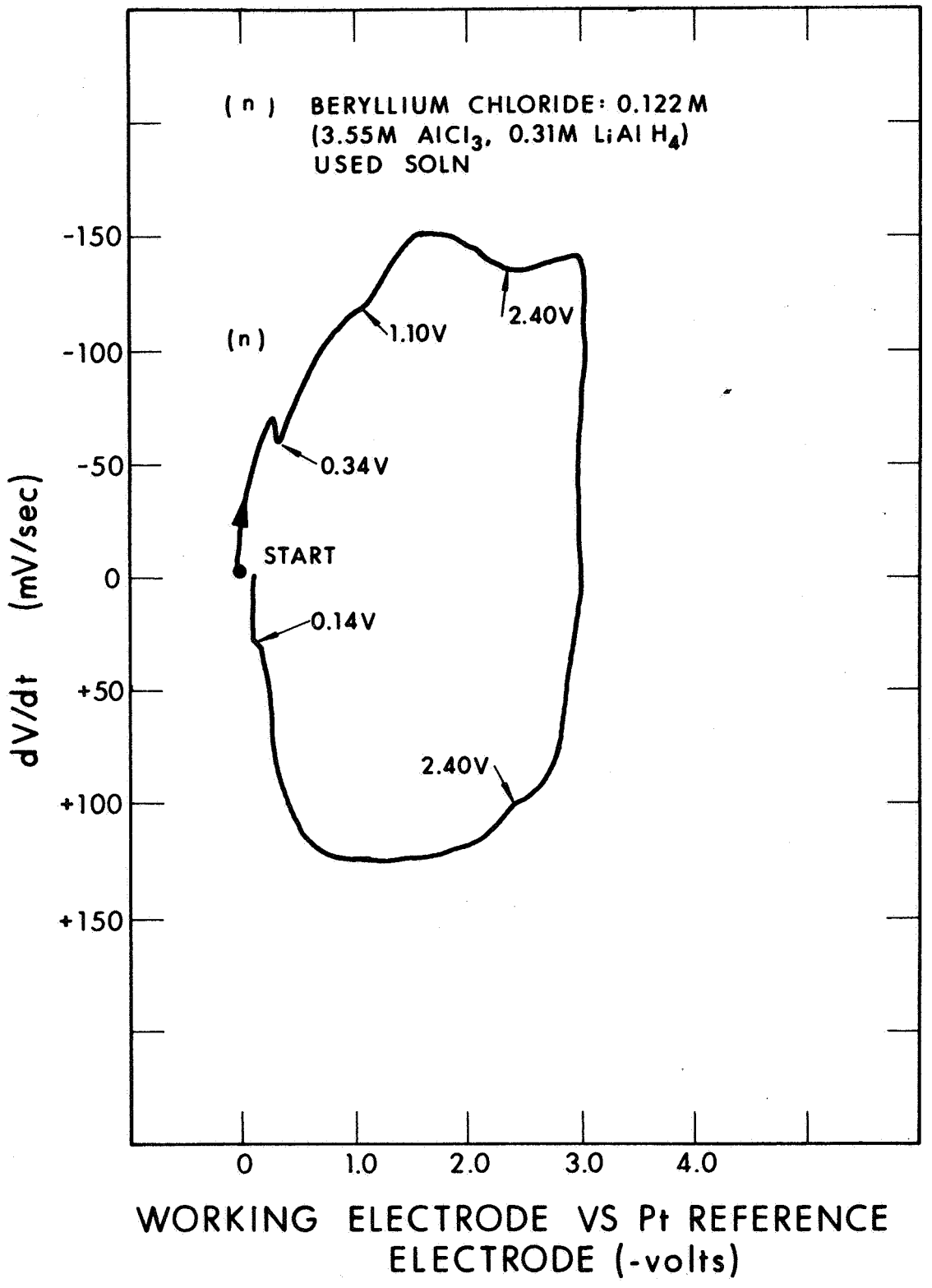

Figure 7A. Voltage Derivative Curves for APS Containing Inert Salt Additives (contd)

The voltage derivative curve for the APS containing $TiCl_4$ (0.099M) was characterized by a large number of incisions (Figure 7A(o)). The incision at -0.15V is probably due to electrodeposition of titanium, while that at -0.33V is due to electrodeposition of aluminum. (Titanium was detected qualitatively in the electrodeposit from the above solution). Undoubtedly, some of the peaks observed in the lower portion of the curve are associated with the electrodeposition processes.

The voltage derivative curve for the APS containing $TiO(AcAc)_2$ (0.038M) was similar to those for the case of the APS containing $TiCl_4$, in that a large number of incisions occurred (Figure 7A(p)). The aluminum peak appears in the same potential range for both systems, namely, -0.30V to -0.35V. A number of peaks in the lower portion of the curve for this system also appeared in the derivative curves for the APS-$TiCl_4$ system, which suggests a similarity in at least a portion of the electodeposition process. Several additional peaks which occurred at potentials in excess of -2.0V were due to solution decomposition.

A qualitative check for titanium in the electrodeposit from the APS-$TiO(AcAc)_2$ bath was positive, although the amount of titanium present was small.

A.2.5 Amine Additives

The derivative curve for the APS containing tetraethylammonium chloride (0.06M) exhibited the characteristic aluminum peak at -0.26V along with two sets of additional peaks due to some organic reduction process (Figure 8A(a)). In the case of the APS containing 2,4-dimethylaniline (0.157M), two additional peaks at -0.60V and -1.35V (lower part of curve) were ~~pres~~ent along with the typical aluminum peak at -0.23V (upper part

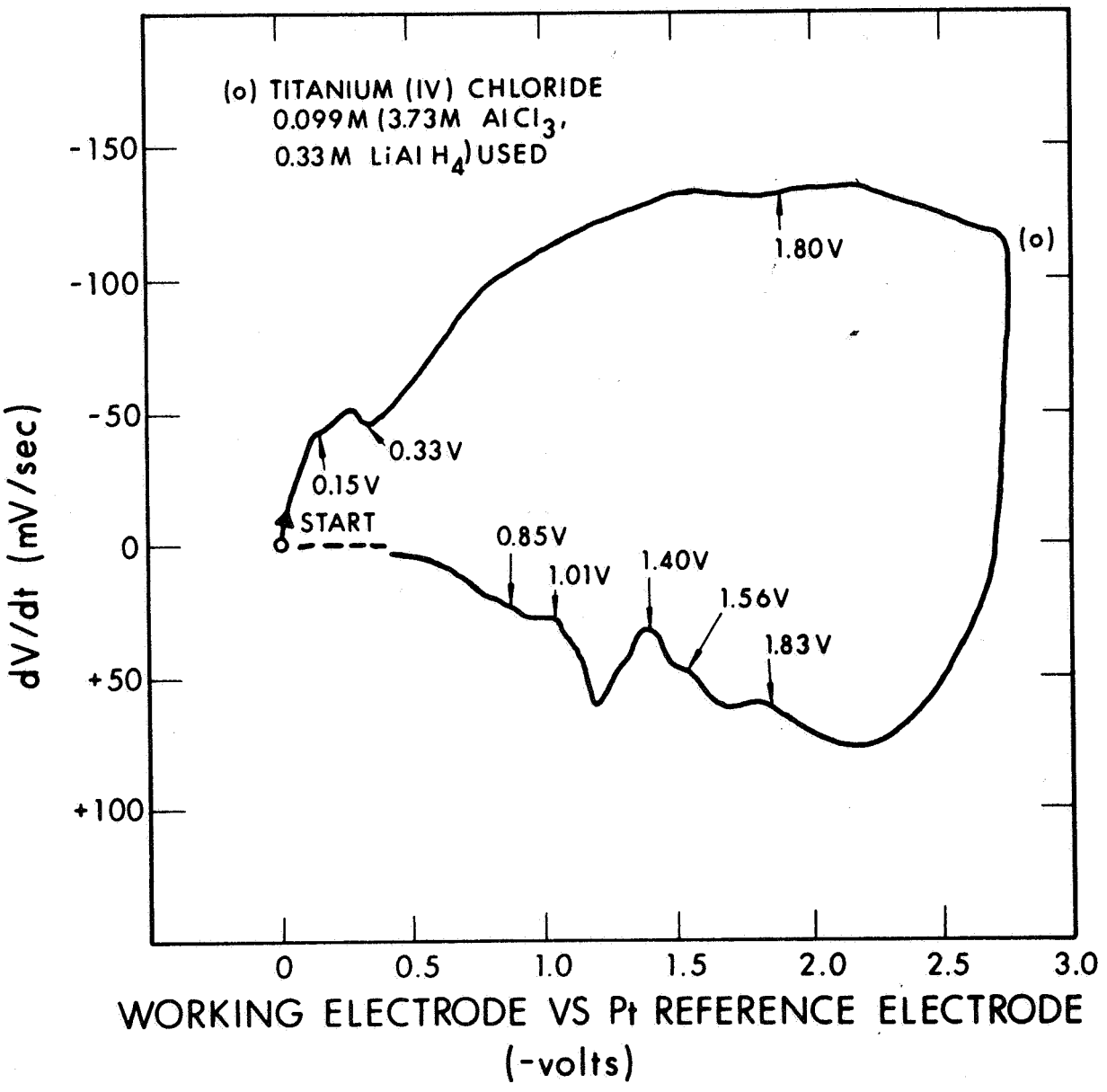

Figure 7A. Voltage Derivative Curves for APS Containing Inert Salt Additives (contd)

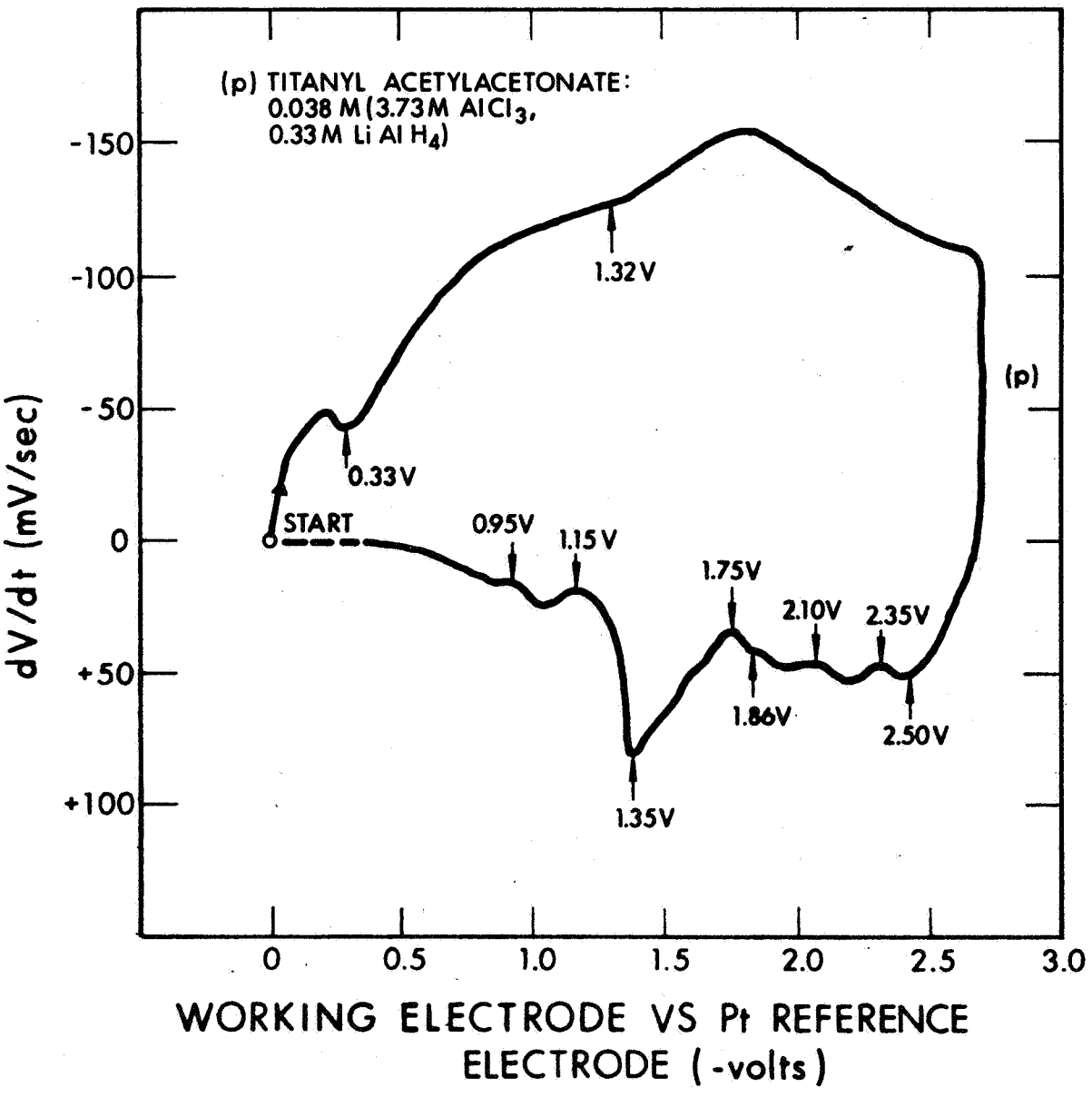

Figure 7A. Voltage Derivative Curves for APS Containing Inert Salt Additives (contd)

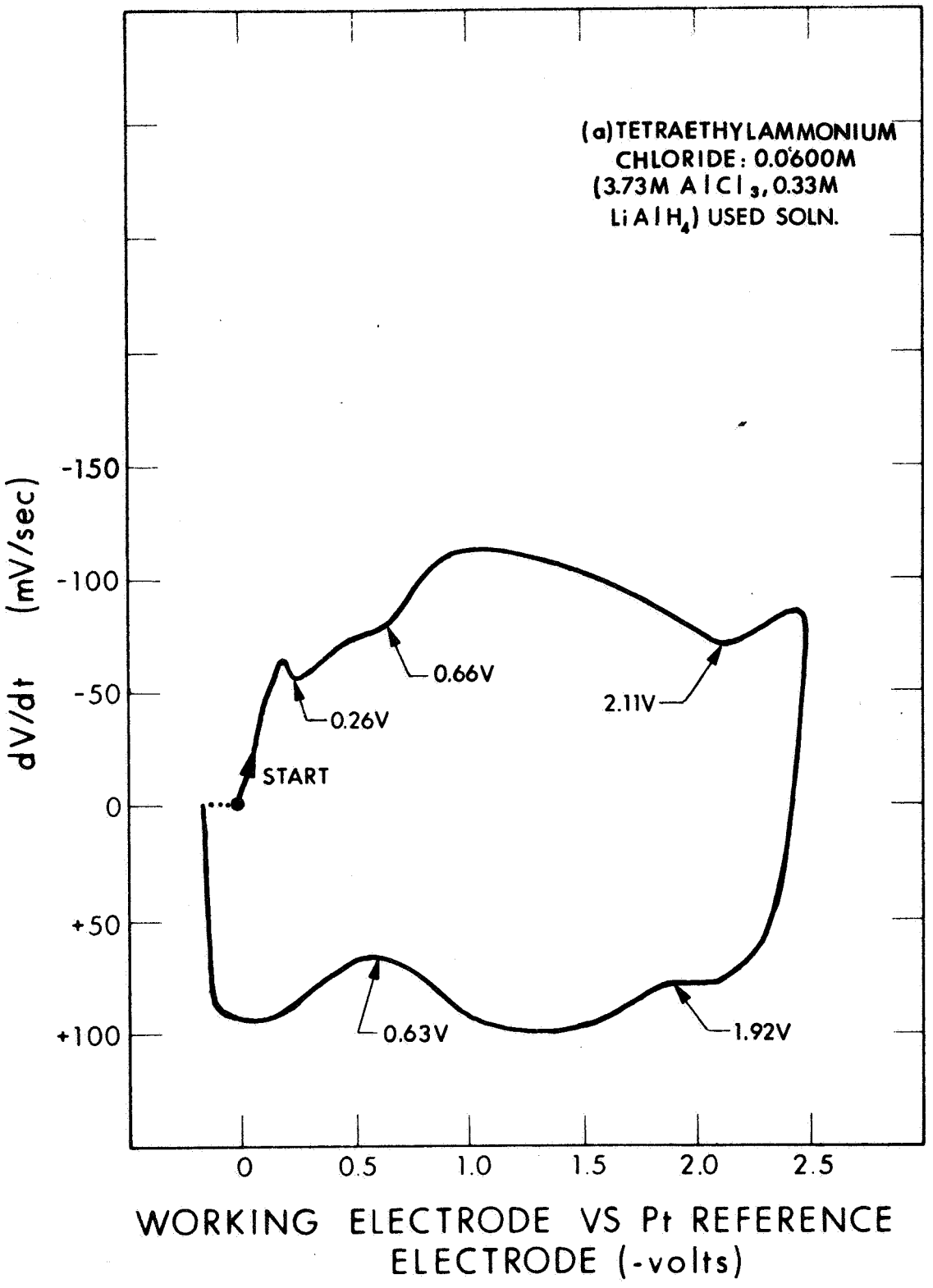

Figure 8A. Voltage Derivative Curves for APS Containing Amine Additives

of curve). (See Figure 8A(b)). A somewhat similar curve was obtained for the APS containing phenylhydrizine hydrochloride (0.0972M), except for two additional weak peaks - one on the upper part of curve (at -0.7V to -0.8V) and the other on the lower part of the curve (at -2.1V to -2.2V). (See Figure 8A(c)).

The voltage derivative curve for the APS containing oxydianiline (0.10M) contained only three incisions: at -0.40V (upper portion of curve), associated with the aluminum electrodeposition process, and at -1.9V and -1.2V (lower portion), corresponding to some organic reduction process (Figure 8A(d)). Apparently, the addition of oxydianiline (4-aminophenyl ether) to the APS has the effect of shifting the reduction potential of aluminum to a higher negative value.

A.2.6 Nitrile Additives

No aluminum peak was noted for the APS containing acetonitrile at a concentration of 0.908M (unused) - only a broad, medium-intensity peak in the range of -1.4V to -1.8V (upper part of curve). A peak at -2.0V to -2.1V also occurred in the bottom part of the curve (Figure 9A(a)). After the above solution had been used (electrolyzed for some time), an additional weak peak at -0.4V to -0.5V appeared (aluminum peak?). (See Figure 9A(b)). In this case, the major solution process was the organic reduction. The scanning data was corroborated by the electrodeposition data in that no metallic deposit was obtained - only a salt coating on the cathode.

In the case of the APS containing benzonitrile, a hardened aluminum deposit was obtained for concentrations up to about 0.175M (Figure 9A(c)). In all cases, the aluminum peak (at -0.15V to -0.20V) was

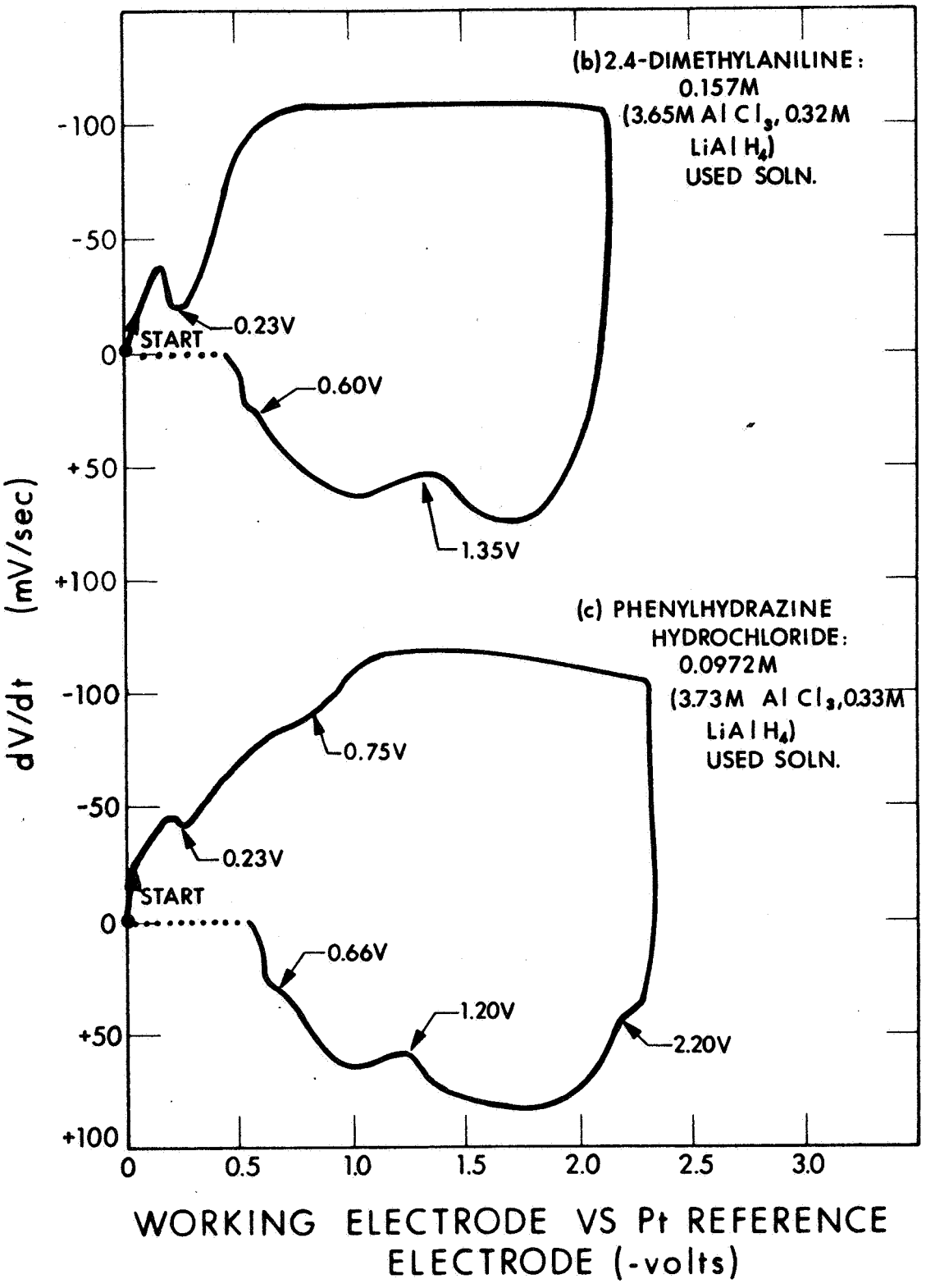

Figure 8A. Voltage Derivative Curves for APS Containing Amine Additives (contd)

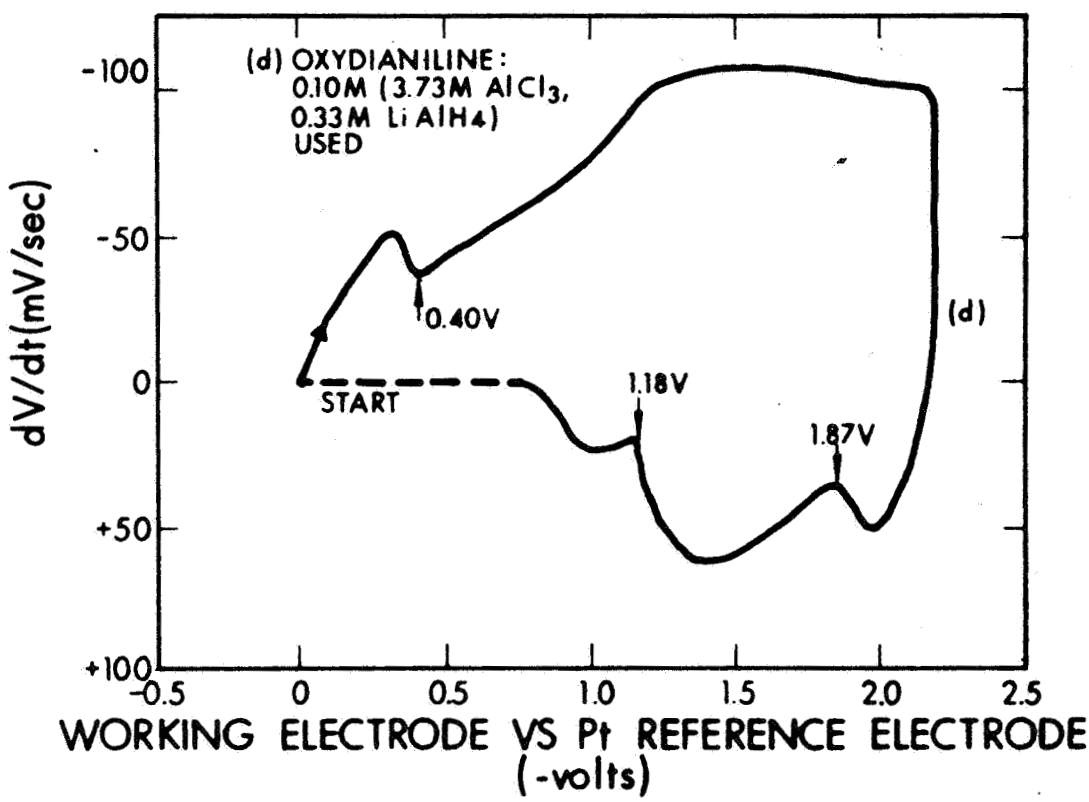

Figure 8A. Voltage Derivative Curves for APS Containing Amine Additives (contd)

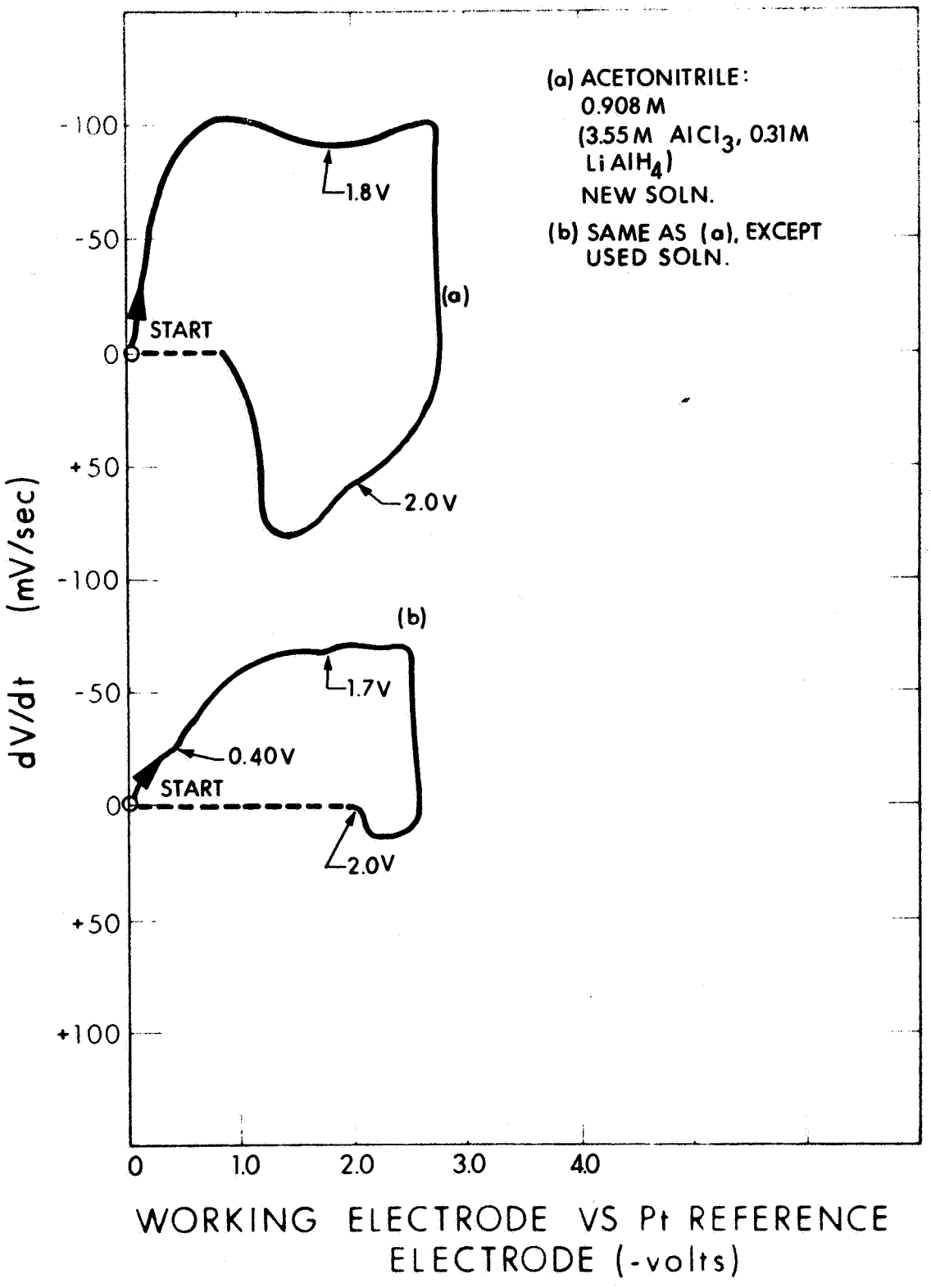

Figure 9A. Voltage Derivative Curves for APS Containing Nitrile Additives

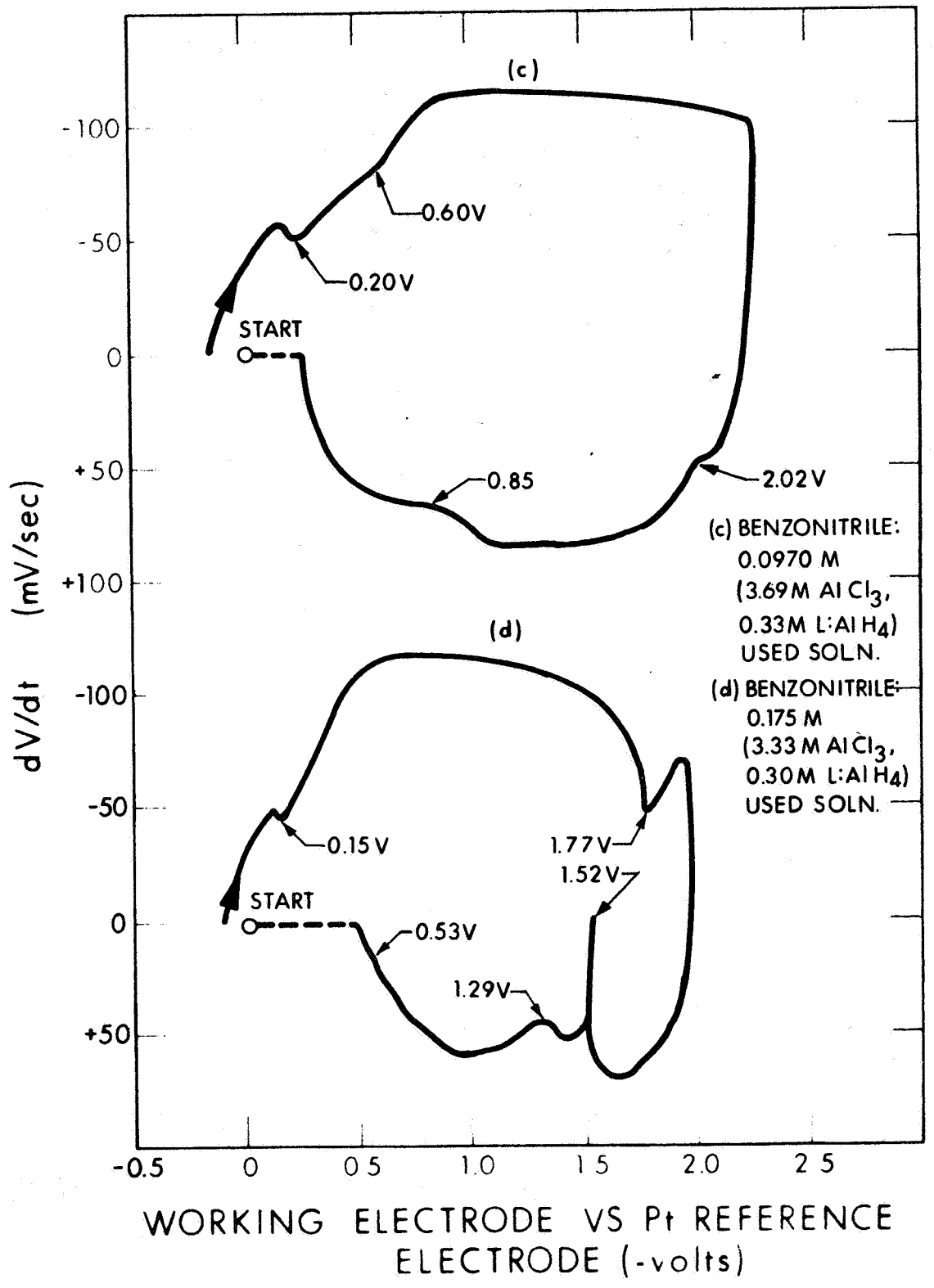

Figure 9A. Voltage Derivative Curves for APS Containing Nitrile Additives (contd)

present in the derivative curve. At a benzonitrile concentration of 0.175M, after a considerable amount of plating time (57 hrs. at 0.5A, 0.5 liter volume), additional strong-intensity peaks appeared indicating an increase in the organic reduction process (Figure 9A(d)).

The voltage derivative curve for the APS containing 0.0855M p-tolunitrile was quite similar to that for the case of the APS alone, except for the peak on the lower portion of the curve at -0.44V (Figure 9A(e)).When the concentration of p-tolunitrile was doubled, additional peaks appeared and the residual polarization voltage was much higher (Figure 9A(f)).

The voltage derivative curve for the APS containing phthalonitrile (0.0851M) was quite similar in shape to that for the same concentration of p-tolunitrile with similar measured reduction potentials (Figure 9A(g)).

The reduction potential values for the voltage derivative curves for the APS containing 4-biphenylcarbonitrile (0.100M) were not very repeatable (Figure 9A(h)). In fact, the derivative curve did not have the same general shape on successive scans in many instances.

A.2.7 Amide Additives

The voltage derivative curve for the APS containing phenylacetamide (0.089M) exhibited the typical aluminum peak at -0.22V with several very weak, broad peaks at -2.05V and -2.50V (upper portion of curve). (See Figure 10A(a)). There were also several somewhat stronger incisions on the lower portion of the curve at -2.30V, -1.95V, and -1.02V.

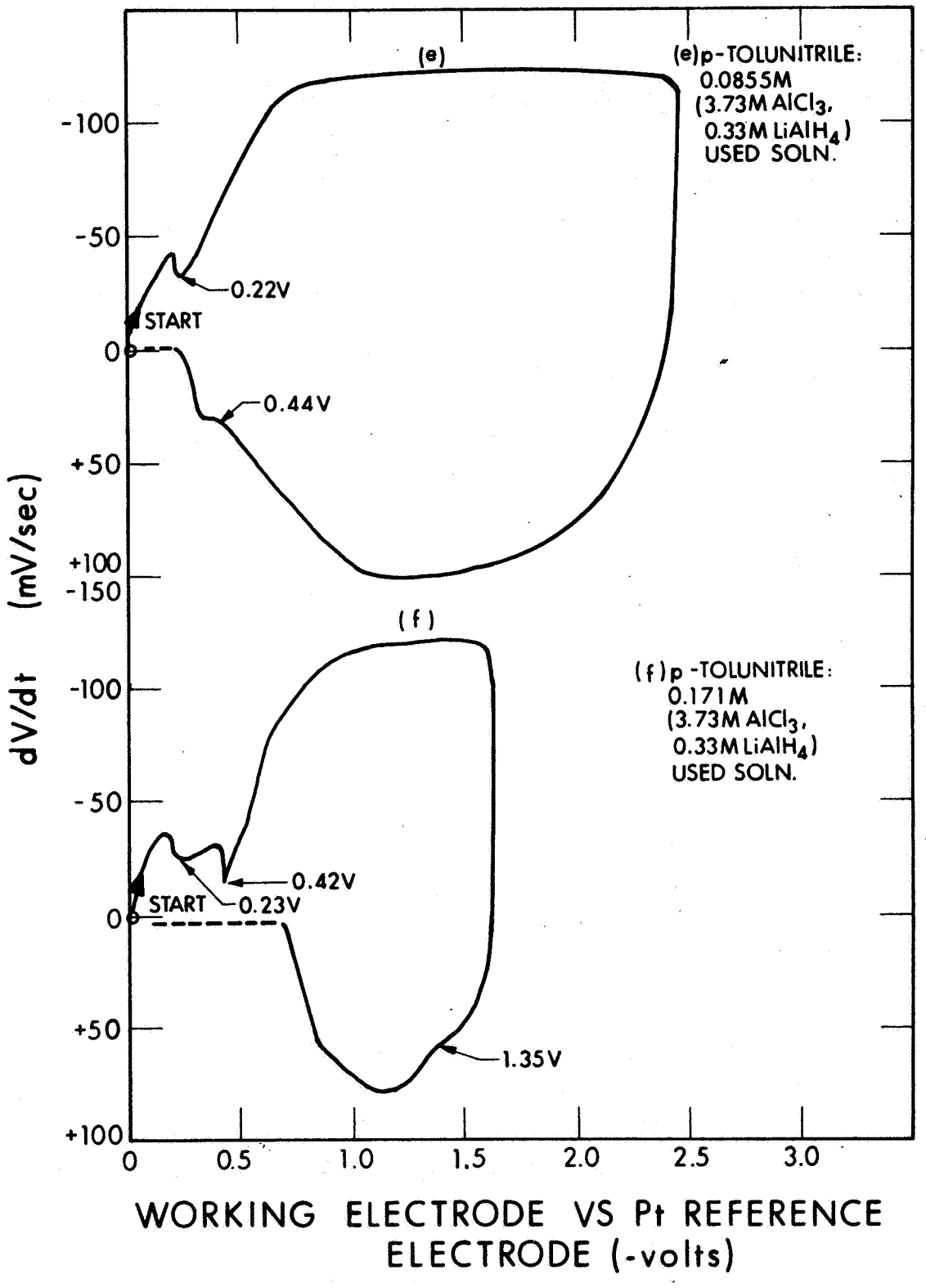

Figure 9A. Voltage Derivative Curves for APS Containing Nitrile Additives (contd)

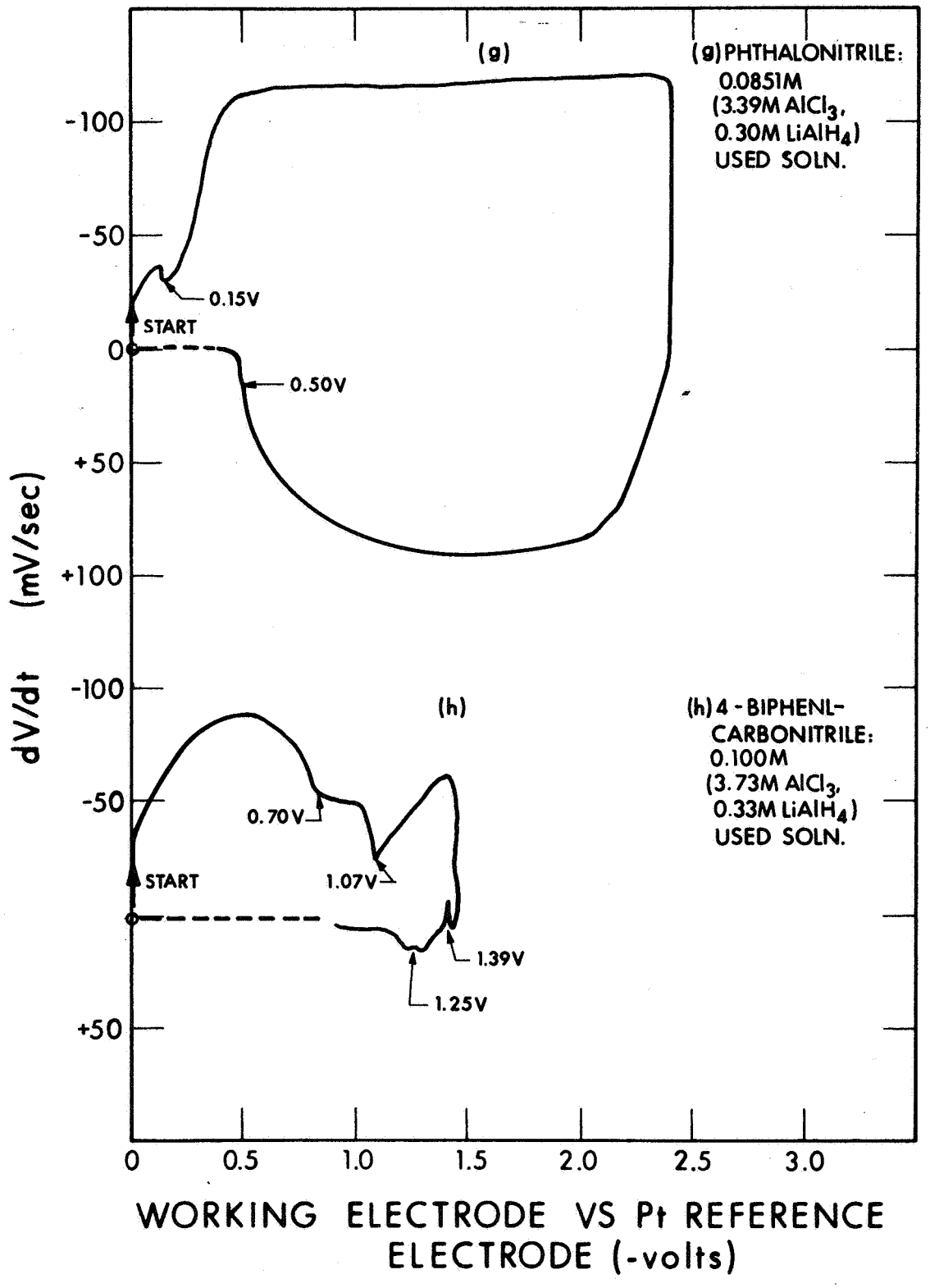

Figure 9A. Voltage Derivative Curves for APS Containing Nitrile Additives (contd)

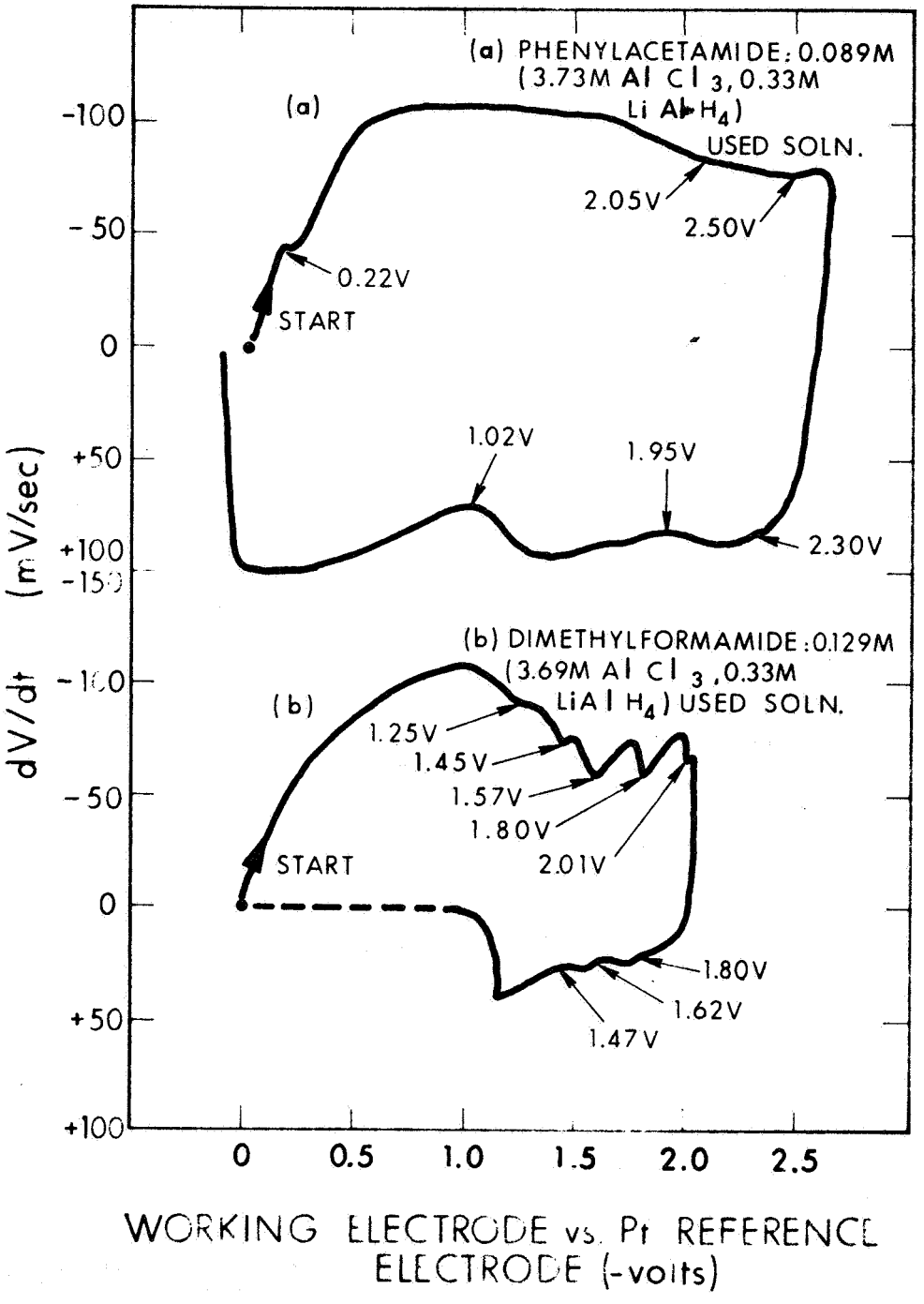

Figure 10A. Voltage Derivative Curves for APS Containing Amide Additives

In the case of the dimethylformide additive (Figure 10A(b)), no aluminum peak was evident where one normally occurs in the voltage derivative curve (at less than -0.50V). However, since a coherent aluminum deposit was obtained, one of the higher valued peaks must be associated with the aluminum electrodeposition process.

The aluminum peak was shifted to slightly more negative potentials (slightly above -0.3V) for the following additives: urea (0.10M), benzamide (0.075M), and p-toluamide (0.074M). (See Figures 10A(c), 10A(d), and 10A(e)). All the above curves exhibited additional peaks due to some secondary reduction process. The derivative curve for the APS containing acetanilide (0.094M) was quite similar to that of the APS alone, with several additional reduction peaks (Figure 10A(f)) at -1.80V and -0.86 V on the lower portion of the curve.

A.2.8 Hetrocyclic Compound Additives

The voltage derivative curve for the APS containing a concentration of pyridine of 0.06M was not very different from that of the APS alone except for some additional broad, rather weak peaks at potentials above the aluminum reduction potential (Figure 11A(a)). The pyridine-containing APS produced the best electrodeposit at a concentration of pyridine of 0.125M. The voltage derivative curve for this solution after and before the electrodeposition test (i.e., "used" and "new"), were completely different indicating a considerable chemical change had taken place as a result of the electrolysis (Figure 11A(b) and 11A(c), respectively). As the concentration of pyridine was increased, the shape of the derivative curve changed somewhat - especially at the higher concentrations. At a concentration of 0.25M, the aluminum peak had become weak and a sharp, much stronger peak now appeared at -0.79V (Figure 11A(d)).

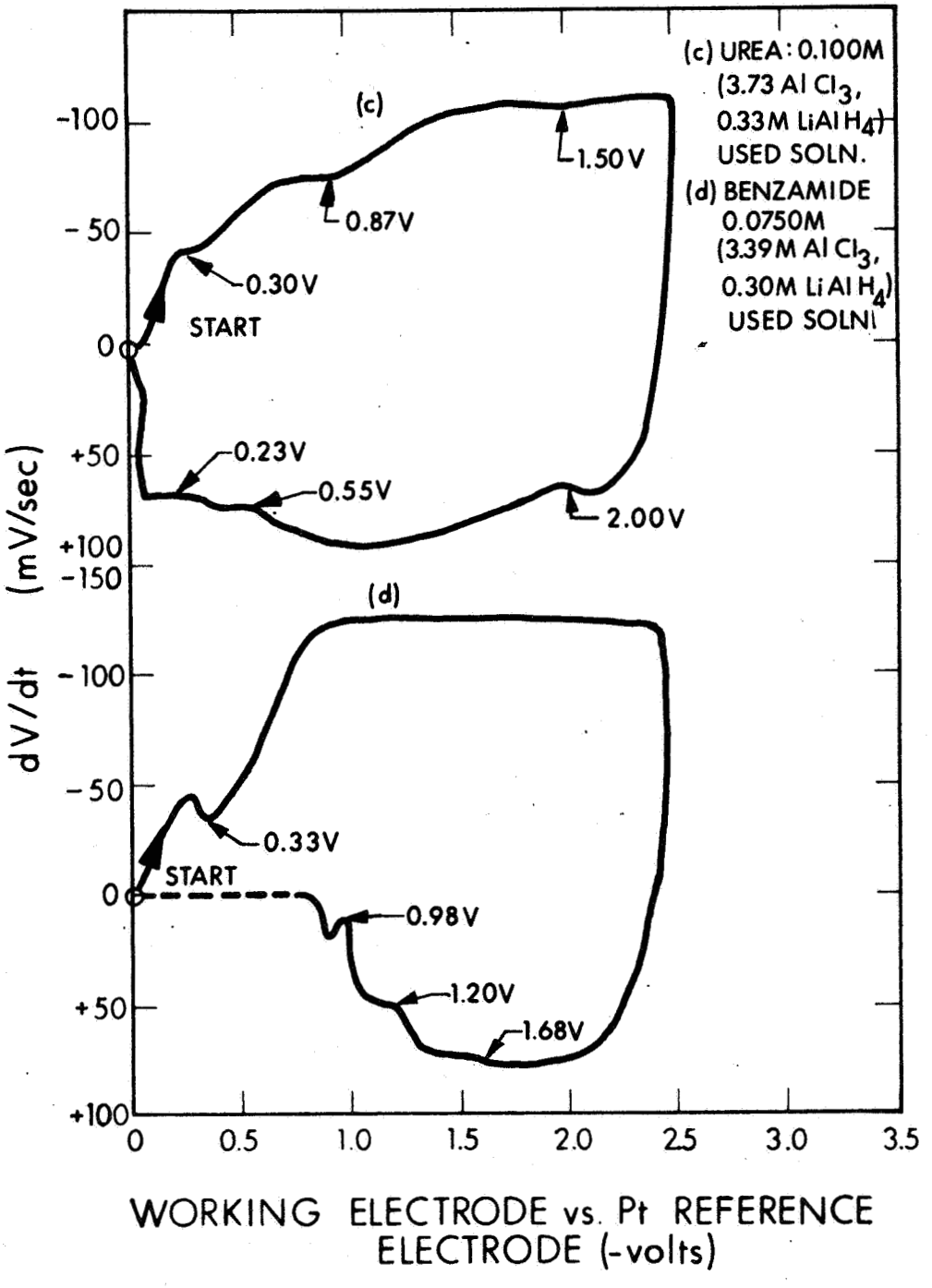

Figure 10A. Voltage Derivative Curves for APS Containing Amide Additives (contd)

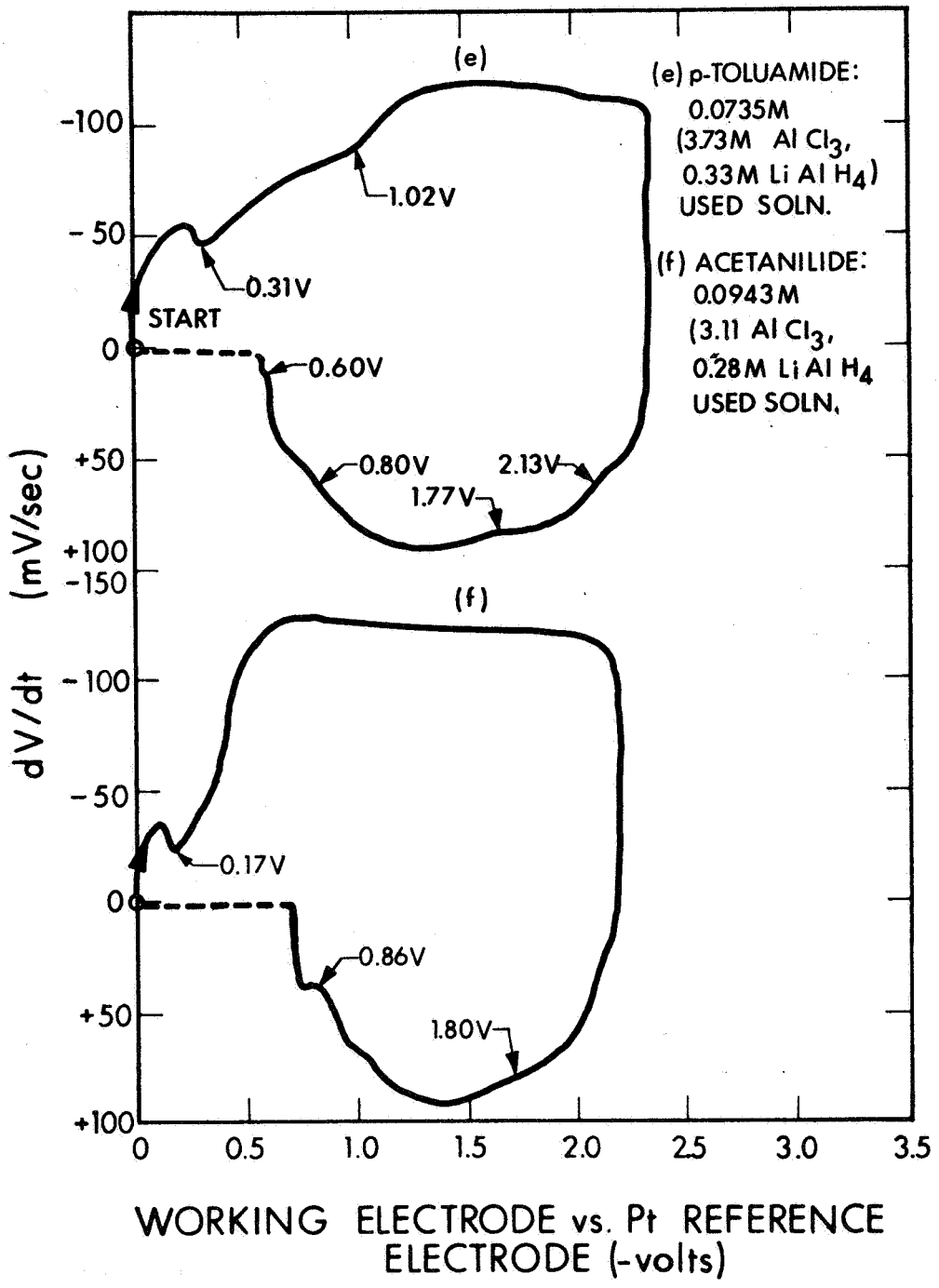

Figure 10A. Voltage Derivative Curves for APS Containing Amide Additives (contd)

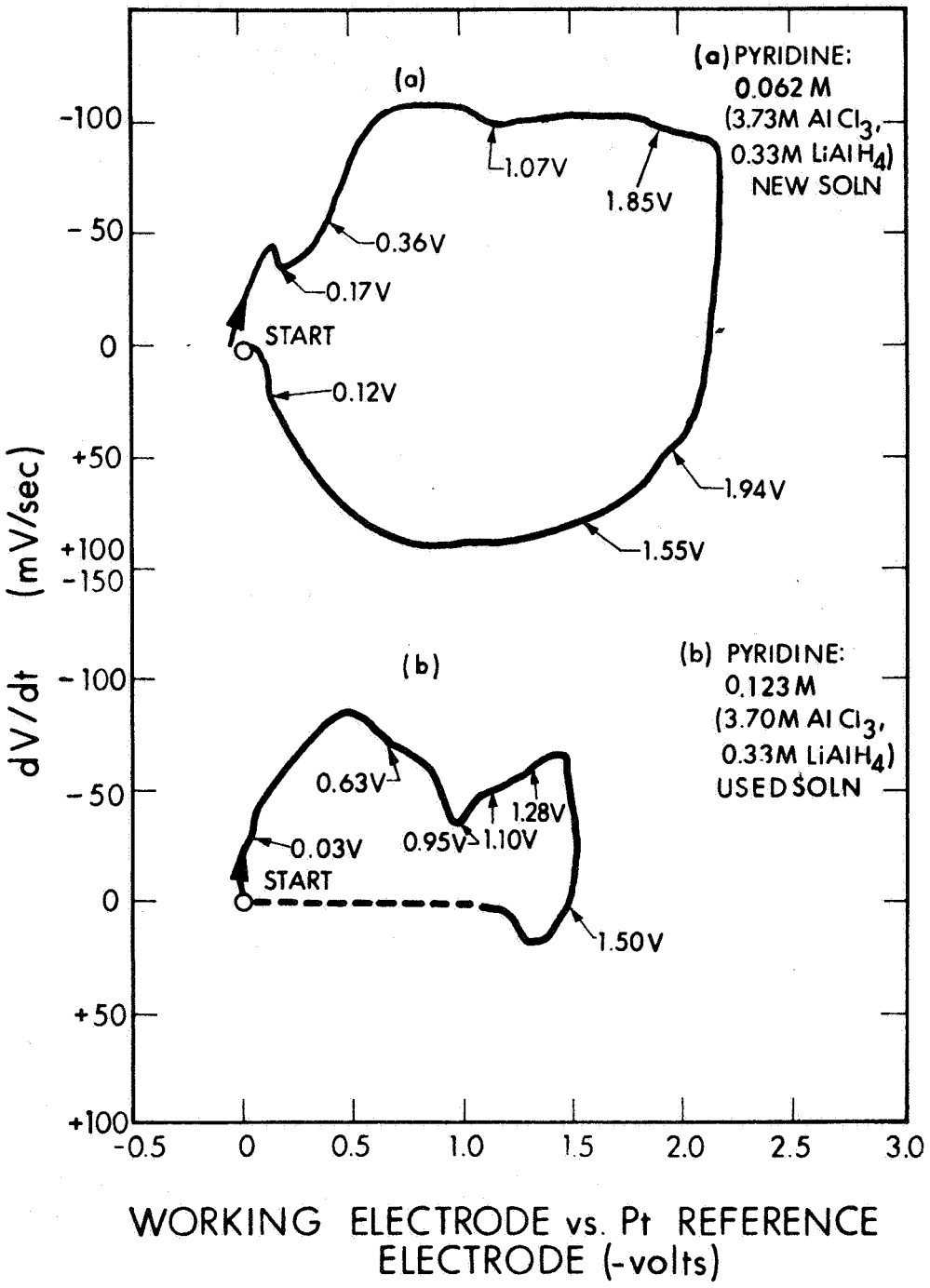

Figure 11A. Voltage Derivative Curves for APS Containing Heterocyclic Compound Additives

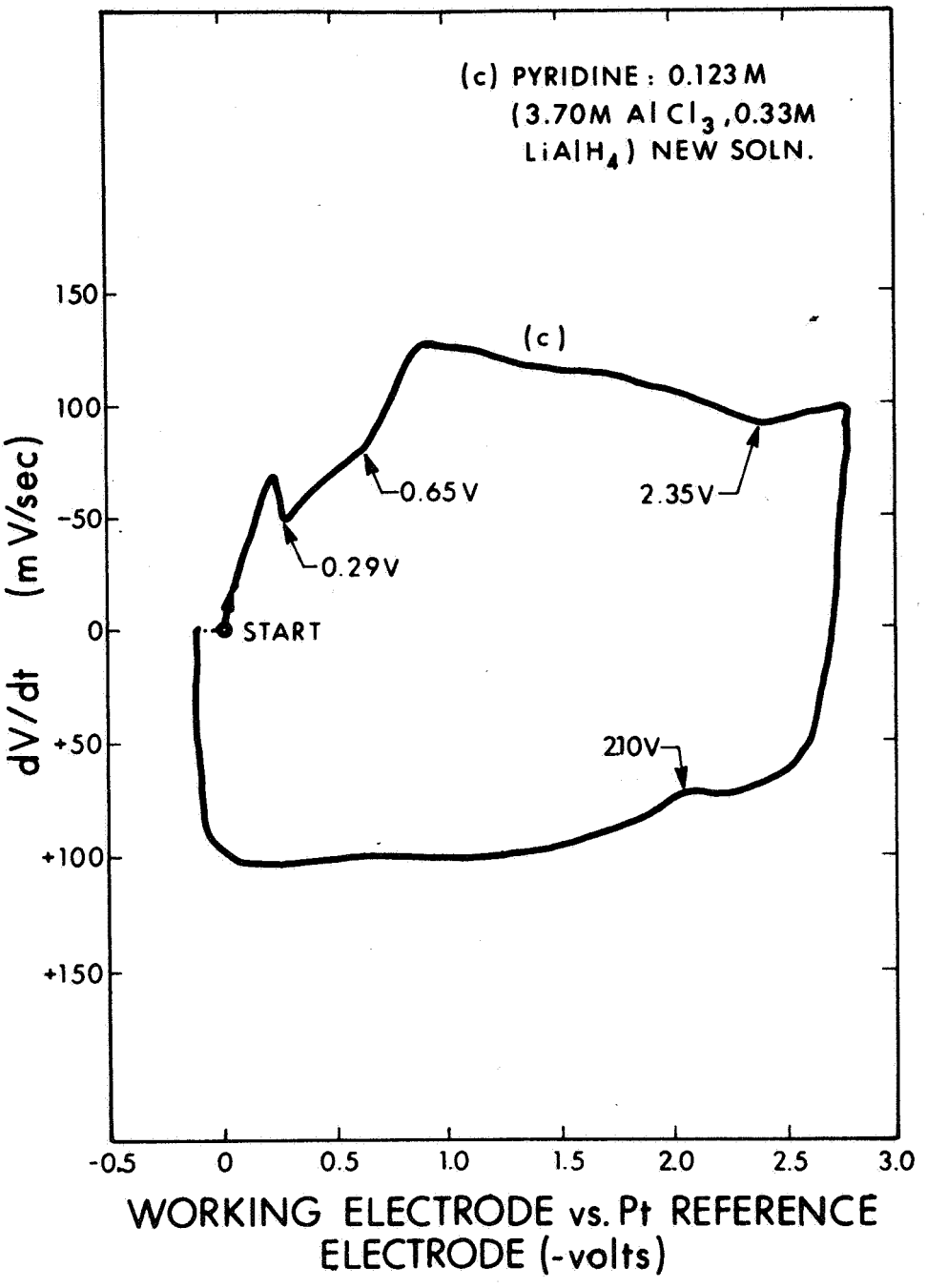

Figure 11A. Voltage Derivative Curves for APS Containing Heterocyclic Compound Additives (contd)

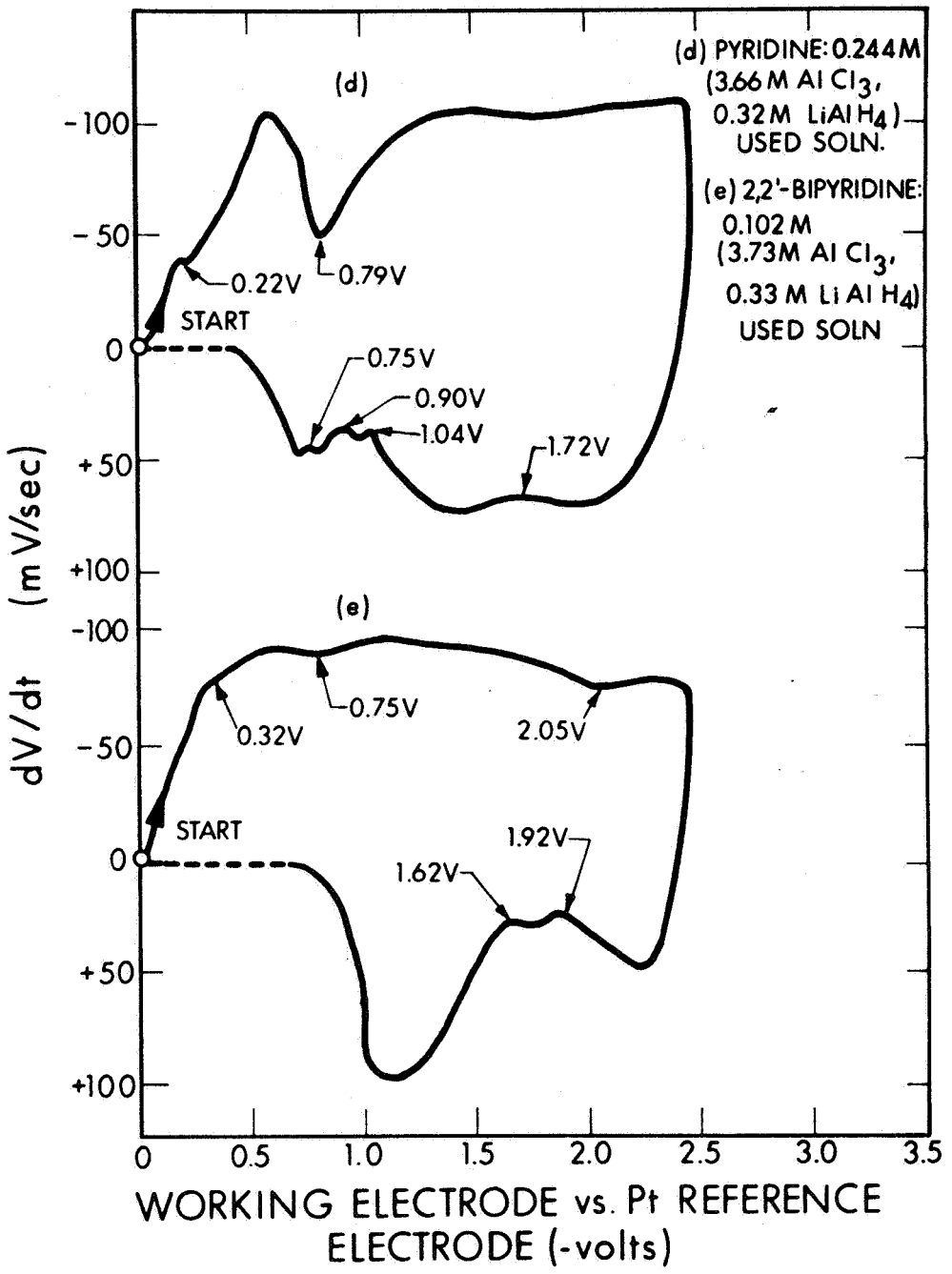

Figure 11A. Voltage Derivative Curves for APS Containing Heterocyclic Compound Additives (contd)

The voltage derivative curve for the APS containing 0.10M of 2,2'-bipyridine (Figure 11A(e)) exhibited an extremely weak and broad peak (at -0.32V) in potential range of aluminum deposition. The electrodeposit in this case was quite poor, being very crumbly and nonmetallic in nature.

The aluminum peak for the case of the indole additive (0.086M) was shifted to a slightly less negative potential relative to that of the APS alone (-0.10V versus -0.25V, respectively). (See Figure 11A(f)).

At a concentration of morpholine of 0.225M (initially) in the APS, the voltage derivative curve exhibited an additional peak at-0.20V in addition to the typical aluminum peak at -0.30V (Figure 11A(g)).

A.2.9 Ester Additives

The derivative curve for the case of the APS containing an organic ester additive, ethyl acetate (0.092M), was similar to that of the APS alone, but with some additional peaks at the higher potentials (Figure 12A(a)).

The derivative curve for the APS containing an inorganic ester additive, tri-n-butyl phosphate (0.097M), was not similar in shape to that for ethyl acetate (Figure 12A(b)). Two closely-spaced peaks were present (at -0.18V and -0.25V in the aluminum deposition potential range, compared to only one for the case of ethyl acetate (at -0.27V).

A.2.10 Organometallic Additives

In the case of ferrocene, the derivative curve was very similar to that of the APS alone (Figure 13A(a)), except for additional peaks in the lower portion of the curve. A qualitative check for iron in the electrodeposit was negative.

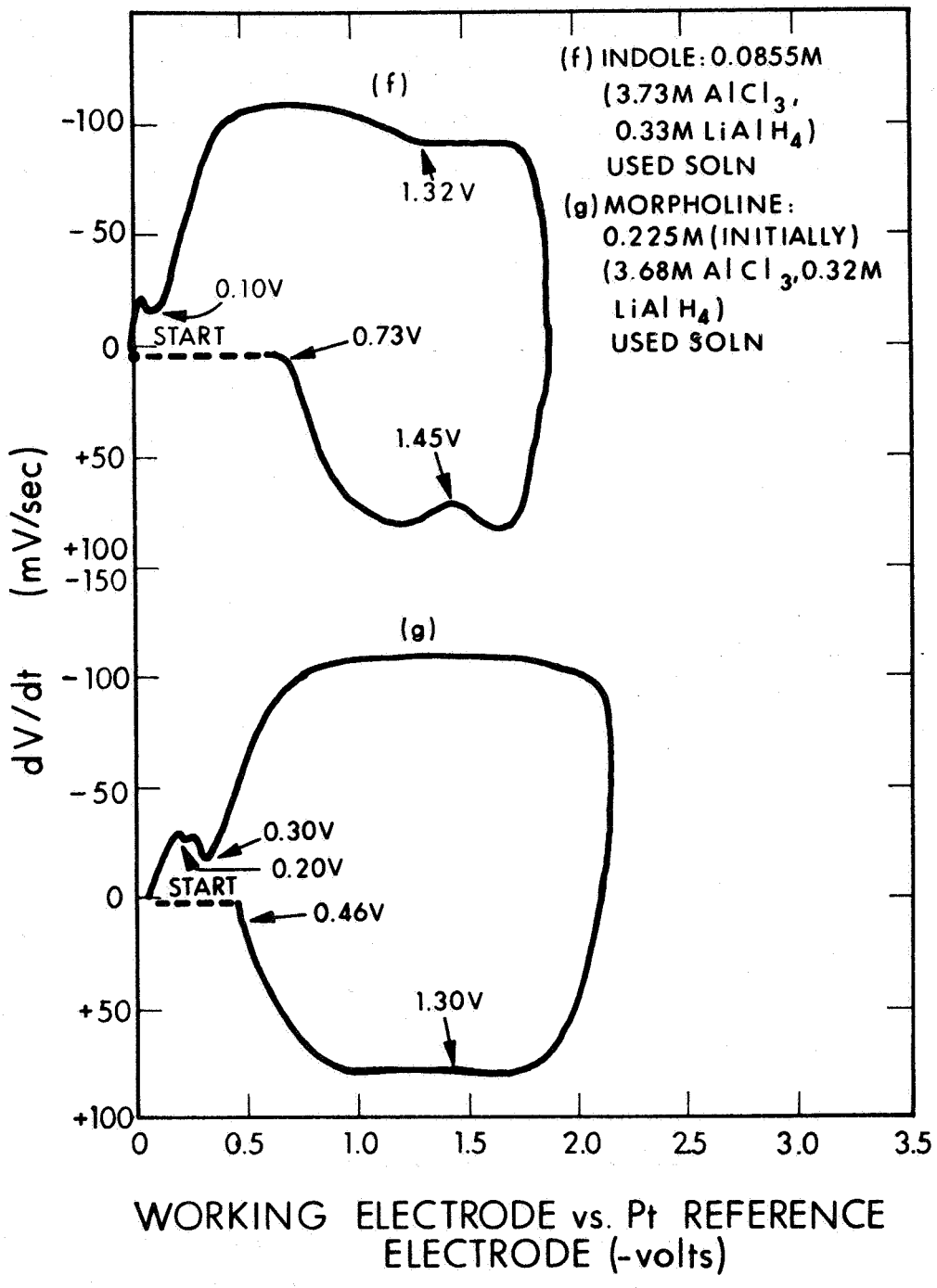

Figure 11A. Voltage Derivative Curves for APS Containing Heterocyclic Compound Additives (contd)

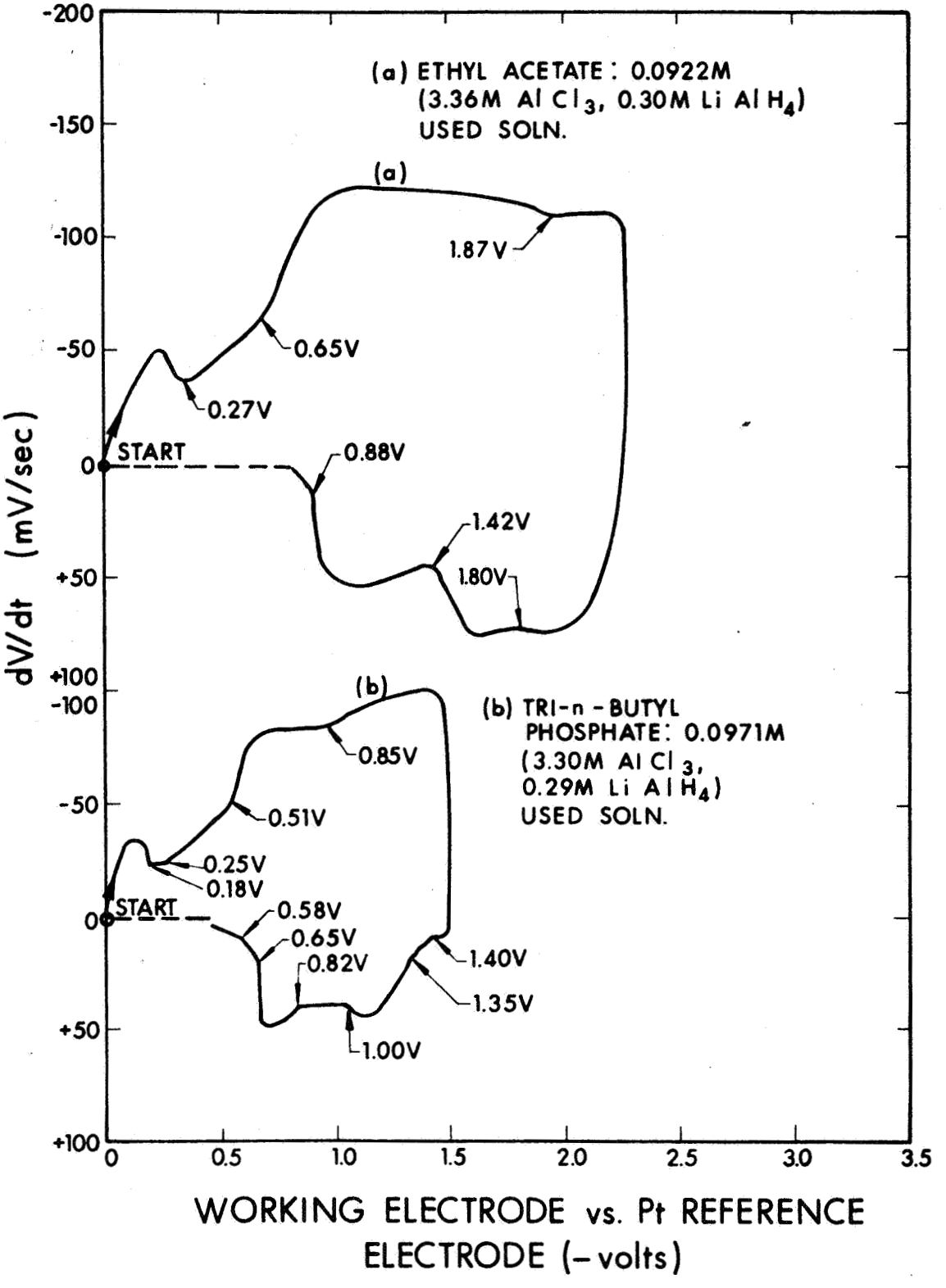

Figure 12A. Voltage Derivative Curves for APS Containing Ester Additives

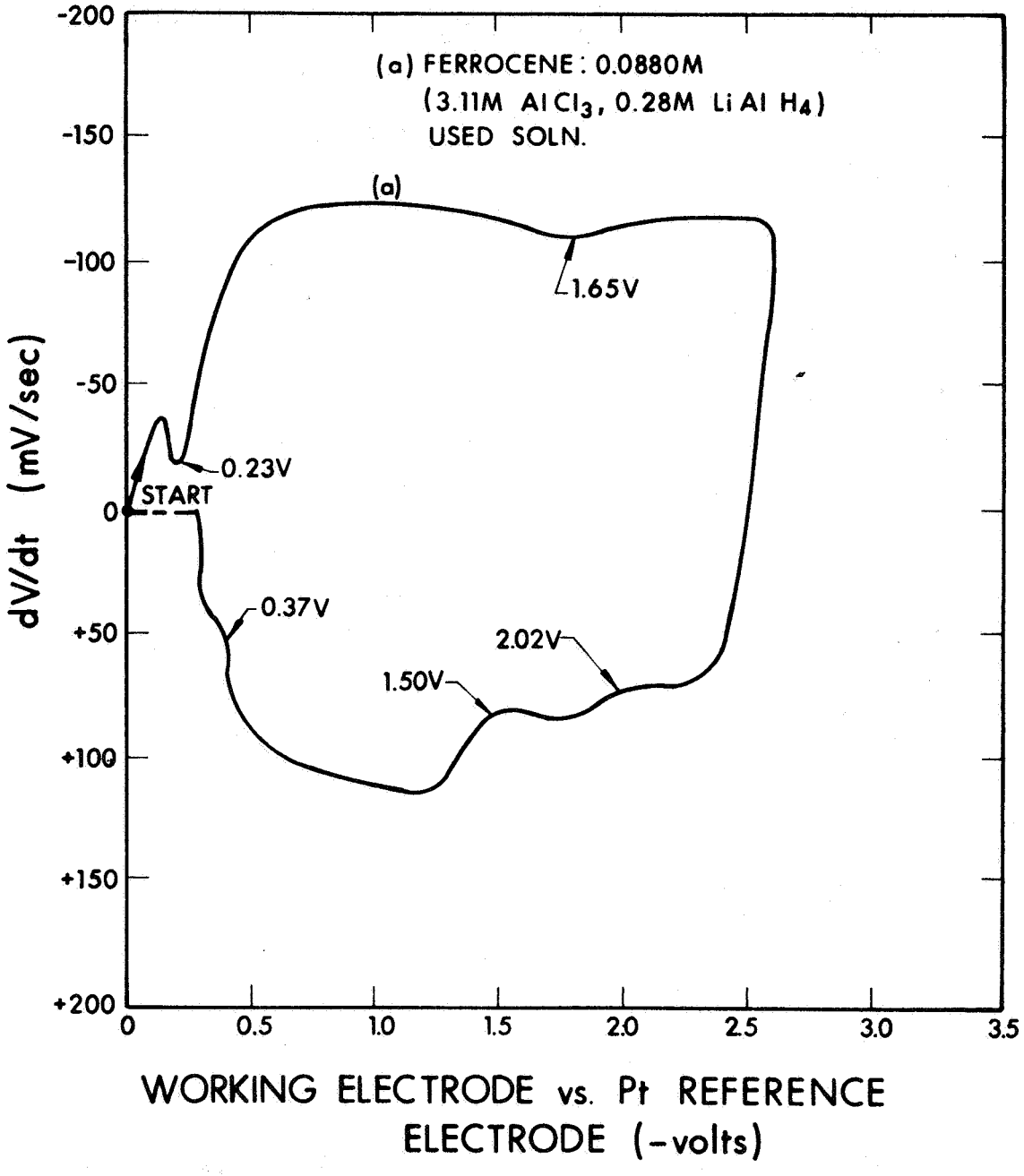

Figure 13A. Voltage Derivative Curves for APS Containing Organometallic Additives

No additional peaks were discernible in the neighborhood of the aluminum peak at -0.33V in the voltage derivative curve for the APS containing titanocene dichloride (0.098M). (See Figure 13A(b)). However, several of the peaks which occurred for the case of the APS containing $TiCl_4$ and titanyl acetylacetonate also were present in the present case, so that similar processes were probably occurring in all three solutions (i.e., titanium electrodeposition). A qualitative check for titanium in the electrodeposit was positive.

A.3 SUMMARY OF ELECTROLYTE SCANNING STUDIES

The majority of the aluminum plating solutions (mainly used) which produced a metallic aluminum deposit were characterized by a well-defined peak in the voltage derivative curve, generally in the potential range of -0.15V to -0.30V (aluminum peak). However, the aluminum peaks for the case of the APS additives KCl (0.089M) and LiBr (0.092M) occurred at a very low potential of -0.03V, while those for 4-biphenylcarbonitrile (0.1M) and dimethylformamide (0.13M) occurred at a potential in excess of -0.50V.

However, the presence of a sharp aluminum peak in the derivative curve of a test solution was no guarantee that a satisfactory aluminum electrodeposit would be obtained; this only indicated that aluminum electrodeposition was taking place. In some cases, these were other electrochemical reactions occurring simultaneously, and the resultant electrodeposit was severely deteriorated (e.g., dark, powdery, with occluded salt), as for example, in the case of the thiocyanate additives KSCN (0.086M) and NH_4SCN (0.066M). The voltage derivative curves in both instances exhibited a second smaller and weaker peak at approximately 0.1V before the aluminum peak.

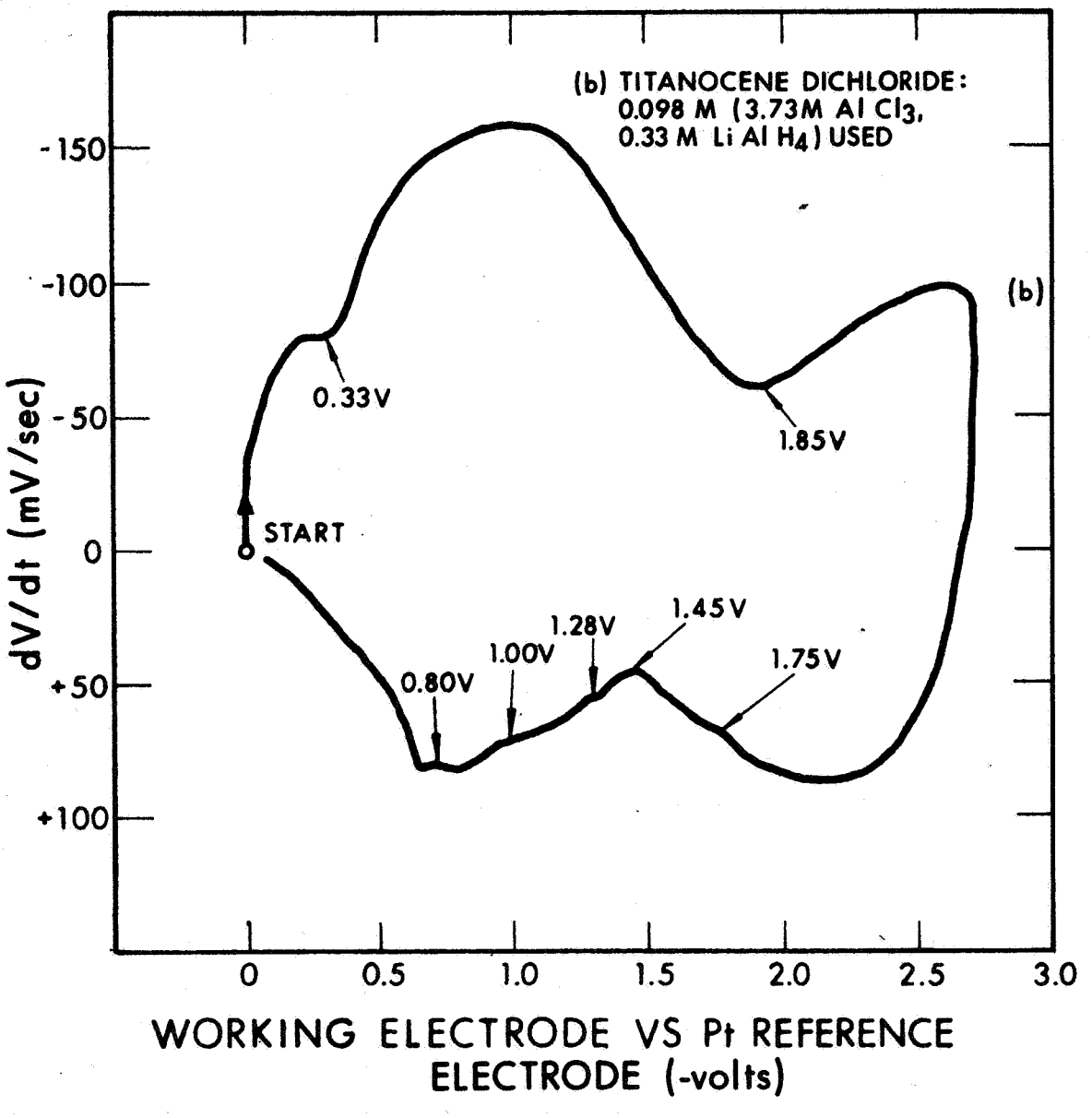

Figure 13A. Voltage Derivative Curves for APS Containing Organometallic Additives (contd)

The perchlorate additives to the APS ($Mg(ClO_4)_2$ and $LiClO_4$) resulted in electrodeposits which were similar in appearance to those for the case of the thiocyanate additives. In this case, however, though no additional peaks were observed adjacent to the aluminum peak in the voltage derivative curve, other peaks were present at potentials more negative than the aluminum peak. This indicates the presence of additional electrochemical reactions (other than aluminum electrodeposition) during electrolysis, such as solvent decomposition (i.e., organic reduction processes). The extent of these reactions can be estimated from the depth and sharpness of the incisions (peaks).

The voltage derivative curves for the APS containing isopropyl ether (29% by volume) or bis (2-butoxyethyl) ether (17% by volume) were similar to those for the case of the thiocyanate APS additives, in that two closely spaced peaks were present at the aluminum reduction potential. However, in the case of the ether additives, the deposit obtained was quite satisfactory, and was not severely deteriorated as in the case of the thiocyanate additives.

During the present study, voltage derivative curves were obtained of the APS when it was fresh and unused, when it had been electrolyzed for an extended period of time (still yielding a satisfactory deposit), and when it had completely deteriorated (Figures 4A(a)-4A(c)). The curves for the first two cases were somewhat similar in appearance, but the curve for the case of the deteriorated APS was drastically different. Thus, APS deterioration can readily be detected through the use of the scanning technique.

Monitoring the bath plating characteristics by use of the scanning technique proved useful in another instance. Unexpected deterioration of a used portion of mixed-ether (anisole-ethyl ether) APS resulted in a black, scum coating on the cathode during electrolysis instead of the usual metallic aluminum deposit. The deterioration was traced to a leak in the refrigeration unit connected to the glove box. A leak in the cooling coils inside the glove box resulted in the contamination of the entire glove-box atmosphere, and, thereby, the plating solution.The usual conductivity measurements showed essentially no difference before and after the deterioration. The respective voltage derivative curves, however, were considerably different. The curve obtained before the deterioration occurred (Figure 14A(a)) showed the typical aluminum peak at about -0.48V, which is somewhat higher than that for the regular APS. In the case of the deteriorated solution, the aluminum peak either was absent or so weak and broad as to be undectable (Figure 14A(b)). Also, the shape of the curve had changed drastically.

By periodically monitoring the plating solution via the scanning technique, therefore, one can save considerable wasted time and effort in aluminum electroforming should any subsequent contamination of the plating solution reoccur.

A.4 CONCLUSIONS TO ELECTROLYTE SCANNING STUDIES

The voltage derivative (scanning) data for the regular APS and the mixed-ether APS were found to be useful for monitoring the plating characteristics in order to detect bath deterioration - especially where the usual conductivity tests failed. This technique can be applied

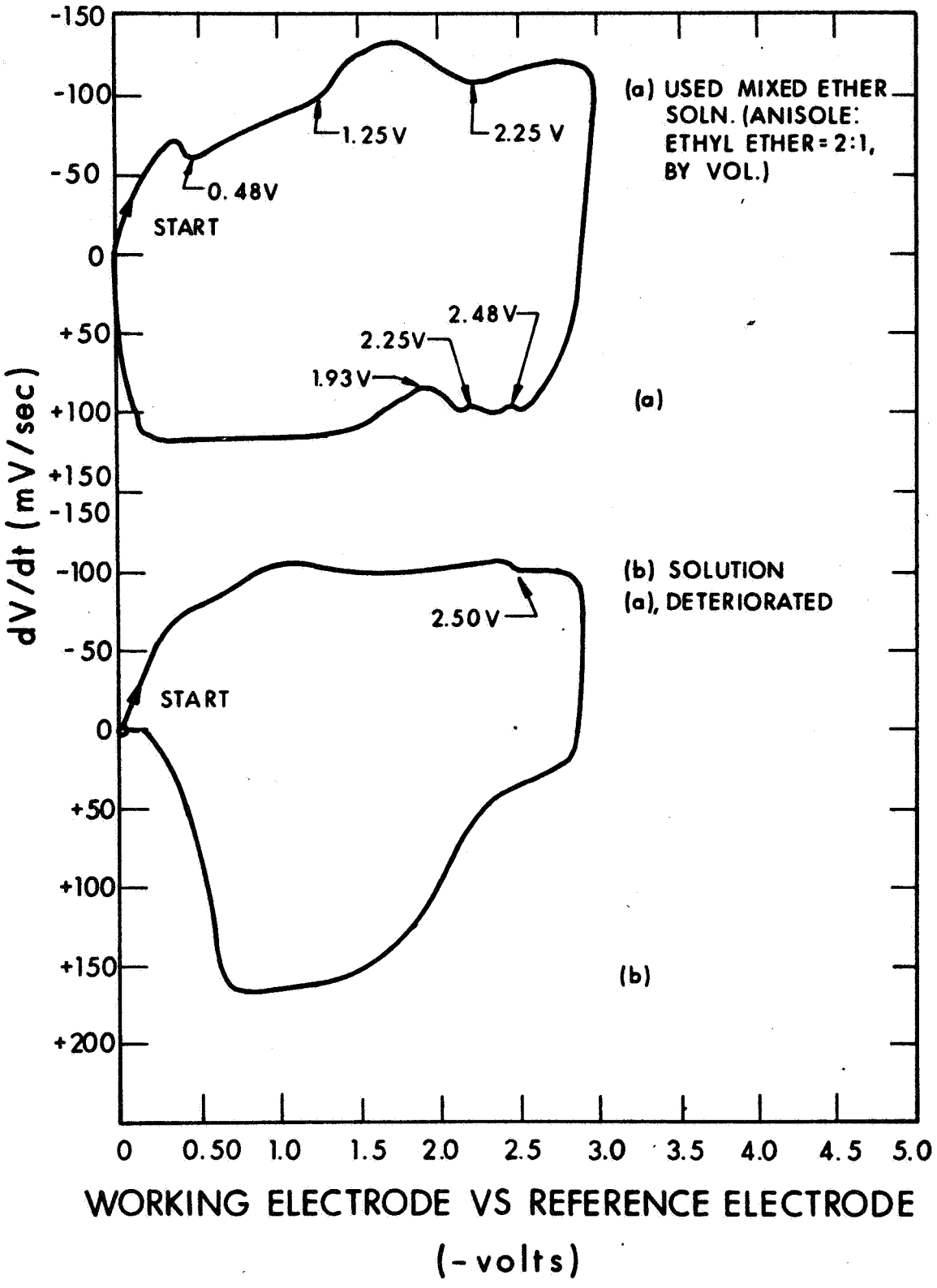

Figure 14A. Voltage Derivative Curves for Mixed-Ether APS

similarly to other test aluminum plating solutions. The present amount of data is insufficient, however, to draw conclusions concerning the use of electrolyte scanning as a means of estimating the life of the plating bath. To explore this possibility further would require an extensive compilation of scanning data over the lifetime of the bath - from the time it was freshly prepared until the time a satisfactory deposit was no longer obtained. Still, the scanning technique was useful for testing for total deterioration in the case of the regular APS and mixed-ether APS.

The data obtained from the voltage derivative curves for the various test solutions (mainly used aluminum plating solutions) were useful for detecting if electrochemical reactions (i.e., organic reduction porcesses) other than aluminum deposition were taking place. The extent of these reactions were indicated by the depth and sharpness of the additional incisions on the derivative curves.

While the electrolyte scanning technique was useful for ascertaining whether aluminum was electrodeposited upon electrolysis of a test APS, it gave no information as to the nature of the electrodeposit. Test solutions which possessed voltage derivative curves which were similar in appearance yielded electrodeposits which were entirely different - as in the case of the ether and thiocyanate additives. Thus, one <u>cannot</u> predict whether the resultant electrodeposit from a test APS will be completely metallic or only partially metallic (with organic occlusions), hard or soft, brittle or strong, coherent or powdery. For this, one ultimately must electrolyze the test solution for a period of time.